
**Department of Pure and Applied Chemistry**

# Synthesis, structural and adhesive evaluation of novel graft meth(acrylate) copolymers

**By**

**Iain I MacDonald**

**PhD Thesis** **May 2011**

This thesis is the result of the author's original research. It has been composed by the author and has not been previously submitted for examination which has led to the award of a degree.



**Signed:** **Date:**

## Acknowledgements

I would like to sincerely thank all those who made the work presented here possible and for making my time spent accomplishing it very enjoyable. Particular thanks must go to my supervisor Prof. David C. Sherrington FRS for all of his great ideas, productive discussions and support throughout this project. Thanks are also due to Prof. Peter Cormack for many useful ideas and advice.

I would also like to thank; Drs Mike Chisholm and Jane Brown from Lucite International for financial backing, supplying materials and helpful discussions; Dr Nick Hudson and Jim Morrow for help with setting up the Instron, Dr Lawrence Tetley for use of the TEM and to Dr Steve Hinder for help with setting up ULAM ToF-SIMS experiments.

Last, but not least, I would like to extend my gratitude to all of the Polymer Group members, past and present, who have supported my research, but especially Roz, Filipe, Pol, Arlene, Toni, Raul, Isabel and Phill for gourmet lunches and coffee.

## Abstract

A facile and inexpensive method of enhancing the adhesion of poly(methyl methacrylate) (PMMA) to the polyolefins polyethylene (PE) and polypropylene (PP), two commercially important but incompatible polymer classes, using a layer of graft copolymer has been demonstrated. In the present work a series of copolymers containing polyethylene, docosyl or branched alkyl grafts along a poly(methyl acrylate) or poly(methyl methacrylate) trunk were synthesised, characterised and adhesion tested. The graft copolymers were prepared by means of free radical polymerisation and grafting through procedure using macromonomers. Characterisation of the copolymers was achieved by NMR spectroscopy and SEC analysis where possible. The vinyl macromonomers employed in the polymerisation reactions were prepared by a straightforward esterification of commercially available starting materials. The copolymers were also tested using both an in-house and a standard method to determine their effectiveness as an adhesive in lap joints. When annealed above their melting temperature thin films of copolymers from the prepared series were found to provide strong adhesion between plaques of polyolefin and PMMA. The effects of overall molecular weight, mole ratio of (meth)acrylate backbone to PE side-chain and side-chain length and branching on adhesive performance were also investigated. Interestingly graft copolymers with a rather low PE content (~10-20%) proved to provide the best adhesion. In addition a method of purifying and characterising the commercially available polyethylene mono-alcohol by column chromatography was found. The mechanism of adhesion was probed using SEM, TEM and EDX spectroscopy of a cryo-fractured adhesion test piece and further investigation of the adhesive-PMMA interface was carried out using ULAM-ToF SIMS. The morphology of a series of PMA-*g*-PE copolymers of different compositions was investigated using TEM. Graft copolymers with low PE content (i.e. the best adhesives) showed no evidence of microphase separation whereas copolymers with higher PE content displayed evidence of continuous crystalline PE domains. Overall the PE grafts seem to increase compatability and toughness possibly acting as thermally labile crosslinks within the amorphous PMA matrix.

## Abbreviations

| | |
|---|---|
| 2-EHA | 2-ethylhexyl acrylate |
| 2-EHMA | 2-ethylhexyl methacrylate |
| 9-BBN | 9-borabicyclo[3.3.1]nonane |
| AIBN | azobis(isobutyronitrile) |
| ASTM | American Society for Testing and Materials |
| ATRA | all-*trans*-retinoic acid |
| ATRP | atom transfer radical polymerisation |
| B36Ac | 2-hexadecylicosyl acrylate |
| BMA | butyl methacrylate |
| DCC | dicyclohexylcarbodiimide |
| DBU | 1,8-Diazabicyclo[5.4.0]undec-7-ene |
| DCU | dicyclohexylurea |
| DIBAL-H | diisobutylaluminium hydride |
| DMA | dodecyl methacrylate |
| DMAP | dimethylaminopyridine |
| DMTA | dynamic mechanical thermal analysis |
| DocAc | docosyl acrylate |
| DSC | differential scanning calorimetry |
| DVB | divinylbenzene |
| EA | ethyl acrylate |
| EDX | energy-dispersive X-ray spectroscopy |
| EVOH | ethylene/vinyl alcohol co-polymer |
| FT-IR | Fourier transform infrared |
| HDPE | high density polyethylene |
| ICI | Imperial Chemical Industries |
| ISO | International Organization for Standardization |
| LDPE | low density polyethylene |
| LLDPE | linear low density polyethylene |
| MA | methyl acrylate |

| | |
|---|---|
| MALDI | matrix assisted laser desorption ionisation |
| MALLS | multi angle laser light scattering |
| MAO | methyl alumoxane |
| MHS | Mark-Houwink-Sakurada |
| MMA | methyl methacrylate |
| MS | mass spectrometry |
| $M_n$ | number average molecular weight |
| $M_w$ | weight average molecular weight |
| $M_z$ | centrifuge average molecular weight |
| NMP | nitroxide mediated polymerisation |
| NMR | nuclear magnetic resonance |
| PA-6 | polyacrylamide-6 |
| PDI | polydispersity index |
| PE | polyethylene |
| PE460Ac | polyethylene acrylate (derived from PE460-OH) |
| PE460MAc | polyethylene methacrylate (derived from PE460-OH) |
| PE460-OH | polyethylene mono-alcohol ($M_n$ = 460 gmol$^{-1}$) |
| PE700Ac | polyethylene acrylate (derived from PE700-OH) |
| PE700MAc | polyethylene methacrylate (derived from PE700-OH) |
| PE700-OH | polyethylene mono-alcohol ($M_n$ = 700 gmol$^{-1}$) |
| PEG | polyethylene glycol |
| PET | polyethylene terephthalate |
| PMA | poly(methyl acrylate) |
| PMMA | poly(methyl methacrylate) |
| *p*-MS | para-methyl styrene |
| PP | polypropylene |
| RAFT | reversible addition-fragmentation chain transfer |
| SAXS | small angle X-ray scattering |
| SEC | size exclusion chromatography |
| SEM | scanning electron microscopy |
| SIMS | secondary ion mass spectrometry |

| | |
|---|---|
| $T_c$ | crystallisation temperature |
| TCB | trichlorobenzene |
| TD-SEC | triple detection SEC |
| TEM | transmission electron microscopy |
| $T_g$ | glass transition temperature |
| THF | tetrahydrofuran |
| $T_m$ | melting temperature |
| TMEDA | tetramethylethylenediamine |
| ToF | time-of-flight |
| ULAM | ultra low angle microtomy |
| XPS | X-ray Photoelectron Spectroscopy |
| $[\eta]$ | intrinsic viscosity |
| $\eta$ | viscosity |

# Table of Contents

# Chapter 1

# Introduction

# 1 Introduction

Polyolefins are plastic materials with excellent properties and are ubiquitous in modern life although due to their inert surface they have yet to gain importance as functional speciality materials. Methods exist to modify polyolefin surfaces, but these are either not cost-effective, or somehow detract from the excellent properties of the polymer. In the present work we sought to find an inexpensive way to prepare block or graft copolymer adhesives that could be used specifically between polyethylene (PE) or polypropylene (PP) with poly(methyl methacrylate) (PMMA). The potential application for these sandwich materials is as a laminated composite material which might be used, for example, to replace PVC in window frames

## 1.1 Polyolefins

Polyethylene (PE) is the most widely used plastic, with production in 2007 worldwide (excluding China where no data was available) of 40.1 million tonnes, whilst polypropylene (PP) production was second at 25.1 million tonnes, with the two commodities together making up roughly half of all polymer production[1]. Applications of polyolefins are copious, from packaging, moulded toys and playground equipment to storage tanks, plumbing and hip-replacements. The combination of chemical inertness, mechanical properties customised to suit specific applications, extremely low cost of production and ease of processing make polyolefin use widespread. However, polyolefins have a lack of chemical and physical interactions with their immediate environment and this is a major problem as it means that they are incompatible with many other materials, including other polymers. This has limited the use of polyolefins in many applications, particularly where adhesion to their surface is required and there has been a great effort, in both academia and industry, to find simple and cost-effective solutions to this problem.

### 1.1.1 Historical Aspects of Polyolefins

At present PE is produced by two distinct processes; free radical polymerisation at high pressure to furnish low density polyethylene (LDPE) and coordination

polymerisation using transition metal based catalysts to provide high density polyethylene (HDPE).† Coordination catalysis is used to prepare polypropylene (PP). LDPE is more flexible, but much less mechanically tough than HDPE. HDPE tends to be too crystalline for some applications however, and a compromise between low and high density PE was also introduced, which possesses a controlled number and length of chain branches. This copolymer of ethylene and other short chain α-olefins (such as 1-hexene) is made by coordination polymerisation and is known as linear low density polyethylene (LLDPE) (Figure 1.1).

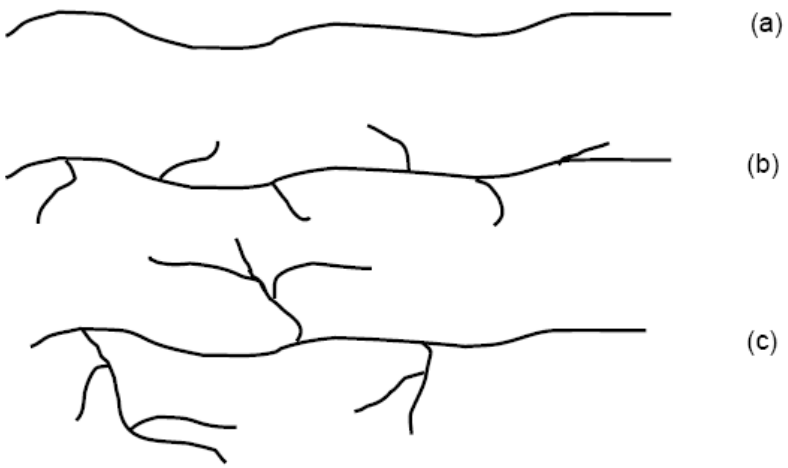


**Figure 1.1: Chemical structures of various kinds of polyethylene (a) HDPE (linear) (b) LLDPE (many equal short branches) (c) LDPE (various branches on branches).**

Although it seems certain to have been accidently prepared by several researchers[2], a method to produce polyethylene commercially was discovered in 1933 by Fawcett, Gibson and co-workers at ICI during a series of experiments involving high pressures. When a mixture of ethylene and benzaldehyde was subjected to a high pressure (2000 atm) and a temperature of 170°C, a white waxy solid PE had coated the inside of the reactor[2]. However the researchers' attempts to replicate this result were problematic and eventually led to the project being abandoned after an explosion. Further investigation at ICI by Perrin and co-workers resulted in control

† LDPE is arbitrarily assigned the density range 0.910 - 0.940 g $cm^{-3}$, while HDPE is defined as a having density greater than or equal to 0.941 g $cm^{-3}$.

over the reaction and reproducibility[3]. They discovered that expeditious oxygen, which had been present as an impurity in the ethylene, was initiating polymerisation *via* a free-radical mechanism. Using an oxygen-free monomer stream and adding a free-radical initiator resulted in a highly controlled, high-yielding and commercially viable synthetic route to polyethylene.

The need for high temperatures and pressures led to high plant set-up and running costs and PE produced by the free-radical initiated route was highly branched due to back-biting by the propagating radical (chain transfer to polymer). Highly branched PE (LDPE) has a lower mechanical strength but is less brittle than linear PE (HDPE) as a result of lower crystallinity due to the inefficient packing of the branched chains. Both LDPE and HDPE possess physical properties that make them useful materials albeit in different applications. Therefore new synthetic routes were sought by several academic and industrial groups, which could produce linear polyolefins and regiochemically control the polymerisation.

In the early 1950s Ziegler and co-workers[4] discovered a new way to make polyolefins using a transition metal catalysed, coordination polymerisation process which produced linear or so called 'high density' PE (HDPE). This material was, in contrast, much tougher both mechanically and thermally than LDPE made by the free-radical process. Ziegler's synthetic route involved heterogeneous catalysts based on titanium halides, $TiCl_3 \cdot \frac{1}{3}AlCl_3$, that produced HDPE upon activation with organoaluminum co-catalysts such as $Al(C_2H_5)_2Cl$ by coordination polymerisation at low temperature and pressure. This system gave highly reproducible results, providing high yields and molecular weights. Working independently at around the same time Natta extended the research accomplished by Ziegler on organometallic catalysts to longer chain α-olefins, discovering that the polymerisation was stereospecific[5]. By modifying Zeigler's catalyst Natta and co-workers were able to synthesise poly(α-olefins), most notably polypropylene with either isotactic or syndiotactic architectures, each being highly crystalline and having different properties and applications.

Polyolefins produced using Zeigler-Natta catalysts are highly linear, and stereo-chemically controlled. This allows the chains to pack closely, giving the materials high crystallinity (often greater than 90%) and therefore higher density. Zeigler and Natta were jointly awarded the Nobel Prize in Chemistry "For their discoveries in the field of the chemistry and technology of high polymers" in 1963.

The mechanism of the Zeigler-Natta catalyst system was elucidated by Cossee and Arlman in the early 1960s (Scheme 1.1)[6]. Recent developments of olefin polymerisations include the more efficient metallocene zirconium 'sandwich' complexes discovered by Kaminsky and co-workers.[7] The metallocene catalysts are activated by methyl-alumoxane (MAO), and generate polymers with even higher regio- and stereo-control than the titanium-based Zeigler-Natta catalysts they are replacing. Recently a new breed of olefin catalysts have been reported by Fujita and co-workers[8] which have still higher efficiencies in olefin polymerisations. It is noteworthy that the drive to find improved polymerisation catalysts has led to the discovery and refinement of alkene metathesis[9] catalysts now used to great effect in organic synthesis.

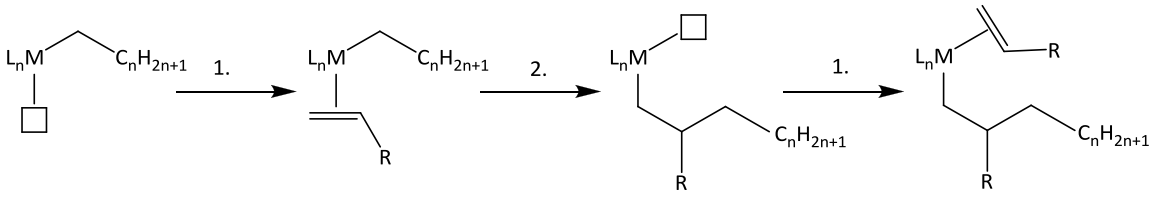


**Scheme 1.1: The Cossee-Arlman mechanism for the polymerisation of olefins, $ML_n$ = metal centre, □ = vacant coordination site. Step 1 is binding of the olefin monomer to the vacant coordination site. Step 2 is migratory insertion of the monomer into the polymer chain.**

### 1.1.2 Making polyolefins compatible

One of the key features of polyolefins is their lack of chemical and physical interactions with their immediate environment; this can be an advantage or a disadvantage depending upon the application being sought. A PE surface can be

envisaged as being made up solely of methylene groups, like an *n*-alkane. The historical name for *n*-alkanes was *paraffin* from the Latin *parum* meaning barely and *affinis* with the meaning here of lacking affinity. Similarly the surface of polypropylene is made up of methine, methylene and methyl groups only. A polyolefin surface is thus very hydrophobic, making it an excellent inert barrier in packaging applications, however this very lack of affinity prevents other materials from adhering to the polymer surface. This can be overcome by either 1) surface modification by post-polymerisation processing, or 2) co-polymerising the olefin with more polar monomers, or 3) by using an adhesive compatibiliser, which might be made by co-polymerisation, either in blends or at the surface.

#### 1.1.2.1 ***Surface modification techniques.***

Surface modification of polyolefins can be achieved by various means, including surface grafting by redox initiators, chemical treatment, corona treatment, halogenations, flame treatment and plasma treatment. Most of these methods are harsh and are therefore complex or expensive to implement industrially. Surface modification often impinges on the properties of the bulk polymer, affecting mechanical strength and durability. Surface treatments are nonetheless effective and are used extensively for many applications.

Surface grafting with redox initiators has been used to modify polymer surfaces by Batich and co-workers[10]. They grafted polyacrylamide onto a LDPE surface by first oxidising the surface with chromic acid, followed by reduction with diborane. This furnished a hydroxyl rich surface from which polyacrylamide grafts were subsequently grown using a $Ce^{4+}/HNO_3$ redox initiator. This provided a hydrophilic surface on the LDPE which was characterised by XPS and FT-IR spectroscopy. Successful as this technique is however, the harsh reagents and their associated costs prevent its commercial exploitation. Surface grafting to PE has also been attained by using thermal and radiochemical methods[11]. These methods are also fairly destructive of the surface, with microscopic imaging of treated areas revealing cracks.

Chemical treatment of LDPE films with an aqueous solution of ammoniacal ammonium persulfate in the presence of $Ni^{2+}$ ions results in the appearance of polar groups (carbonyl and carboxyl) on the polymer surface[12]. The reagent mixture is aggressive enough to oxidise polymer main-chain carbons. $Ni^{3+}$ ions generated by the action of the persulfate have been proposed to be the oxidising species. The authors reported the increased strength of laminates of LDPE with epoxy resins, which they attributed to improved mechanical interlocking through surface roughness and chemical bonding at the interface (Figure 1.2).

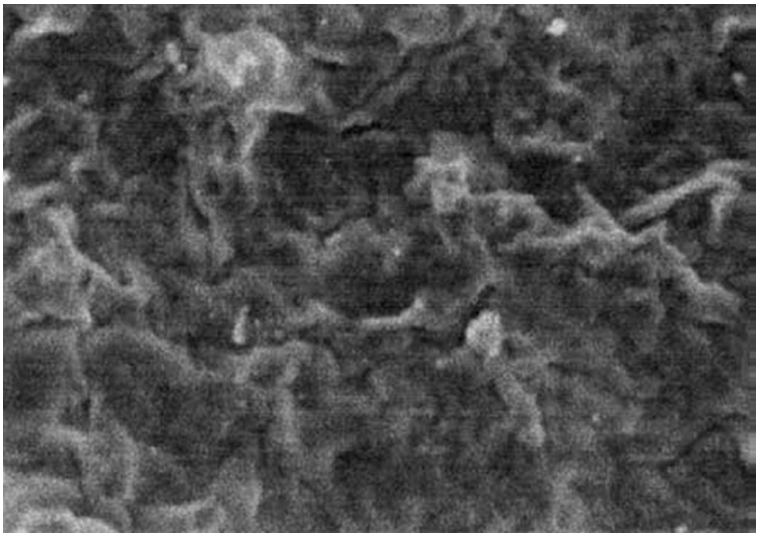

**Figure 1.2: A SEM micrograph of the morphology of LDPE film treated with ammonium persulfate and nickel sulfate[12a]**

Several groups have studied the effect of corona discharge followed by functionalisation or grafting. Being relatively simple, corona discharge is the most widely used continuous process for the surface treatment of polyolefin films[12b]. The technique is mainly used in the polymer industry to improve the printability[13] and adhesion[14] of polyolefin films. The corona treatment device is simple and cost effective. It consists of a high voltage–high frequency generator, an electrode and a grounded metal roll covered with a dielectric material as shown in Figure 1.3. The whole system works like a large capacitor, with the electrode and the grounded roll as the plates of the capacitor and the roll covering and air as the dielectric. The high voltage applied across the electrodes ionises the air producing plasma, which brings

about physical and chemical changes on the polymer surface to improve surface properties.

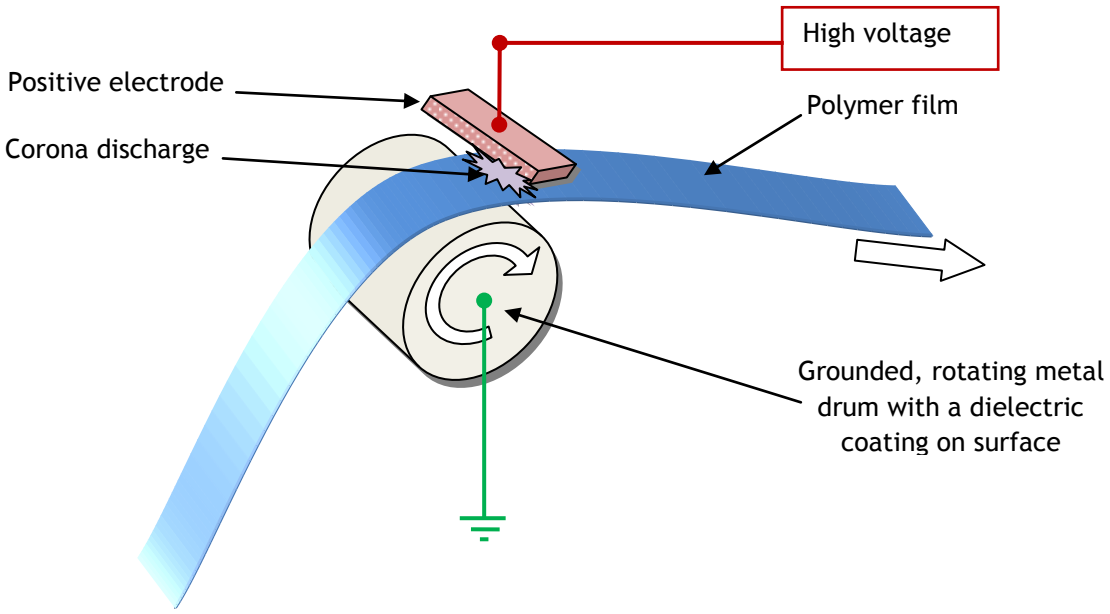


**Figure 1.3: A basic schematic of corona discharge equipment.**

Park and co-workers[13] exposed films of LDPE to corona discharge and subsequently grafted acrylic acid onto the surface to improve its properties, in particular to improve adsorption of basic dyes. Using X-ray photoelectron spectroscopy (XPS) they confirmed the presence of polar carboxyl, carbonyl and hydroxyl groups bound to the surface.

Fluorination[15] has been used to change both the permeability and surface properties, particularly in the manufacture of fuel tanks for automotive applications, where fuel loss can be reduced by a factor of 50-100[16]. This makes HDPE fuel tanks impermeable enough to meet stringent environmental emission controls. Studies have also shown that if oxygen is present during fluorination of the polymer surface, this creates -COF groups on the surface which increase its polarity and render further modification possible, by grafting for example.

#### 1.1.2.2 *Copolymerisation of olefins with functional monomers*

Copolymerisation has also been used to improve the surface adhesion of polyolefins, but this can have a detrimental effect on the mechanical properties of the bulk material as it disrupts the packing of the polymer chains and can therefore lower the crystallinity. Direct copolymerisation of ethylene with polar monomers is difficult as this type of monomer can poison the Zeigler-Natta catalyst system, owing to their Lewis basicity[17]. The non-bonded electron pairs on heteroatoms (e.g. O or N) of functional monomers tend to compete for and form complexes with the active site of the catalyst diminishing its activity. To overcome this protected functional monomers can be used which are de-protected in a subsequent step, alternatively modified catalysts have been used which can tolerate the comonomer functionality.

Chung and co-workers[18] have extensively studied incorporating functionality into polyolefins, by both copolymerisation of functional monomers and by post-polymerisation treatment of olefin polymers. Co-monomers for olefin copolymerisations used by the group included *p*-methyl styrene (*p*-MS), divinylbenzene (DVB) and vinyl boranes such as 5-hexenyl-9-borabicyclo[3.3.1]nonane (5-hexenyl-9-BBN).

By selecting a metallocene catalyst with constrained ligand geometry, the group found that *p*-MS was incorporated well in copolymerisations with ethylene, with conversions of *p*-MS up to 90% in the copolymer[19]. Subsequently the group applied similar methodology to the preparation of propylene/ethylene/*p*-MS and ethylene/1-octene/ *p*-MS elastomeric terpolymers[20]. Copolymerisations involving propylene and *p*-MS did not work. The researchers postulated that steric hindrance between the phenyl ring of *p*-MS and the Zr catalyst ligands during the cross-over reaction prevented incorporation of the relatively bulky comonomer. The PE-co-*p*-MS copolymers were then metallated using *s*-butyl lithium (*s*-BuLi), which lithiated at the benzylic methyl group[20]. Styrene was then added and this grafted from the PE backbone in a living anionic polymerisation (Scheme 1.2).

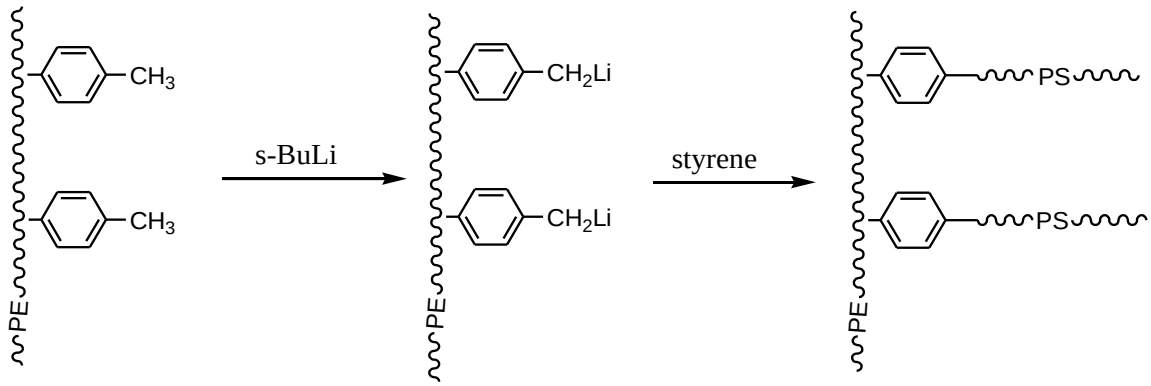


**Scheme 1.2: Modification of PE-co-*p*MS copolymers with PS grafts**

The graft copolymers were used as compatibilisers (10 % by weight) in PE/PS blends and, confirmed by scanning electron microscopy (SEM), improved the dispersion of PS in a PE matrix relative to no compatibiliser being used. This approach to polyolefin-containing copolymers seems to be useful as the comonomer *p*-MS and the catalysts are commercially available, however the use of stoichiometric amounts of *s*-BuLi could prevent exploitation of this method on an industrial scale.

Chung and co-workers[21] have also reported the preparation of copolymers of ethylene and 5-hexenyl-9-BBN by using similarly constrained metallocene catalysts. Since the borane copolymer contains an alkyl portion next to the double bond it was relatively small when compared to *p*-MS and could also be copolymerised with propylene. The borane was found to be stable to the catalyst system whilst still being reactive enough to allow facile modification in post-polymerisation steps. The same group have also reported the preparation of borane-terminated polypropylene and polyethylene by using 9-BBN as a chain transfer agent[22]. By adding oxygen to the polymer, a B—O—O—C peroxide was generated at the borane end-group. Methyl methacrylate was then added to this macroinitiator to create a PE/PMMA diblock copolymer, which was ~1:1 by mass, using 'living' free radical polymerisation.

The newer Kaminsky-type[7] metallocene catalyst systems show improved tolerance to polar monomers, and several groups have managed to co-polymerise ethylene in the presence of oxygen-containing comonomers. Aaltonen and co-workers[23] used 10-undecen-1-ol as a co-monomer containing an alkyl 'spacer', with the length of alkyl chain between the alkene and the hydroxyl group helping to prevent complete catalyst poisoning. In recent studies the same group[24] have prepared polypropylene with hydroxyl-side chain functionality of up to 8.2 weight percent by a similar co-polymerisation. They used T-peel adhesion tests of the copolymer between aluminium adherands and found the copolymer had significantly higher adhesive strength than polypropylene. They attributed the improved adhesion to the copolymer having a more polar surface and backed up these findings with contact angle measurements which confirmed the increased surface polarity with respect to PP.

In a similar vein, Borbado and co-workers[25] used 10-undecenoic acid as the co-monomer in an ethylene polymerisation using both titanium and zirconium metallocene catalysts in the presence of MAO. They detected a threefold increase in polymer adhesion, even with the low incorporation of carboxyl co-monomer observed, however decreased catalyst activity was again a problem.

Copolymerisation with functional monomers to provide better surface properties is an approach that detracts from one of the great advantages of polyolefins; their straightforward and inexpensive manufacture. There have however been great advances in catalysis that may allow copolymerisation to become a viable method for the production of compatibilisers and adhesives.

### 1.1.2.3 *PE-containing block copolymers*

There has been great progress in the last 20 or so years toward the controlled polymerisation of olefins, with recent advances in catalysis also allowing end-functional polyethylenes to be prepared[26]. Using these end-functional or telechelic polyolefins as building-blocks could provide attractive routes to new types of block and graft copolymers.

Bergbreiter and co-workers[27] have used living anionic polymerisations of ethylene to synthesise PE oligomers and polymers terminated with functional groups. They used tetramethylethylenediamine (TMEDA) as a ligand to increase the reactivity of *n*-BuLi. The group also reported the quenching of the living polyethylene by electrophilic substitution with a wide selection of different functional groups, including hydroxyl, carboxyl, chlorocarbonyl and amine (Scheme 1.3).

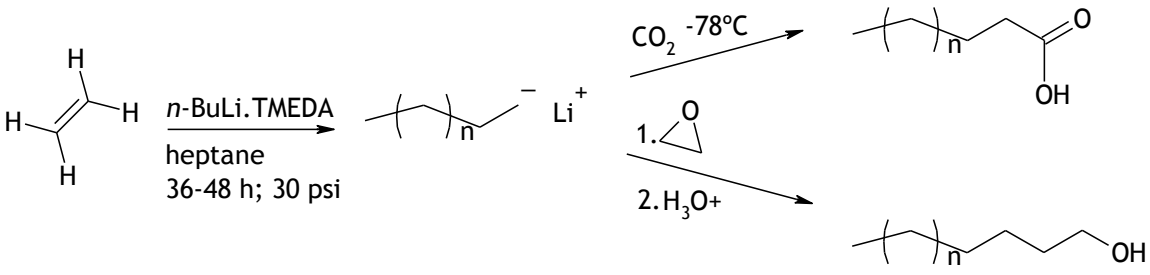


**Scheme 1.3: A method of preparing hydroxyl and carboxyl terminated polyethylenes. n = ~40 to ~200.**

In a subsequent study, Bergbreiter and co-workers[28] have reported using diblock co-polymers of PE and polyethylene glycol (PEG) to functionalise polyethylene. They prepared the copolymers by acid-catalysed transesterification, coupling carboxyl-terminated PE that was prepared as described above, with a commercially available monomethyl ether terminated PEG. The polymers were blended at low concentration into PE. Contact angle and X-ray photoelectron spectroscopy (XPS) studies of the surface revealed that it had a more polar surface than pure polyethylene, which suggested that the PEG chains had migrated to the surface.

Although this was elegant research and a good proof of principle, the drawbacks of using anionic polymerisation (e.g. the need for highly pure and dry monomers; the use of stoichiometric quantities of pyrophoric Li reagents) preclude the use of this olefin polymerisation method on a commercial scale.

Endo and co-workers[29] have also reported the synthesis of diblock co-polymers of PE and PMMA. They first prepared polyethylenyllithium from ethylene gas using *s*-BuLi complexed with TMEDA, then added 1,1-diphenylethylene to create a stabilised anion at the end of the living PE chain. Methyl methacrylate (MMA) was then added at low temperature to create the second block. The reported yields for these polymerisations were low, with PMMA either making up a smaller block than the PE or not being incorporated at all. Although this polymerisation was performed in one pot, it nonetheless seems to have been an over-complicated approach.

Gibson and co-workers have also reported the preparation of end-functional polyethylenes by a degenerative transfer polymerization of ethylene using a bis(imino)pyridine iron catalyst and triethylzinc as a co-catalyst[30]. The low reaction temperature resulted in precipitation at fairly low molecular weight (~700 $gmol^{-1}$), which could be seen as a drawback. It seems possible that the commercially available polyethylene alcohols used in the present work were prepared by this method.

Matyjaszewski and co-workers[31] have recently reported the preparation of methacrylate monomers with alkyl chain length of ~22 carbon atoms which are similar to those in the present work, using the methodology of Gibson and co-workers[30]. They reported that, even under mild conditions, the reaction of their 'PE-OH' with methacryloyl chloride was accompanied by the formation of side-products. Instead the researchers dehydrobrominated a polyethylene macroinitiator they had already prepared for an atom transfer radical polymerisation (ATRP) to provide the methacrylate (similarly to Scheme 1.4, steps 4 and 5). The article also describes the copolymerisation of the macromonomer with *n*-butyl acrylate and then *t*-butyl acrylate using an ATRP method. These resulted in incomplete and low incorporation of the macromonomer into the copolymers (they were able to fractionate the

relatively insoluble macromonomer from both copolymers). This is in contrast to the present work (see Section 3.3) where complete conversion is repeatedly seen for a range of different monomers with longer PE chain lengths and for various, selectable, composition ratios. Perhaps surprisingly the researchers did not attempt to use a straightforward conventional free-radical reaction to prepare their polymers.

In more recent work Matyjaszewski and co-workers have used a vinyl-terminated ($M_w$ = ~1800 gmol$^{-1}$) polyethylene acquired from Matsui chemicals, converted this to a PE-OH and subsequently to a PE macromonomer which was used to prepare polystyrene-*graft*-polyethylene *via* an ATRP method[32]. As with the previous work a two-step route to the PE-methacrylate was taken, with the macromonomer being characterised by $^1$H NMR spectroscopy (Scheme 1.4).

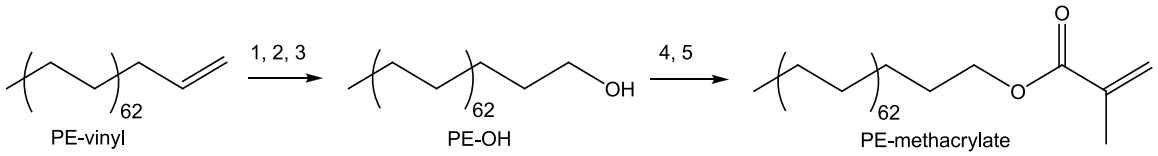


**Scheme 1.4: Preparation of a PE-methacrylate macromonomer from vinyl-terminated PE[32]. Conditions: 1. diisobutylaluminium hydride (DIBAL-H), *o*-xylene, 100°C. 2. Dry air, *o*-xylene, 100°C. 3. $HCl_{(aq)}$. 4. 2-bromo-2-methylpropionyl bromide, $NEt_3$, PhH, 100°C. 5. 1,8-Diazabicyclo[5.4.0]undec-7-ene (DBU), PhH, 100°C.**

The final PE-methacrylate was found to be 60% pure, with the major impurity being non-functional PE of a similar molecular weight, which the researchers attributed to reaction of the alkyl aluminium intermediate with expeditious moisture during the conversion of PE-vinyl to PE-OH.

In two recent patents[33], Everaerts *et al.* at the 3M Corporation claimed (meth)acrylate-based copolymers containing alkyl side-chains of over 20 carbons in length as useful heat-activated adhesives. Although the precise details of the formulation and composition are vague, the researchers have claimed that 20 to 70 % of the copolymer should be made up from an alkyl (meth)acrylate monomer with a

carbon chain comprising at least 20 carbon atoms. These materials were described as becoming tacky at temperatures over 40 °C and as being useful where an adhesive is required to be non-stick until needed when it can be activated by heating.

In another patent from Sugimoto *et al.* at the Asahi Glass Co. similar poly(meth)acrylates are described with uses as oil and water repellent coatings[34]. The copolymers were made by free radical polymerisation with a range of different monomers, including perflouroalkyl (meth)acrylates and alkyl acrylates. The monomers pertinent to the present work were alkyl (meth)acrylates with chain lengths of $C_{16}$ to $C_{22}$.

Chatterjee and co-workers[35] have studied the crystallinity of poly(methacrylic acid)-*g*-docosyl acrylate copolymers that are similar to those described in the present work (Section 3.3). They prepared the docosyl acrylate monomer by reacting methacrylic acid with 1-docosanol in the presence of para-toluenesulfonic acid. They copolymerised the docosyl acrylate with a range of different mole fractions of methacrylic acid from 0 to 0.91. The copolymers were characterised by SEC and DSC. From the DSC studies the group found that the crystalline fraction decreased from 0.52 to 0.07 and that the melting point decreased as the mole fraction of methacrylic acid was increased.

Shanahan and Guiu[36] have studied the adhesive effects of a PE graft copolymer (PE*) between layers of HDPE and an ethylene/vinyl alcohol copolymer (EVOH). They co-extruded the polymers together as a five layered system consisting of two outer layers of HDPE, a central layer of EVOH and layers of PE* at each LDPE/EVOH interface. Using ‘L-peel’ adhesion tests of the multilayered polymer structure they studied the adhesive strength at various temperatures. It is interesting to note that no mention is made of the structure of the adhesive polymer (PE*) in either publication.

In a recent patent, Kneafsey *et al.*[37] of Henkel Loctite Corporation describe a two component adhesive formulation specifically designed for bonding polyolefin surfaces. The first component (the ‘initiator’) seems to contain a mixture of an organoborane, a polyaziridine and some other unspecified complexing agents to

stabilise the organoborane. Organoboranes such as those described in the patent are highly reactive and tend to be pyrophoric when exposed to open air, making them unsuitable for use in an adhesive formulation. The complexing agents described seem to limit the reactivity of the borane allowing them to be stored and used without an inert atmosphere. The second component is a mixture of the vinyl monomers tetrahydrofurfuryl methacrylate (THFMA), 2-ethylhexyl methacrylate (2-EHMA) and hydroxylethyl methacrylate monoester of succinic acid and a core-shell toughener (Blendex 336; GE Speciality Chemicals). The hydroxylethyl methacrylate monoester of succinic acid, which is acidic, has the purpose of de-complexing the organoborane when the two components are mixed. The organoborane reacts with the polyolefin surface and initiates polymerisation of the vinyl monomers from the surface at the same time. In this way polymer grafts grow from the polyolefin surface and if a second polyolefin surface is present, the two will become covalently bonded together. The patent reports some data from ASTM D1002 adhesion tests with this formulation on untreated substrates (Table 1.1). It is worth noting that the polypropylene used was 'filled polypropylene' and as such may have different and unknown surface energy from the substrates used in the present work which were unfilled.

| Substrates | Shear strength / MPa |
|---|---|
| PE/PE | 4.2 |
| PP/PP | 2.2 |
| mild steel/mild steel | 5.7 |
| GBMS/GBMS* | 9.0 |

**Table 1.1: Adhesion test data from the Henkel patent.**

Although the Henkel adhesive is now commercially available and indeed appears to be available as a consumer product, it remains too expensive (at present in the UK it costs over £16 for 35 mL) and exotic for most industrial-scale applications.

* GBMS is grit blasted mild steel.

## 1.2 **Poly(methyl methacrylate)**

Poly(methyl methacrylate) (PMMA) was one of the very first plastics to be derived from petrochemicals[38]. It was originally described by Otto Rohm in his doctoral thesis early in the 20th Century although at this point its technological importance was not realised and PMMA was eventually commercialised in the late 1920s by a number of companies including Rohm and Haas in Germany (Plexiglas), DuPont in the US (Lucite) and ICI in the UK (Perspex). PMMA is prepared industrially by the free-radical polymerisation of methyl methacrylate (MMA), often with casting directly into the final product form which is often translucent sheeting. The polymer has excellent mechanical strength and can be easily moulded when heated above its $T_g$. One of the first applications of PMMA was as a substitute for glass, particularly in the aviation industry where it is still used today. PMMA has a higher impact strength than glass and on impact, unlike glass, the polymer shatters into blunt pieces making it much safer. A drawback of pure PMMA (i.e. a homopolymer of MMA) is that it possesses a relatively low ceiling temperature (220-230 °C), above which it undergoes depolymerisation and MMA vapour is released[39]. The risk of depolymerisation must be considered, particularly on large-scale applications of PMMA. Small amounts of ethyl acrylate (EA) are often copolymerised with MMA in commercial grades destined for thermal processing, which serve to improve stability. EA segments in the PMMA chain enhance the thermal stability as they prevent depolymerisation by acting as 'stops' on the backbone. PMMA is an amorphous polymer, having a glass transition temperature ($T_g$) of around 110 °C it must be heated to above this temperature in order to process it into useful objects and therefore thermal stability is important for most applications. Typically PMMA is produced by either extruded sheets of the material or by cell-casting, where the polymerisation is performed with the bulk monomer already in its final form. When free from monomer residues the polymer is highly biocompatible making it suitable for a wide range of medical applications from intra-ocular lenses to bone cement. Other applications of PMMA include aircraft and submarine windows, riot control shields automotive light lenses and adhesives.

## 1.3 Polymer synthesis and characterisation

### 1.3.1 Addition Polymerisation

Addition polymerisation, using vinyl monomers, allows a simple route to high molecular weight material, without the need for the bi-functional monomers required by condensation (or step-growth) polymerisation (Scheme 1.5). A vinyl monomer is bifunctional, the π-bond is susceptible to attack from free radicals, and either anions when R' is electron withdrawing, or cations when R' is electron-donating.

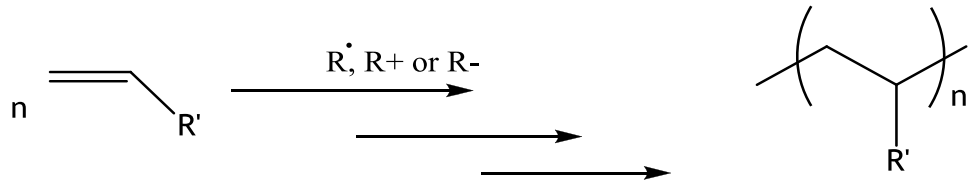


**Scheme 1.5: Free radical addition polymerisation of a vinyl monomer.**

### 1.3.2 Free Radical Polymerisation.[40]

A free radical polymerisation reaction has three distinct stages:

1) Initiation - the formation of an active centre from whence the polymer can grow.

2) Propagation - chain growth by repeated addition of monomer units.

3) Termination - where chain growth is halted by annihilation of the active centre.

#### 1. Initiation.

A free radical polymerisation can be initiated by any species that has the tendency to decompose readily to form radical species when perturbed by some means. The source of this perturbation is typically thermal, photochemical or chemical. Examples of commonly used thermal initiators include azobisisobutyronitrile

(AIBN), and benzoyl peroxide (Scheme 1.6 and 1.7). AIBN can also be decomposed photochemically, using UV light of wavelength 360 nm.

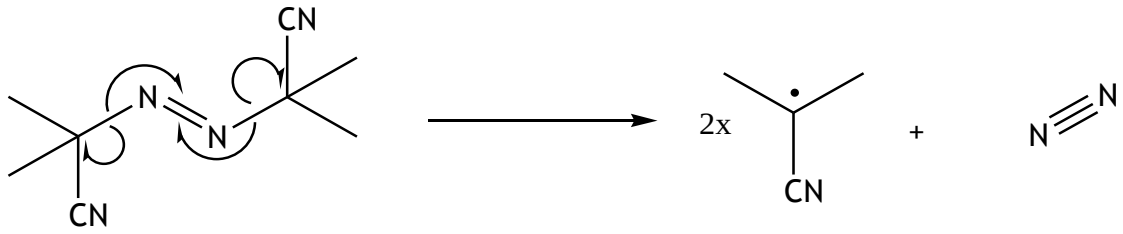


**Scheme 1.6: The decomposition of AIBN.**

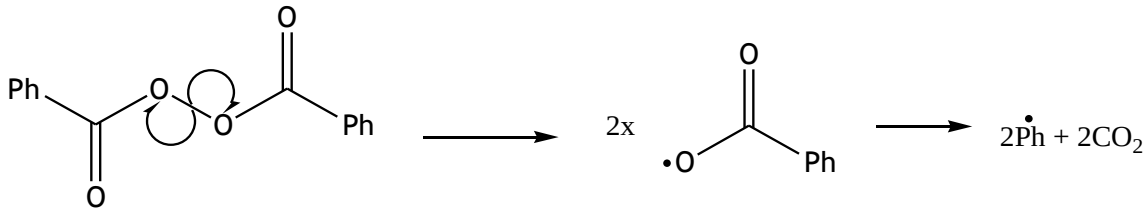


**Scheme 1.7: The decomposition of benzoyl peroxide.**

Redox initiators include the $H_2O_2/Fe^{2+}$ system (Scheme 1.8) and persulfates such as $S_2O_8^{2-}/HSO_3^-$.

$$H_2O_2 + Fe^{2+} \longrightarrow Fe^{3+} + OH^- + OH^{\cdot}$$

**Scheme 1.8: The reaction between hydrogen peroxide and ferrous ion, generating a hydroxyl radical.**

Once the radical comes into contact with the unsaturated monomer it reacts with it, forming an active centre on a monomer, which is able to propagate into polymer (Scheme 1.9).

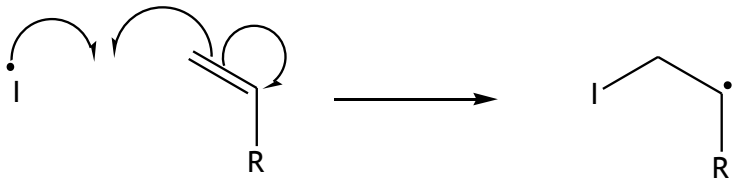


**Scheme 1.9: Initiation of monomer with an initiator derived free radical. I = initiating fragment.**

**2. Propagation.**

In what is typically a highly exothermic process to form saturated polymer chains, the initiated monomer goes on to react with a second monomer unit and a fast chain reaction ensues (Scheme 1.10). Polymer chains with a high degree of polymerisation ($DP_n$) are formed early in the reaction with only small consumption of monomer. In theory this chain reaction should be able go on indefinitely, but in reality there are numerous termination processes that quench the propagating radical.

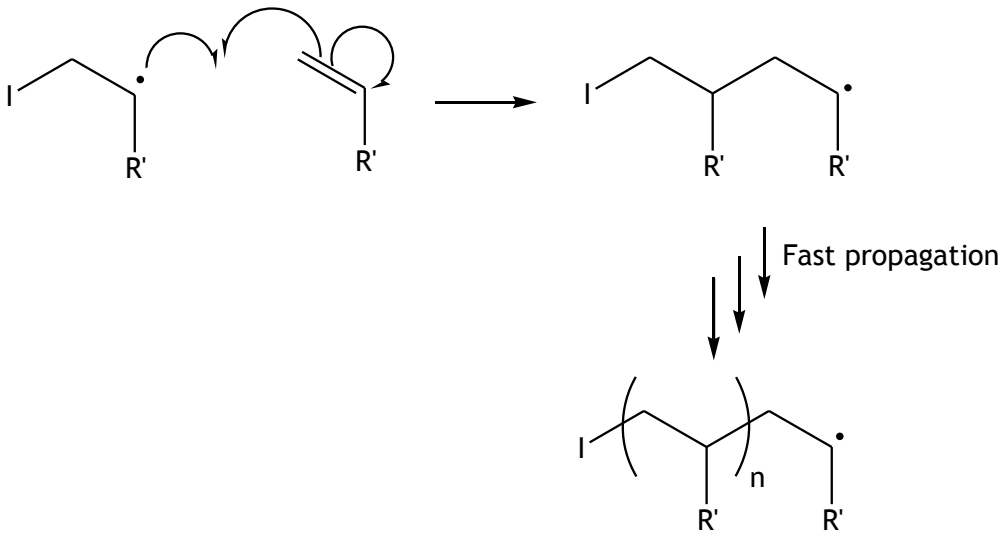


**Scheme 1.10: Free radical chain propagation.**

### 3. Termination

Active radical centres at the end of the growing polymer chain can be terminated in numerous ways. The most important termination mechanism is the reaction of two active chain ends although combination of an active chain end with an initiator radical fragment or the transfer of the active centre to another molecule in the reaction pot, for example to the solvent are also observed. Chain transfer agents such as alkyl thiols are often added to free radical polymerisations to limit molecular weight or, in conjunction with bi-functional monomers, to introduce branching[41]. Radical-scavenging impurities such as oxygen or inhibitors are also important chain terminators which must be removed prior to initiation. Reaction of two chain ends can occur by two different routes; combination or disproportionation. Combination is where two chain ends couple to yield one long chain (Scheme 1.11).

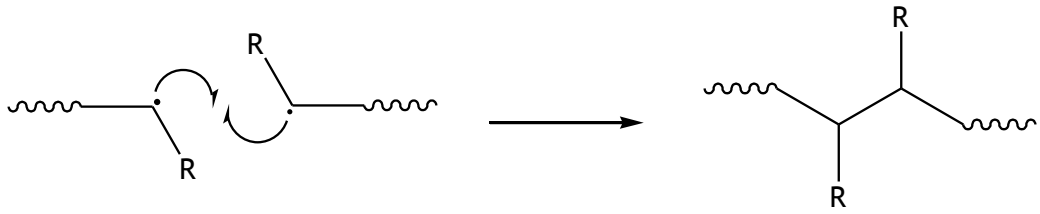


**Scheme 1.11: Free radical chain termination by combination.**

Disproportionation is where one chain abstracts a hydrogen atom from the other providing two dead polymer chains, one with an unsaturated group at the end (Scheme 1.12). The mechanism by which termination occurs is monomer and temperature dependant. At temperatures above 330 K[†] disproportionation is the main termination mechanism for both MMA and MA, two monomers used extensively in the present work.

[†] Below 330 K MMA terminates mostly by combination.

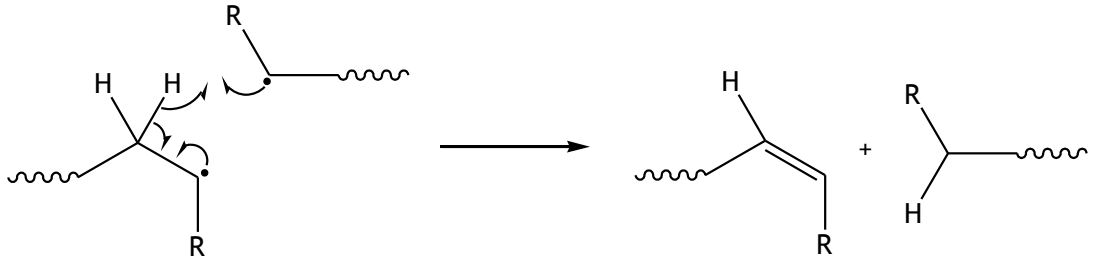


**Scheme 1.12: Free radical chain termination by disproportionation with hydrogen abstraction.**

### 1.3.3 **Free radical vinyl copolymerisation.**[30]

In a free radical copolymerisation the comonomers involved will have different relative reactivity towards the propagating radical at the end of the polymer chain. These differences are determined by factors such as the relative electron richness and steric encumbrance of the monomers. Staudinger[42] first noted the effects of relative monomer reactivity when he observed a composition drift with time during the course of a copolymerisation of vinyl acetate with vinyl chloride. Polymer produced early in the reaction was rich in vinyl acetate, whilst that generated later in the reaction was rich in vinyl chloride. This demonstrated the higher reactivity of vinyl acetate towards the propagating radical at the end of the polymer chain. A kinetic survey of the elementary reactions involved in copolymerisation by Dostal and Mark[43] presented a method of predicting the composition of a copolymer at a given time. The method employs the so-called 'instantaneous copolymer composition equation' (Equation 1.1).

**Equation 1.1: The instantaneous copolymer composition equation, where;**

——: (number of $M_1$ units in polymer)/(number of $M_2$ units in polymer) at a given time *t*,

$r_1$, $r_2$: relative reactivity ratio of monomer 1 and 2 respectively,

$[M_1]$, $[M_2]$: concentrations of monomer 1 and 2 respectively.

Copolymerisation composition outcomes can therefore be established when monomer concentrations are known using the equation and numerical values for $r_1$ and $r_2$ that have been determined experimentally for a large range of vinyl monomers[44]. The most common values for the reactivity ratios are either $r_1$ and $r_2$ are both < 1 or $r_1$ >1 and $r_2$ is small. It is unusual to find systems where $r_1$ and $r_2$ are both > 1. Usually if one of the radicals is very reactive, it will be reactive with both monomers, *i.e.* $r_1 > 1$ and $r_2 < 1$ means that the radical derived from monomer 1 will be very reactive. Where $r_1$ and $r_2$ are roughly equal and < 1, then both monmomers will be incorporated into the propagating chain fairly randomly. Where $r_1$ is >1 and $r_2$ is small (or *vice versa*) then there is a tendancy to get large blocks of monomer 1 units broken by individual monomer 2 segments. In the final case $r_1 << 1$ and $r_2 << 1$, here each propagating radical preferentially reacts with the opposite monomer giving rise to a 1:1 alternating copolymer.

There are two types of copolymerisation system, 'ideal' and 'non-ideal', information which can be gleaned from the reactivity ratios. In ideal systems the propagating radicals of both monomers show the same preference for adding one of the monomers over the other and thus $r_1 = 1/r_2$. In this case the radical derived from the last monomer (whether it is monomer 1 or 2) added to the propagating chain has no influence on the rates of addition of either of the comonomers. The controlling factors are therefore the relative reactivities of the monomers themselves and their concentrations at a given time during the polymerisation. For non-ideal systems the propagating radicals derived from each monomer have a preference for either the

same monomer or the other monomer and thus this becomes an additional controlling factor to those influencing an ideal system.

If a copolymer with well-defined proportions of both monomers is required, the more reactive monomer can be fed into the reaction mixture to keep its concentration constant according to the value determined using the equation, consequently preventing composition drift from occurring. By integrating the instantaneous copolymer equation, mean sequence lengths of each monomer unit in a copolymer can also be statistically determined using the relative reactivity ratios of both monomers and their concentration ratio (—— in the polymer.

### 1.3.4 **Chain transfer in free radical polymerisation**

Chain transfer is a phenomenon which occurs during polymerisation where the propagating radical at the end of the growing polymer chain is quenched by abstracting hydrogen from some species in the reaction pot. Since the propagating radical is generally a highly reactive species, chain transfer can occur between it and monomer, solvent or polymer (back-biting or disproportionation). Although they ultimately control the molecular weight by terminating chain growth, these chain transfer reactions are relatively uncommon during polymerisation unless the new radical formed from hydrogen abstraction is stabilised by resonance and/or inductive effects. So-called chain transfer agents (CTAs) are often added to a polymerisation as a means of limiting the molecular weight. The most common CTAs are thiols, where the radical formed resides on the electron-rich sulfur atom (Scheme 1.13).

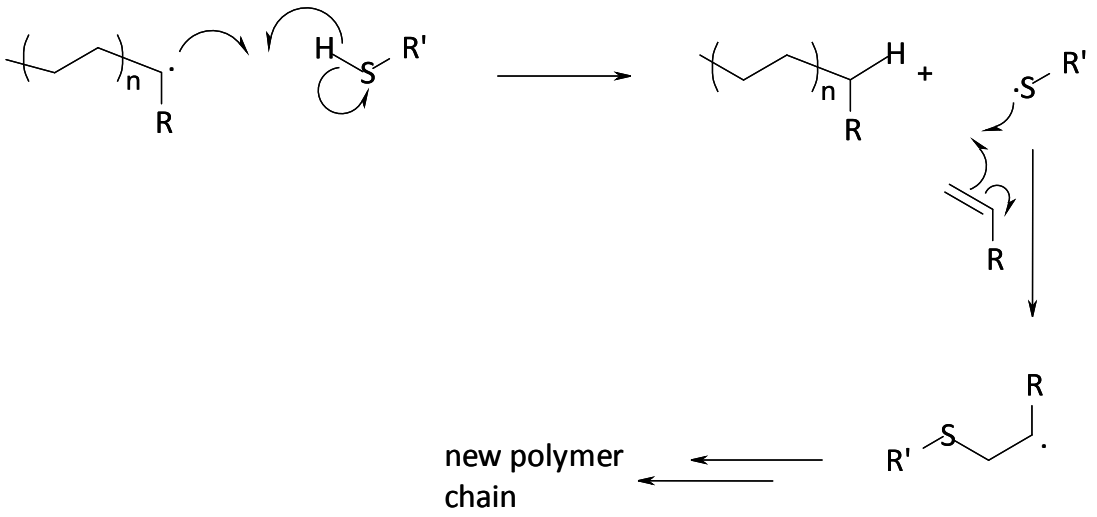


**Scheme 1.13: The reaction mechanism of chain transfer to a thiol CTA**

The efficiency of the chain transfer process with different reagents depends on the reactivity/stability of both the propagating radical and CTA radical. Chain transfer agents have been studied extensively for many different monomers[44] and a theory on the chain transfer process was developed by Mayo[45]. The Mayo equation can be used to determine the *chain transfer constant* (*C*) for a particular CTA/monomer combination (Equation 1.2).

$$\frac{1}{Dp} = C\frac{[S]}{[M]} + \frac{1}{Dp_0}$$

**Equation 1.2 The Mayo equation**

where *Dp* is the degree of polymerisation, $Dp_0$ is the *Dp* with no CTA present, [*S*] and [*M*] are the CTA and monomer concentrations respectively. A plot of 1/*Dp* vs. [*S*]/[*M*] will give a straight line for an efficient process with the slope of the line equal to *C*. The chain transfer constant supplies information on the effectiveness of the chain transfer process and, in general, a value of $C > 1$ means that the process is highly efficient. Once the chain transfer constant is known for a particular reaction, the average molecular weight can be predicted for a given concentration of the CTA.

### 1.3.5 **Graft copolymers.**

There are three main synthetic methods for preparing graft copolymers (1) grafting 'from', (2) grafting 'onto' or (3) grafting 'through' *via* macromonomers. Since the polymers discussed here were synthesised by grafting through (also known as the macromonomer technique) this is reviewed in the greatest depth, although some other synthetic strategies are covered briefly.

#### 1.3.5.1 ***Grafting 'from'.***

This technique uses an existing polymer that has reactive or functional groups along its chain length, these act as initiators for new polymer chains to grow from. Some of the emerging controlled radical polymerisation (CRP) systems have been successfully used to initiate graft growth from the trunk macroinitiator. For example alkyl halides along the trunk polymer backbone can be used as atom transfer radical polymerisation (ATRP) macroinitiators from whence vinyl monomers can add to form grafts of controlled length. ATRP was first developed in the mid 1990s independently by the research groups of Sawamoto[46] in Japan and Matyjaszewski[47] in the United States. The methodology uses an initiator, a transition metal catalyst (Cu or Ru), and a ligand. The technique is tolerant of a wide range of monomers and can produce polymers with a high degree of control over the molecular weight and narrow polydispersity, due to the low number of chain termination reactions that occur. The method, although elegant, has not become industrially important to date due to the cost of the reagents and the difficulty of removing catalyst residues from the final product (the polymers are frequently coloured by catalyst residues). Using a CRP method to synthesise the polymers discussed here might provide more controlled architectures, but this is unlikely to provide any benefit with the given application and the approach used in the present work employs far less complicated and thoroughly proven chemistry. Examples of other CRP methods include reversible addition fragmentation chain transfer (RAFT)[48] and nitroxide mediated polymerisation (NMP)[49]. These emerging technologies along with ATRP are now areas of concentrated research and all rely on harnessing the propagating radical to control the molecular weight.

#### 1.3.5.2 *Grafting 'onto'.*

As the name suggests, this technique uses reactive groups along the backbone of an existing polymer and grafting the second polymer, which has complementary reactivity, onto these functional groups.

Wesslén and co-workers[50] have reported the preparation of amphiphilic graft copolymers by the trans-esterification of poly(2-ethylhexyl acrylate-*co*-methyl methacrylate) with poly(ethylene glycol) monomethyl ether, in a melt phase reaction. By blending the copolymer into PMMA, they observed changes in the surface energy relative to pure PMMA. Baskar and co-workers[51] have prepared amphiphilic graft terpolymers of octadecyl methacrylate, acrylic acid and poly(ethylene glycol) (PEG). The group grafted methoxy-terminated PEG chains (Mw = 5000 $gmol^{-1}$) onto an acrylic acid-*co*-octadecyl methacrylate copolymer *via* acid-catalysed transesterification reactions The polymers were water-soluble with an approximate octadecyl content of 27 mol%, and displayed surfactant properties.

Grafting onto has also been extensively used in polymer surface modification, where the surface is first exposed to an aggressive reagent which functionalises it, then the second polymer is introduced as surface grafts. Boyer and co-workers[52] have recently studied the effect of surface grafting of PMMA onto maleinated PP by reaction in the melt phase. They have found a 15-fold increase in adhesion of PP onto poly(vinylidene fluoride).

This technique could also be used to synthesise polymers of similar architecture to those made in the present work. Starting with a poly(alkyl acrylate) or poly(alkyl methacrylate) backbone as the trunk polymer, this could be trans-esterified in a post-polymerisation modification step with a polyethylene mono-alcohol.

#### 1.3.5.3 *Grafting 'through' via macromonomers.*

The polymers prepared in the present work were all made by grafting through[53]. This method uses polymerisable macromonomers and conventional techniques like free-radical or transition-metal catalysed coordination polymerisations can be applied

to produce grafted polymer architectures. The process has the advantage of providing grafts of equal length (provided that the macromonomer is itself monodisperse) although the frequency of graft points along the main polymer chain is controlled by the polymerisation method employed and the relative reactivity ratios of any co-monomers involved. Using a macromonomer alone furnishes well-defined comb structures, with regular spacing of graft points along the main chain according to the monomer structure (Figure 1.4).

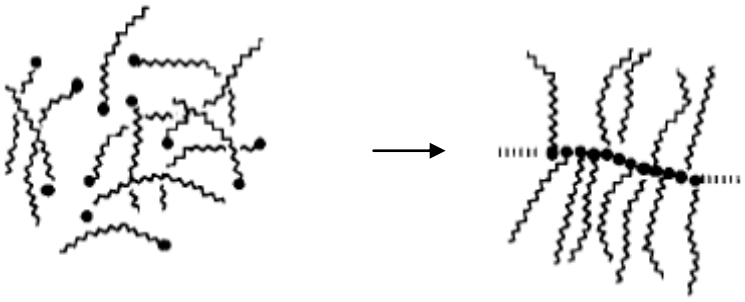

**Figure 1.4: The macromonomer technique; homopolymerisation to yield a comb copolymer.**

If a comonomer is employed, the physical properties of the resulting copolymer can be tuned to allow either the side-chain or the main-chain to dominate the molecular structure (Figure 1.5). This was found to be especially useful in the present work where the highly non-polar PE side chains began to dominate the copolymer properties if they were present at over ~20% by mass (see Section 3.5.7.3). The co-monomer can also be selected to control properties like the $T_g$ of the polymer.

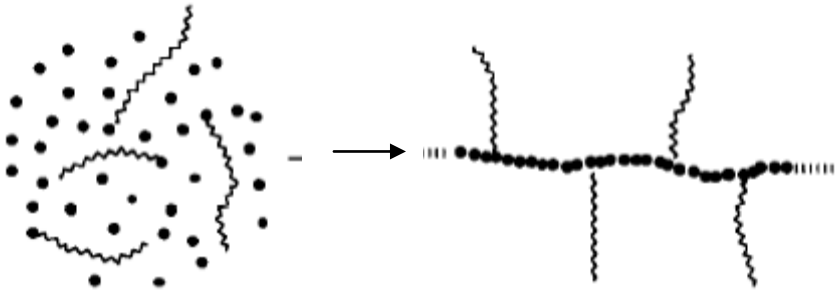

**Figure 1.5: The macromonomer technique; copolymerisation with a co-monomer to yield a graft copolymer.**

### 1.3.5.4 *Macromonomer synthesis.*

In the present work several new acrylate and methacrylate monomers were prepared by the esterification of an alcohol with acryloyl or methacryloyl chloride. This type of esterification between an acid chloride and an alcohol is an established and well-known reaction for preparing methacrylates and acrylates[54] (Scheme 1.14). Acryloyl or methacryloyl chloride can themselves be prepared by reacting methacrylic or acrylic acid with benzoyl chloride in the presence of hydroquinone to prevent polymerisation[55]. Although the acid chlorides used in this reaction are moisture-sensitive and tend to be toxic, lachrymatory and corrosive, they are readily available, inexpensive and usually provide relatively clean reactions with high yield. The presence of a base is essential to activate the reaction and to neutralise the acid by-product produced. If the acid generated is not neutralised it can catalyse hydrolysis of the ester and may add across the double bond of the methacrylate or acrylate. Stoichiometric amounts of base have to be used, with tertiary amines such as pyridine or inorganic bases like sodium bicarbonate being common choices. There are several alternative esterification reactions, each with their own associated advantages and disadvantages.

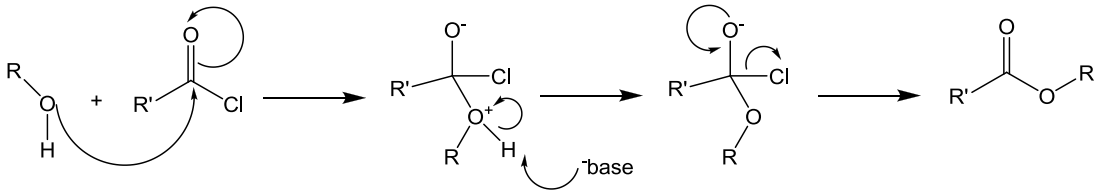


**Scheme 1.14: Esterification of an alcohol using an acyl chloride.**

A good alternative is to use the acid anhydride instead of the acid chloride, this follows a similar mechanism, but with acetate as the leaving group. Using the anhydride generally needs slightly more forcing conditions than if the corresponding acid chloride is used and is not very economical. At least two equivalents of the anhydride are required.

In the Fischer esterification, the starting materials are an alcohol and a carboxylic acid. The reaction is acid catalysed, is often heated quite strongly and water (which

is eliminated during the reaction) is often removed azeotropically using a Dean-Stark trap to drive the reaction to completion. The reaction is reversible and often results in mixtures. This type of esterification, using either methacrylic acid or acrylic acid has been used to prepare methacrylates or acrylates but inhibitors must be added to prevent polymerisation. Mineral acids can be used to catalyse the reaction although organic-soluble acids like para-toluene sulfonic acid (*p*-TSA) are generally preferred.

A more recent mild and effective esterification uses a stoichiometric amount of dicyclohexylcarbodiimide (DCC) and a catalytic amount of dimethylaminopyridine (DMAP) to couple the alcohol and carboxylic acid directly[56] (Scheme 1.14).

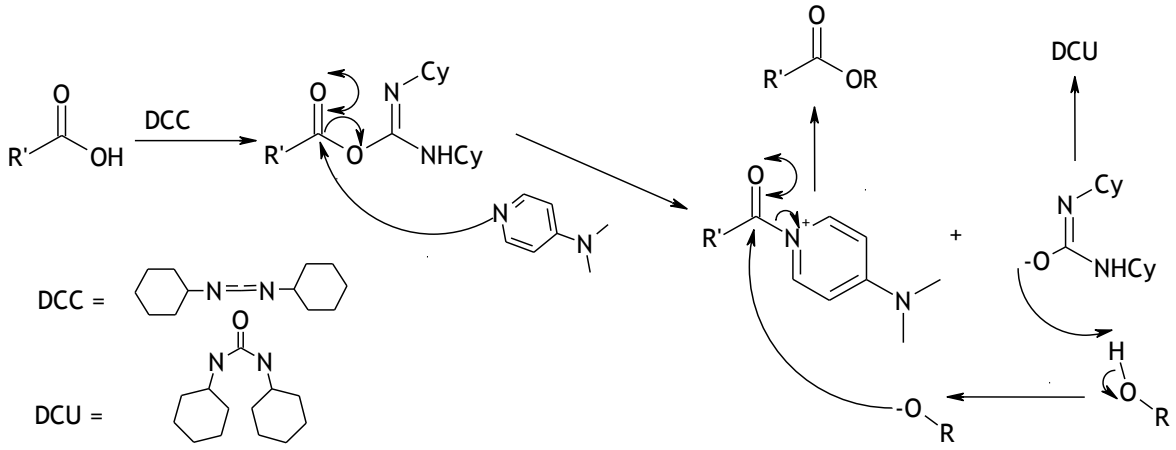


**Scheme 1.15: The DCC/DMAP coupling.**

This method is especially useful for acid sensitive substrates as it operates under mildly basic conditions and can give clean conversions with very high yields at room temperature. The reaction takes advantage of the high efficiency of DMAP as a nucleophilic catalyst. Although the so-called DCC/DMAP coupling is highly efficient the large quantities of DCC needed and the highly toxic nature of DMAP make it best suited only to small scale work where a high coupling efficiency is required. In addition a stoichiometric amount of dicyclohexylurea (DCU) is generated which can be difficult to separate from the product. In a recent study Yoda and co-workers[57] have used DCC/DMAP to prepare poly(**L**-lactic acid) in supercritical $CO_2$. The absence of water and acid prevented depolymerisation and hence the group reported high molecular weights for this type of polymer.

### 1.3.6 **Molecular weight**

Synthetic polymers usually have a distribution of chain lengths, which can be broad or narrow depending on the method used to prepare them. In order to obtain a single number for molar mass it is necessary to average over the distribution. There are several ways of defining the average which use different weighting factors. The most useful average molecular weights are:

Number average molecular weight $$\overline{M}_n = \frac{\sum N_i M_i}{\sum N_i}$$

**Equation 1.3**

Weight average molecular weight $$\overline{M}_w = \frac{\sum N_i M_i^2}{\sum N_i M_i}$$

**Equation 1.4**

Centrifuge average molecular weight $$\overline{M}_z = \frac{\sum N_i M_i^3}{\sum N_i M_i^2}$$

**Equation 1.5**

where $N_i$ is the number of molecular species i of molar mass $M_i$.

The weight average gives greater weighting to higher molar mass species and is always larger than the number average (Figure 1.6). Since the $M_w$ is more representative of where the *mass* of polymer chains lie, rather than the *number* of polymer chains, the former is usually more pertinent to the physical properties of the polymer. The $M_z$ is derived from the sedimentation equilibrium.

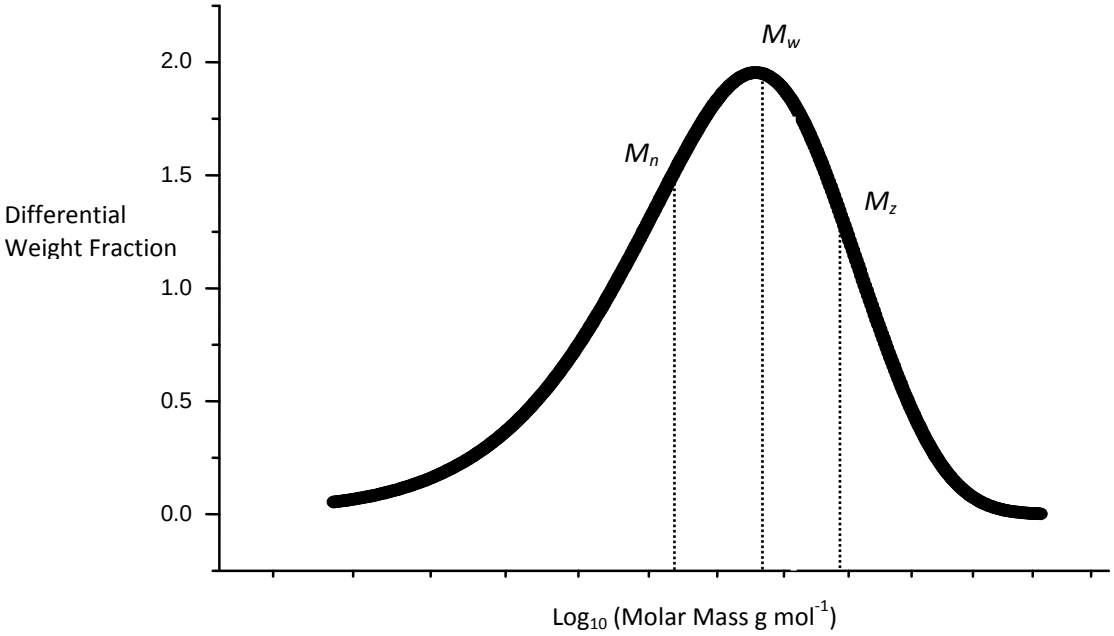


**Figure 1.6: A typical example of a molar mass distribution curve for a polymer prepared by free-radical polymerisation**

From the molar mass averages the polydispersity index *PDI* can also be calculated.

$$PDI = \frac{\overline{M}_w}{\overline{M}_n}$$

**Equation 1.6**

The *PDI* is a measure of the breadth of the molar mass distribution. For example, a hypothetical polymer with all chains of equal length will have *PDI* = 1. For polymers produced by conventional free radical polymerisation the *PDI* is typically in the range of 1.5-2.0. Controlled free-radical polymerisation methodologies such as ATRP or RAFT can achieve polydispersity indices close to 1.

There are numerous means of determining the molar mass of a polymer and these can be divided into relative and absolute methods. Relative methods include intrinsic viscosity measurements and size exclusion chromatography (SEC) calibrated with standard samples. Absolute methods include: membrane osmometry and centrifugal analysis which are accurate but nowadays are not convenient and routine methods, or SEC with multi-angle light scattering detection (SEC-MALLS). SEC-MALLS is

convenient, rapid and was used in the present work to determine the molecular weights of those polymers that were soluble in THF.

### 1.3.7 **Molecular weight determination**

#### 1.3.7.1 ***Intrinsic viscosity measurements***

The viscosity of a polymer solution is closely related to the molar mass and architecture of the polymer molecules. Relative molecular weight can be calculated from the viscosity of a dilute polymer solution. This works on the principle that larger polymer molecules increase the solution viscosity relative to smaller ones for the same concentration. The intrinsic viscosity [$\eta$] is defined as the limiting value of the ratio of specific viscosity $\eta_{sp}$ (Equation 1.7).

$$\eta_{sp} = \frac{\eta - \eta_0}{\eta_0} = \frac{t - t_0}{t_0}$$

**Equation 1.7**

where $\eta$ and $\eta_0$ are the viscosities of the solvent and the solution respectively, which can be substituted directly with the time taken for the pure solvent ($t_0$) and the polymer solution ($t$) to flow through a capillary. As the concentration $c$ tends towards zero, the intrinsic viscosity is reached as shown by the equation below (Equation 1.8).

$$[\eta] = \lim\left(\frac{\eta - \eta_0}{\eta_0 c}\right) = \lim\left(\frac{\eta_{sp}}{c}\right) \quad \text{as } c \to 0$$

**Equation 1.8**

The intrinsic viscosity of a polymer can be measured by using dilute solution viscometry. This method uses a capillary viscometer (Ubbelohde or Ostwald) which comprises a capillary of uniform diameter over a reservoir of the solution being measured. A second reservoir above the capillary is filled by applying a vacuum and then a measured volume of the solution is allowed to flow through the capillary

under gravity. The time taken for this volume to flow through the capillary is measured with a stopwatch and typically multiple replicate measurements are made. The solvent is first measured to provide a value for $\eta_{0,}$ in fact the time can be directly substituted into the equation for specific viscosity. A polymer solution is then made up such that the time taken to flow through the capillary is at least twice that for the pure solvent (typically 2 wt%). This solution is then diluted and measured several times to provide enough data such that the plot of $\eta_{sp}$ /c vs. 1/c gives a straight line. The plot is extrapolated to c = 0 to give a value for [$\eta$]. If this technique is performed well the data obtained can be very accurate but it is time-consuming and tedious. Since viscosity varies considerably with temperature, this is kept constant using a thermostatic bath. Dust, debris or insoluble polymer can also cause serious measurement errors to occur if they are present in the solution; typically the polymer solution is filtered prior to measurement.

Once the intrinsic viscosity of a polymer [$\eta$] has been measured by dilute solution viscometry, the Mark-Houwink-Sakurada equation (MHS) can be used to calculate the relative viscosity average molecular weight (Equation 1.9).

$$[\eta] = K' M_v^a$$

**Equation 1.9**

where *K'* and *a* are the MHS constants and $M_v$ is the viscosity average molecular weight. This relation applies over a wide range of molar masses above a threshold of around 10,000 $gmol^{-1}$. A specific set of MHS constants exists for every common homopolymer, solvent and temperature combination. However such data may not be available for specific copolymers.

#### 1.3.7.2 *Size Exclusion Chromatography*[58]

Size exclusion chromatography (SEC) or gel permeation chromatography (GPC) is a facile, rapid and routine technique used to determine polymer molecular weights and molecular weight distributions. Preparative SEC can be used to fractionate polymers according to their molecular weight. SEC separates polymer molecules on the basis of their hydrodynamic volume relative to the size of the pores in the chromatographic stationary phase. The chromatographic column(s) are packed with a non-adsorbing porous material, usually a crosslinked polystyrene polymer. A conventional HPLC instrument can be equipped with this type of column although the choice of detectors can differ for SEC. The choice of solvent depends upon the polymer being analysed, the polymer sample must be freely soluble to allow analysis.

When a polydisperse solution is applied to the column in the solvent flow, the smaller molecules can enter further into the porous structure of the stationary phase than the larger molecules and will be delayed for a longer time in the column than the larger molecules. The largest molecules are eluted first and small ones last (Figure 1.7).

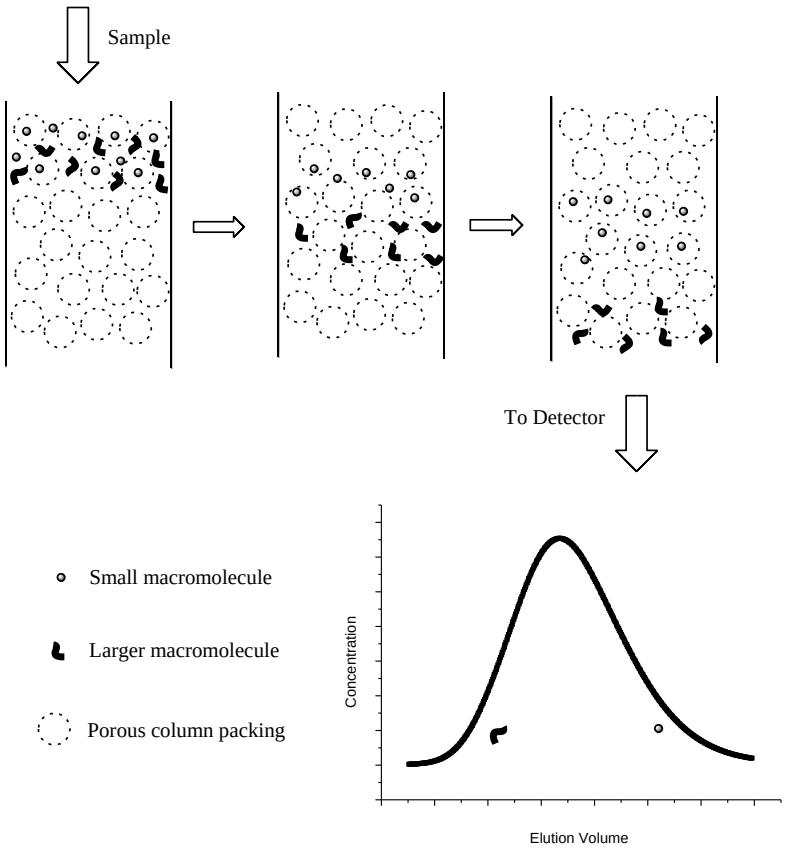


**Figure 1.7: A schematic representation of separation by size of polymer molecules in a SEC column**

Conventional or relative SEC uses narrow-polydispersity polymer standards of known molecular weight to provide a calibration curve for that polymer in that instrument. The retention time, measured using conventional liquid-chromatography detectors (e.g. refractive index and UV absorbance), can then be used to provide the molecular mass of an unknown sample. Whilst this technique is useful for linear polymer samples where a set of standards are available, it cannot be reliably applied to samples where branching, structural or chemical variations from the standards are present.

Two specialised detectors have been developed for specific application to SEC. The laser light scattering detector was first developed in the 1980s and has been steadily

improved with new electronics and computer data acquisition capabilities. The substitution of small, inexpensive diode lasers for the original bulky He-Ne gas lasers has greatly reduced the size and cost of laser light-scattering detectors. The development of the reference flow viscometer has provided similar size reduction, ease of use and cost advantages. The combination of these two detectors with a concentration detector (usually a differential refractive-index (DRI) detector) on a SEC instrument provides a means of quickly determining the absolute molecular weight of a sample, this combination is known as triple-detection SEC (TD-SEC).

Each detector in a TD-SEC system measures a different and complementary variable. The light scattering detector response is proportional to molecular size and concentration, likewise the viscometer detector response is proportional to the intrinsic viscosity and concentration of the polymer solution. As both of these detector responses are proportional to the concentration of the sample, the concentration is measured by a DRI.

#### 1.3.7.3 *The light scattering detector*

In order to quantify light scattering (LS) it is necessary to know the concentration of each eluting fraction as well as its differential refractive index increment (*dn/dc)*. For most types of homopolymers as well as many types of copolymers, the value of *dn/dc* will be constant over the entire range of masses measured. An off-line measurement of *dn/dc* from the bulk polymer solution is often sufficient to characterise the entire sample. A more complex strategy for copolymers is required since *dn/dc* may vary at each elution fraction. If the copolymer has homogeneous distributions of each monomer in the polymer for all fractions, then *dn/dc* will be constant over the entire size distribution and the off-line measurement of an average *dn/dc* will suffice. Where the copolymer is made from monomers where the *dn/dc* values of the individual homopolymers are nearly equal, an average *dn/dc* value can usually be used.

The *dn/dc* can be calculated accurately for chemically monodisperse fractions, if co-monomer weight fractions $w_i$ and homopolymer *dn/dc* values are known as described by the following equation (Equation 1.10).

$$\frac{dn}{dc} = \sum w_i (dn/dc)_i$$

**Equation 1.10**

A differential refractive index (DRI) detector is sufficient to measure (at low solute concentrations) the concentration change of an eluting fraction. This requires measurement of *dn/dc*, which is also a requirement for determining the light scattering constant $K^*$, defined as: (Equation 1.11)

$$K^* = \frac{4\pi^2 n_0^2 (dn/dc)^2}{\lambda_0^4 N_A}$$

**Equation 1.11**

where $N_A$ is the Avogadro constant, $n_0$ is the refractive index of the solvent and $\lambda_0$ the wavelength.

In a LS detector, the light scattered from a laser beam passing through the sample cell is measured at angles other than zero. The "excess" intensity of the scattered light at the angle $\Theta$ ($R(\Theta)$) is related to the weight-average of molar mass $M_w$ as expressed by the following (Equation 1.12)

$$\frac{K^* c}{R(\Theta)} = \frac{1}{M_W P(\Theta)} + 2A_2 c$$

**Equation 1.12**

where $c$ is the concentration of the polymer, $A_2$ is the second virial coefficient, and $P(\Theta)$ describes the scattered light angular dependence. In a plot of $K^* c / R(\Theta)$ *versus* $\sin^2(\Theta)$, $M_w$ can be obtained from the intercept and $R_g$ from the slope. In most cases, the injected concentration is small and $A_2$ can be neglected. Thus, if the optical properties ($n_0$ and *dn/dc* from equation 33) of the polymer solution are known, the molar mass at each elution volume increment can be determined as expressed by Equation 1.13.

$$M_{W,i} = \frac{R(\Theta)}{K^* P(\Theta)_i c_i}$$

**Equation 1.13**

If a low-angle LS instrument is used, $P(\Theta)$ is close to unity and $M_{w,i}$ can be calculated directly.

### 1.3.8 **NMR spectroscopy**

Nuclear magnetic resonance (NMR) spectroscopy is probably the most powerful method available for the molecular structural characterisation of organic compounds[59]. The technique is relatively new, first being used widely in the early 1960s. It uses the interaction of the magnetic moment of a nuclear spin with a static magnetic field, which is known as the Zeeman interaction. It follows that only nuclei with non-zero spins have an observable interaction, such as $^{1}H$ and $^{13}C$. The strength of this interaction is different for each of the chemically distinct nuclei, with each having a measurable chemical shift. The chemical shift of a nucleus is mainly influenced its immediate environment. Improvements like the addition of Fourier transforms and pulsed-sequence methods have greatly increased the power of the technique for structure elucidation.

When applied to polymers NMR spectroscopy can be used to not only identify the composition, but also information on the sequence distribution and molar mass can often be obtained. Information about the presence of or degree of branching and stereochemical configuration can sometimes also be gleaned, although the broadness of the peaks found in polymer spectra can make analysis problematic or impossible.

## 1.4 The influence of structure and morphology on properties

The morphology of a polymer is, to a large extent, governed by its molecular structure i.e. the monomer(s) used, their relative bulk and the polymerisation method used. Linear polymers with side groups that can pack effectively (e.g. HDPE, isotactic PS and syndiotactic PP) tend to be highly crystalline, whereas polymers with bulky side groups (e.g. PMMA, PMA) tend to be amorphous. If the polymerisation method used introduces branching to the molecular structure, then the degree of crystallinity will be less than for a linear method (e.g. LDPE vs. HDPE). Below a threshold value of ~20,000 $gmol^{-1}$, the $M_w$ also affects morphology and hence the mechanical and thermal properties.

### 1.4.1 Crystalline or semi-crystalline polymers

The molecular structure of some polymers can allow segments of them to close pack, forming crystalline domains. Intramolecular (and intermolecular) interactions such as van der Waals forces or hydrogen bonding are the driving force behind the crystallisation of a polymer. Where such interactions exist, polymer chains and/or pendent groups arrange themselves into the most favourable, lowest energy close-packed state. Since these interactions exist in the polymer melt at close to the crystallisation temperature, a degree self-organisation of these mesogenic segments will already be present. Although it is impossible in practice to make a 100% crystalline polymer due to the unavoidable presence of defects such as branching and a distribution of different chain lengths, some materials in practice come very close to this figure, with HDPE and PP being good examples. The crystalline domains exist as densely packed spherulites, separated by smaller amorphous regions. Having a large amount of crystallinity increases the elastic modulus of a polymer, and although this is desirable for some applications, this also makes the material prone to brittle failure. Therefore it is often desirable to curtail the modulus by decreasing the degree of crystallinity to make the material less brittle, sacrificing some of the hardness. A good example of this is the copolymerisation of ethylene with small amounts of longer-chain α-olefins such as hex-1-ene, to produce so-called linear low density polyethylene (LLDPE). The presence of short side chains disrupts the close

packing of the PE chains and reduces the crystallinity relative to HDPE. By altering the molar ratio of the two co-monomers, or indeed the chain length of the comonomer, the material properties can be tailored according to the desired application.

### 1.4.2 **Amorphous polymers**

Many polymers, such as PMMA, have no crystalline content and therefore present no long-range order but are nonetheless equally important materials. For polymers which show no crystallinity and for the portions of semi-crystalline polymers that are not crystalline, a phenomenon known as the glass transition is observed. The glass transition is a second-order phase transition as it involves a change in the heat capacity of a material with temperature. The glass transition temperature ($T_g$) of a polymer is the temperature above which it becomes rubbery (below its $T_g$ the polymer is glass-like) and is associated with changes in the free-volume of the polymer and hence the modulus. The modulus of a polymer decreases markedly at its $T_g$; this effect can be observed and quantified by using dynamic mechanical thermal analysis (DMTA). Melting ($T_m$) and crystallisation ($T_c$) transitions are first-order as they involve changes in the latent heat of the sample and are often not observed for polymers with low crystallinity.

### 1.4.3 **Characterising Polymer Morphology**

#### 1.4.3.1 ***Differential scanning calorimetry***

Crystallinity can be measured by using wide angle X-ray scattering (WAXS) or, more routinely, by thermal methods such as differential scanning calorimetry (DSC). DSC allows the thermal phase transitions of a material to be accurately characterised. With polymeric samples it can allow the observation of the glass transition ($T_g$), melting ($T_m$) and crystallisation ($T_c$) temperatures and energy changes. By measuring the change in heat capacity with temperature of a known mass of sample, the instrument can supply information on the nature and size of the phase transition. With thermal analysis methods, polymer samples with crystalline content will display well-defined crystallisation and melting transitions with the energy

associated with these being proportional to the degree of crystallinity present. The degree of crystallinity observed in a polymer sample is often governed by its thermal history; if it has been quench-cooled from the melt the amount of crystallinity will be much lower than if it were annealed and allowed to crystallise. Similarly in DSC experiments, the heating rate can influence the results as recrystallisation will be competing with melting as the sample is heated. Therefore measurement of the degree of crystallinity is often subject to the sample preparation method and the measurement technique.

#### 1.4.3.2 *Transmission electron microscopy*

The morphology of a polymer sample can also be investigated by transmission electron microscopy[60] (TEM). In a conventional transmission electron microscope a beam of electrons illuminate the specimen in an analogous way to a light microscope. The specimen must be thin enough to allow some of the electrons to pass through and features of the specimen which scatter electrons are seen as dark regions by the detector, usually a charge capture device (CCD) or photographic film. Since electrons have a much shorter wavelength than light a higher resolution can be achieved, but the microscope must be operated in a vacuum since air scatters electrons. Most polymers only scatter electrons weakly unless they contain atoms with high atomic numbers therefore methods have been developed to stain them using heavy atoms. In the case of block copolymers or polymer blends, these can be chosen to selectively stain one component allowing the morphology to be observed, in addition the crystalline and amorphous domains of a homopolymer can sometimes stain to different degrees providing contrast.

## 1.5 **Adhesion**[61]

A basic definition for an adhesive is a material which when applied to the surfaces of materials can join them together and resist separation[62]. Adhesive formulations contain polymers, and/or monomers that can be polymerised ('cured') once the substrate surfaces have been brought together. The most basic, essential properties of an adhesive are that it wets the substrate surfaces and provides a cohesively strong solid. There are six theories of adhesion; physical adsorption, chemical, diffusion, electrostatic, mechanical (interlocking) and the theory of weak boundary layers. Of these, physical adsorption will always make a contribution to adhesion as it is generated when molecules are in intimate contact. Electrostatic theory can only be applied to electrical conductors so does not usually apply to the treatment of polymeric adhesives (for example, it is useful in the treatment of the adhesion of two metals).

#### Physical adsorption

Although physical adsorption is usually the weakest force in an adhesive joint, its contribution is nonetheless significant and frequently important. At the adhesive-substrate interface molecules of the adhesive and substrate are close enough together for van der Waals forces to hold them together. Van der Waals forces cover three different types of interaction; permanent dipole-permanent dipole (4-20 $kJmol^{-1}$), permanent dipole-induced dipole (<2 $kJmol^{-1}$) and instantaneous dipole-induced dipole (dispersion forces) (0.08-40 $kJmol^{-1}$). The potential energy of van der Waals forces are inversely proportional to the $6^{th}$ power of the distance of separation and so it follows that the adhesion force will only be experienced by the topmost surface layers of adhesive and substrate.

#### Chemical bonding

Where covalent (60-700 $kJmol^{-1}$), ionic (600-1100 $kJmol^{-1}$) or hydrogen bonds (10-25 $kJmol^{-1}$) are made across the adhesive-substrate interface, the chemical bonding theory of adhesion can be applied. The presence of these types of bonds can make the adhesive joint very much stronger, although functional groups will need to be

present or created on the substrate surface. Some adhesive formulations can achieve covalent bonds by incorporating reagents that react with the substrate surface (for an example see the patent in from Kneafsey *et al.*[37] described in Section 1.1.2.3). Hydrogen bonding is important for many adhesives, for example poly(vinyl alcohol) is excellent for bonding wood or paper.

#### Diffusion

Where polymers come into contact across an interface, there is the possibility that they can diffuse into each other, particularly if they are of the same type or are compatible. Flory and co-workers have shown that for incompatible, high molecular weight species interdigitation of even the chain ends is highly unlikely[63]. For interdiffusion to occur both polymers need to be above their $T_g$, when the chains have sufficient mobility to move across the interface. This can be achieved by heating the joint or by using a solvent to plasticise the polymer. The reptation model for polymer chain motion predicts that this type of diffusion exists for alike polymers above their $T_g$[64].

#### Mechanical interlocking

Since most adhesives are liquids when applied, they are able to flow into voids and unevenness on the substrate surface before hardening. Often the presence of surface irregularity or porosity will improve the strength of a joint as the surface area of the interface is greater than for a smooth surface, but in addition the adhesive is mechanically locked together with the substrate. A good example of this is in dentistry where the decayed tooth is drilled to provide an undercut, 'inkwell'-type hole which is then filled (increasingly using UV-cured PMMA rather than Hg-based amalgam). Since the largest part of the filling is bigger than the hole in the tooth, it is now mechanically held.

#### Weak boundary layers

A weak boundary layer is a surface layer which is cohesively weak. It could be a contaminant like oil or grease, or a feature of the material such as oligomers or plasticisers at a polymer surface or a weakly-coherent oxide at a metal surface. If a

weak boundary layer exists between adhesive and substrate then the overall strength of the joint may be compromised. Therefore surface preparation which removes contamination can help to improve adhesive performance.

### 1.5.1 **Adhesion testing[62].**

In order to quantify the strength of an adhesive, different types of test have been developed. The simplest type of test to implement is the lap-shear test (Figure 1.8). In this type of test two substrates (the adherands) are glued together in a lap joint with a specified overlap.

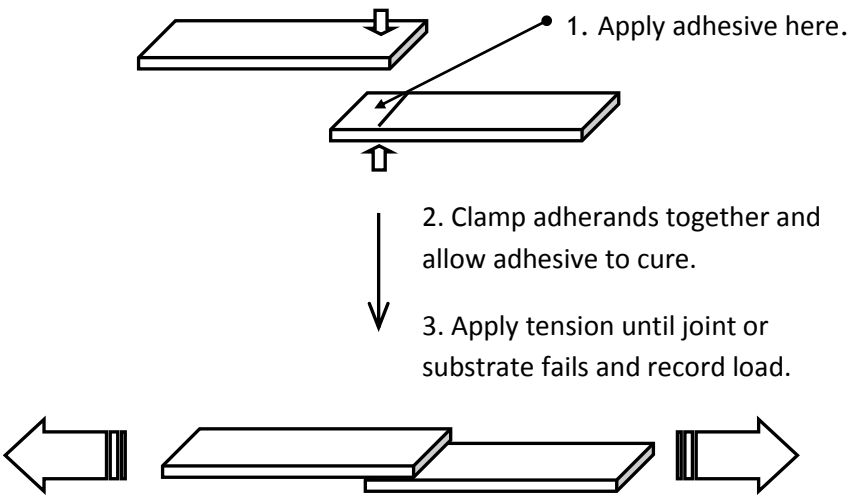


.

**Figure 1.8: The simple lap-shear adhesive strength test.**

The bonded adherands are then pulled apart using a tensile testing instrument fitted with a load cell of an appropriate capacity. The simple lap-shear test at first glance appears to be an accurate representation of the type of real-life situation that many adhesives will be encountered in. This is not the case as the test creates a complex stress situation. The shear strength and modulus of the substrates can also impinge on the test results.

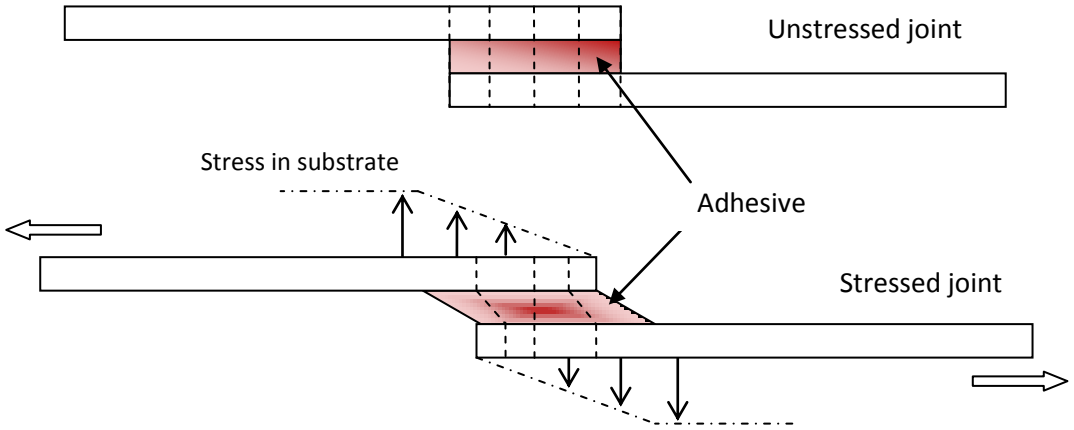


**Figure 1.9: Distortion under stress of a single lap joint showing the stresses generated in the joint during tensile testing[65]. The dotted lines represent stress in the sample (Not to scale).**

**Figure 1.10: Side-on view of a lap-shear joint under stress.**

Research by Tsai and co-workers[66] has shown that this method does not test the true lap-shear yield stress of an adhesive. During the test the adhesive joint becomes misaligned in such a way that it bends under load, creating a complex stress situation which was initially modelled by Volkersen[65] (Figure 1.9) who ignored the contribution of substrate distortion (Figure 1.10). In the present work this effect could be clearly seen during tensile testing (Figure 1.11), indeed the two different substrates lead to an additional imbalance in the stress between them as they distort to different extents.

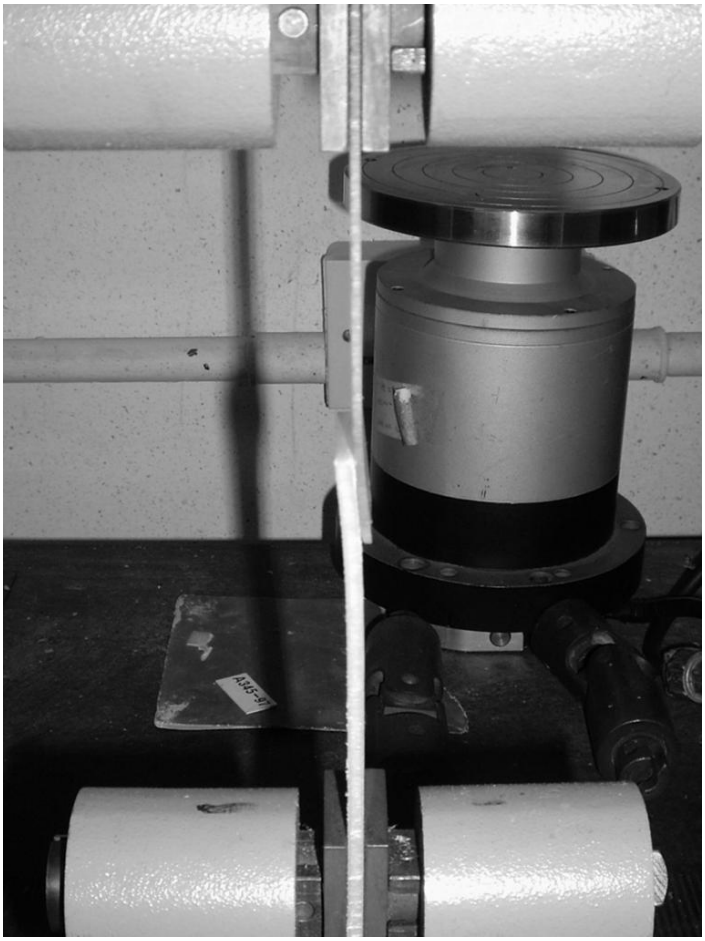

**Figure 1.11: A photograph of an ASTM-specification adhesion test piece fitted to the Instron materials testing apparatus under a load of ~0.4 KN showing the bending of the adherands.**

The results of this type of test depend upon a number of factors, namely joint characteristics, geometry and surface preparation. If these are kept constant however the results of different tests can be compared to one another. Examples of specifications for this type of test include the ASTM D1002-05[67] (Figure 1.12), which was used in the present work with the modification for plastic adherands ASTM D3163-1[68], or the ISO 4587:2003[69].

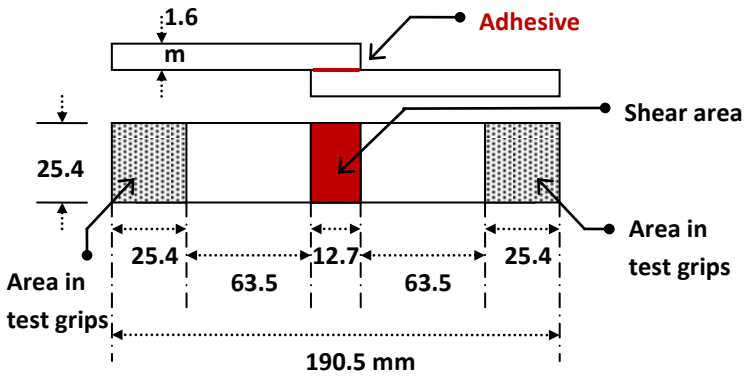


**Figure 1.12: The dimensions of an ASTM D1002 test specimen[63]. Measurements are in mm.**

More realistic measures of true adhesive strength require more complex test arrangements and/or sample preparations that minimise the contribution of adherand strength and modulus, while keeping the stress in a shear direction. Some test method designs include the so-called thick adherand tests ISO 11003-2 (Figure 1.13) and ASTM 3983. The adhesion test pieces are made by constructing a sandwich laminate of adherand-adhesive-adherand, which is subsequently milled to remove parts of the adherand, and then cut into the individual test pieces. This approach provides more control over the adhesive layer, giving greater consistency between individual test specimens. Using thicker adherands also minimises the contribution to the stress-strain curve from adherand bending and stretching. To minimise the effect further, extensometers can also be placed in line with the adhesive bond to measure extension of the adhesive rather than the whole test piece. The stresses generated at the adhesive bond are still complex like the simple test so results from this method are not perfect, however it is still relatively easy to perform.

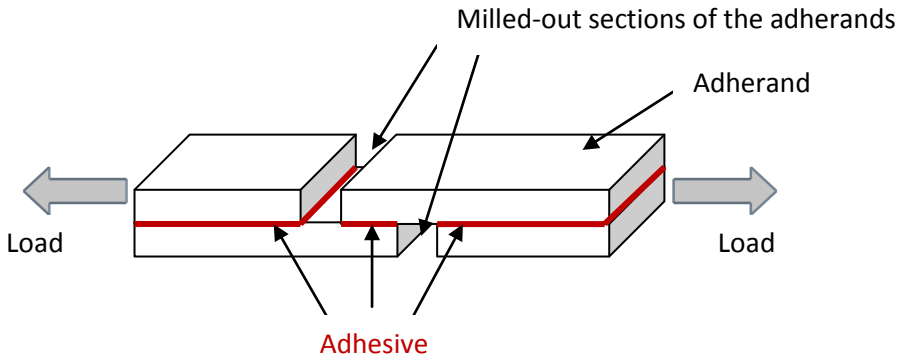


**Figure 1.13: The thick adherand test, ISO 4587:2003[65].**

The shear butt-joint torsion test gives a true representation of the shear stress of an adhesive, but test specimens are difficult to fabricate. The method uses two thin-walled cylinders of the same diameter which must be bonded together in perfect alignment (Figure 1.14). One cylinder is anchored and the other is subjected to a torsional load. The torsional stress and the resulting rotation are measured. The main problem with employing this method is in the complexity of the required equipment, which is the apparatus used to generate the torsion and the means of measuring the rotation. Standards exist for this method and they include the ISO 11003-1.

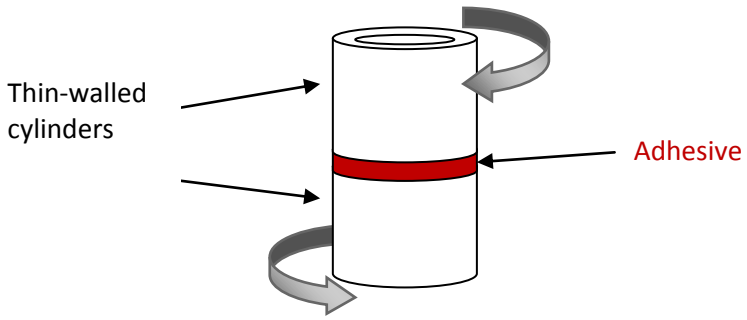


**Figure 1.14: The shear butt joint torsion test.**

## 1.6 **Objectives of the proposed study.**

The present work was essentially to be a continuation and expansion of a small project which was undertaken by the author as part of the requirements for a Masters degree[70]. The ultimate target of the latter, and that of the present work, was to find a cost-effective method of forming strong 'sandwiches' of PMMA and PP or PE films. The target end-use of such a laminated structure was to be as a replacement material for poly(vinyl chloride) (PVC) in the manufacture of window frames, which would have an outer barrier layer of filled PMMA to improve the weather resistance of the material. Polypropylene possesses the required mechanical properties to use for such an application, however it does not weather well compared to PVC, being more susceptible to degradation in the presence of sunlight in particular. PVC on the other hand is currently used to make a wide range of structural materials such as window frames and exterior cladding due to its excellent properties but it does have a serious drawback in that it is very difficult to either recycle (when heated it tends to degrade rather than melt) or to dispose of (when incinerated PVC has been shown to give off highly toxic benzo-*p*-dioxins and polychlorinated dibenzofurans, therefore a very efficient afterburner and scrubber system are needed in the incinerator flue[71]). It also seems likely that concerns over the manufacture and use of PVC due to these by-products will lead to restrictions on its use. This has led to a renewed interest in alternative polymeric materials such as those described in the present work as well as more traditional materials such as wood.

In order to find adhesive materials for a PMMA-PP laminate, polymers potentially giving good adhesion between films of PMMA and LDPE were to be synthesised, characterised and evaluated. Poly(methyl acrylate)-*graft*-polyethylene acrylate copolymers were thought to be good targets and materials with a range of mass ratios were to be examined as optimal 'adhesion compatibilisers' All graft copolymers were to be prepared during the project using a "grafting through method" and the PE macromonomers were to be prepared by esterification of commercially available polyethylene alcohols and docosanol with methacryloyl and acryloyl chloride. The molecular structures of the macromonomers and copolymers were to be characterised by $^{1}$H NMR spectroscopy and SEC, and the thermal properties by DSC.

It was planned to evaluate graft copolymers for adhesive effectiveness by melt-pressing them between thin films of PMMA and either LDPE or HDPE. The adhesive sandwich was then to be annealed at a temperature above that at which the copolymer melted. Once cold the film sandwich was to be pulled apart manually to test the efficacy of the copolymer as an adhesive (in practice this 'in-house' test was found to be very limited and an Instron-based ASTM test was also applied.

In order to provide some mechanistic insight into the observed adhesion behaviour it was anticipated that an extensive portfolio of physical-chemical characterisation procedures might be required, as indeed proved to be so.

## 1.7 References


(1) McCoy, M.; Reisch, M. S.; Tullo, A. H.; Tremblay, J.-F.; Voith, M. *Chem Eng News* **2009**, *87*, 51.

(2) (a) Friedrich, M. E. P.; Marvel, C. S. *J Am Chem Soc* **1930**, *52*(b) Fawcett, E. W.; Gibson, R. O.; Perrin, M. W.; Patton, J. G.; Williams, E. G.; GB471590, Ed., 1937.

(3) Perrin, M. W. *Transactions of the Faraday Society* **1939**, *35*.

(4) (a) Ziegler, K.; US2699457, Ed., 1955(b) Ziegler, K.; Holzkamp, E.; Breil, H.; Martin, H. *Angew Chem Int Edit* **1955**, *67*, 541.

(5) (a) Natta, G. *J Polym Sci* **1955**, *16*, 143(b) Natta, G.; Pino, P.; Corradini, P.; Danusso, F.; Mantica, E.; Mazzanti, G.; Moraglio, G. *J Am Chem Soc* **1955**, *77*, 1708.

(6) Arlman, E. J.; Cossee, P. *J Catal* **1964**, *3*, 99.

(7) Kaminsky, W. *Adv Catal* **2002**, *46*, 89.

(8) Yoshida, Y.; Matsui, S.; Fujita, T. *J Organomet Chem* **2005**, *690*, 4382.

(9) Grubbs, R. H. *Tetrahedron* **2004**, *60*, 7117.

(10) Batich, C.; Yahiaoui, A. *J Polym Sci Pol Chem* **1987**, *25*, 3479.

(11) Zhao, J. Q.; Geuskens, G. *Eur Polym J* **1999**, *35*, 2115.

(12) (a) Bandopadhay, D.; Panda, A. B.; Pramanik, P. *J Appl Polym Sci* **2001**, *82*, 406(b) Sun, C.; Zhang, D.; Wadsworth, L. C. *Adv Polym Tech* **1999**, *18*, 171.

(13) Park, S. J.; Jin, J. S. *J Colloid Interf Sci* **2001**, *236*, 155.

(14) Lei, J. X.; Liao, X. *Eur Polym J* **2001**, *37*, 771.

(15) Kharitonov, A. P.; Taege, R.; Ferrier, G.; Teplyakov, V.; Syrtsova, D. A.; Koops, G. H. *J Fluorine Chem* **2005**, *126*, 251.

(16) Kharitonov, A. P. *J Fluorine Chem* **2000**, *103*, 123.

(17) Boffa, L. S.; Novak, B. M. *Chem Rev* **2000**, *100*, 1479.

(18) Chung, T. C. *Prog Polym Sci* **2002**, *27*, 39.

(19) Chung, T. C.; Lee, S. H. *J Appl Polym Sci* **1997**, *64*, 567.

(20) Chung, T. C.; Lu, H. L.; Ding, R. D. *Macromolecules* **1997**, *30*, 1272.

(21) Chung, T. C.; Lu, H. L.; Li, C. L. *Polym Int* **1995**, *37*, 197.

(22) Xu, G. X.; Chung, T. C. *J Am Chem Soc* **1999**, *121*, 6763.

(23) Aaltonen, P.; Lofgren, B. *Macromolecules* **1995**, *28*, 5353.

(24) Paavola, S.; Uotila, R.; Lofgren, B.; Seppala, J. V. *React Funct Polym* **2004**, *61*, 53.

(25) Santos, J. M.; Ribeiro, M. R.; Portela, M. F.; Bordado, J. M. *Chem Eng Sci* **2001**, *56*, 4191.

(26) (a) Hustad, P. D. *Science* **2009**, *325*, 704(b) Kempe, R. *Chemistry - A European Journal* **2007**, *13*, 2764.

(27) Bergbreiter, D. E.; Blanton, J. R.; Chandran, R.; Hein, M. D.; Huang, K. J.; Treadwell, D. R.; Walker, S. A. *J Polym Sci Pol Chem* **1989**, *27*, 4205.

(28) Bergbreiter, D. E.; Srinivas, B. *Macromolecules* **1992**, *25*, 636.

(29) Endo, K.; Otsu, T. *Macromol Rapid Comm* **1994**, *15*, 233.

(30) (a) Britovsek, G. J. P.; Cohen, S. A.; Gibson, V. C.; Maddox, P. J.; Meurs, M. v. *Angewandte Chemie International Edition* **2002**, *41*, 489(b) Britovsek, G. J. P.; Cohen, S. A.; Gibson, V. C.; van Meurs, M. *J Am Chem Soc* **2004**, *126*, 10701.

(31) (a) Inoue, Y.; Matsugi, T.; Kashiwa, N.; Matyjaszewski, K. *Macromolecules* **2004**, *37*, 3651(b) Kaneyoshi, H.; Inoue, Y.; Matyjaszewski, K. *Macromolecules* **2005**, *38*, 5425.

(32) Kaneyoshi, H.; Matyjaszewski, K. *Journal of Applied Polymer Science* **2007**, *105*, 3.

(33) (a) Everaerts, A. I.; Nguyen, L. N.; Bharti, V.; Pearson, S. D. *Worldwide Patent Application* **2005**, 010117A1(b) Everaerts, A. I.; Nguyen, L. N. *Worldwide Patent Application* **2005**, 010118A1.

(34) Sugimoto, S.; Takashige, M. *United States Patent* **2005**, 6933338B2.

(35) Bisht, H. S.; Pande, P. P.; Chatterjee, A. K. *European Polymer Journal* **2002**, *38*, 2355.

(36) (a) Guiu, A.; Shanahan, M. E. R. *J Polym Sci Pol Phys* **2001**, *39*, 2843(b) Guiu, A.; Shanahan, M. E. R. *Int J Adhes Adhes* **2002**, *22*, 415.

(37) Kneafsey, B. J.; G. Coughlan, U. p., 2004/ (2004) *United States Patent* **2004**, *0010099*.

(38) Neher, H. T. *Ind Eng Chem* **1936**, *28*, 267.

(39) Smolders, K.; Baeyens, J. *Waste Management* **2004**, *24*, 849.

(40) Cowie, J. M. G. *Polymers : chemistry and physics of modern materials*; 2nd ed.; Blackie: Glasgow, 1991.

(41) (a) O'Brien, N.; McKee, A.; Sherrington, D. C.; Slark, A. T.; Titterton, A. *Polymer* **2000**, *41*, 6027(b) Isaure, F.; Cormack, P. A. G.; Graham, S.; Sherrington, D. C.; Armes, S. P.; Butun, V. *Chem Commun* **2004**, 1138(c) Isaure, F.; Cormack, P. A. G.; Sherrington, D. C. *Macromolecules* **2004**, *37*, 2096.

(42) Staudinger, H. *Nobel lectures including presentation speeches and laureates' biographies Chemistry 1942-1962*; Elsevier publishing company, 1964.

(43) Dostal, H.; Mark, H. *Transactions of the Faraday Society* **1936**, *32*, 0054.

(44) Brandrup, J.; Immergut, E. H. *Polymer handbook*; 3rd ed.; Wiley: New York, 1989.

(45) Mayo, F. R. *J Am Chem Soc* **1943**, *65*, 2324.

(46) Kamigaito, M.; Ando, T.; Sawamoto, M. *Chem Rev* **2001**, *101*, 3689.

(47) (a) Wang, J. S.; Matyjaszewski, K. *J Am Chem Soc* **1995**, *117*, 5614(b) Matyjaszewski, K.; Xia, J. *Chem Rev* **2001**, *101*, 2921.

(48) (a) Moad, G.; Rizzardo, E.; Thang, S. H. *Aust J Chem* **2005**, *58*, 379(b) Moad, G.; Rizzardo, E.; Thang, S. H. *Aust J Chem* **2006**, *59*, 669.

(49) Hawker, C. J. *Accounts Chem Res* **1997**, *30*, 373.

(50) Zhu, L. M.; Gunnarsson, O.; Wesslen, B. *J Polym Sci Pol Chem* **1995**, *33*, 1257.

(51) Gaspar, L. J. M.; Baskar, G.; Mandal, A. B. *Chem Phys Lett* **2001**, *348*, 395.

(52) Boyer, C.; Boutevin, B.; Robin, J. J. *Polym Degrad Stabil* **2005**, *90*, 326.

(53) Ito, K. *Prog Polym Sci* **1998**, *23*, 581.

(54) Burtle, J. G.; Turek, W. N. *J Org Chem* **1954**, *19*, 1567.

(55) Stempel, G. H.; Cross, R. P.; Mariella, R. P. *J Am Chem Soc* **1950**.

(56) Neises, B.; Steglich, W. *Angewandte Chemie-International Edition in English* **1978**, *17*, 522.

(57) Yoda, S.; Bratton, D.; Howdle, S. M. *Polymer* **2004**, *45*, 7839.

(58) Munk, P. *Introduction to macromolecular science*; Wiley, 1989.

(59) Brandolini, A. J.; Hills, D. D. *NMR spectra of polymers and polymer additives*; Marcel Dekker: New York, 2000.

(60) Sawyer, L. C.; Grubb, D. T.; Meyers, G. F. *Polymer microscopy*; 3rd ed. / Gregory F. Meyers. ed.; Springer: New York ; London, 2008.

(61) Kinloch, A. J. *Adhesion and adhesives : science and technology*; Chapman and Hall: London, 1987.

(62) Comyn, J. *Adhesion science*; Royal Society of Chemistry, Information Services: Cambridge, 1997.

(63) Flory, P. J.; Eichinger, B. E.; Orwoll, R. A. *Macromolecules* **1968**, *1*, 287.

(64) de Gennes, P. G. *The Journal of Chemical Physics* **1971**, *55*, 572.

(65) Volkersen, O. *Luftfarhtforschung* **1938**, *15*, 41.

(66) (a) Tsai, M. Y.; Oplinger, D. W.; Morton, J. *Int J Solids Struct* **1998**, *35*, 1163(b) Tsai, M. Y.; Morton, J. *Mech Mater* **1995**, *20*, 183.

(67) D1005-05; ASTM International: West Conshohocken, PA, 2005.

(68) D3163-1; ASTM International: West Conshohocken, PA, 2001.

(69) ISO4587:2003; ISO: Geneva, 2003.

(70) MacDonald, I. I. *Unpublished results* **2006**.

(71) Mininni, G.; Sbrilli, A.; Maria Braguglia, C.; Guerriero, E.; Marani, D.; Rotatori, M. *Atmos Environ* **2007**, *41*, 8527.

# Chapter 2

Experimental

# 2 Experimental

## 2.1 Materials

| Substance | Supplier | Purity/grade | Purification |
|---|---|---|---|
| 1-docosanol | Aldrich | 97% | Used as supplied |
| 2-ethylhexyl acrylate | Aldrich | 98% | Passed through a plug of neutral alumina |
| 2-ethylhexyl methacrylate | Aldrich | 98% | Passed through a plug of neutral alumina |
| 2-hexadecyl icosanol | Sasol | 97% | Used as supplied |
| acryloyl chloride | Aldrich | 96% | Used as supplied |
| azobis(isobutyronitrile) | BDH | 97% | recrystallised from acetone |
| butyl methacrylate | Aldrich | 99% | Passed through a plug of neutral alumina |
| dimethylaminopyridine | Aldrich | 99% | Used as supplied |
| dodecyl methacrylate | Aldrich | 96% | Passed through a plug of neutral alumina |
| low-density polyethylene | BDH | | Used as supplied |
| Lowicryl HM20 Kit | Agar Scientific | | Used as per instructions |
| methacryloyl chloride | Aldrich | 97% | Used as supplied |
| methyl acrylate | Aldrich | 99% | Passed through a plug of neutral alumina |
| methyl methacrylate | Aldrich | 99% | Passed through a plug of neutral alumina |

| Substance | Supplier | Purity/grade | Purification |
|---|---|---|---|
| $NaHCO_3$ | BDH | 99% | Used as supplied |
| osmium tetroxide | Aldrich | 4% in $H_2O$ | Used as supplied |
| phosphorous tribromide | Aldrich | 99% | Used as supplied |
| polyethylene | Aldrich | Mn = 1,700 $gmol^{-1}$ | Used as supplied |
| polyethylene mono-alcohol (Mn = 700 $gmol^{-1}$) | Aldrich | 80-85% | Used as supplied |
| polyethylene mono-alcohol (Mn = 460 $gmol^{-1}$) | Aldrich | 80-85% | Used as supplied |
| retinoic acid (ATRA) | Aldrich | 98% | Used as supplied |
| ruthenium dioxide | Johnson Matthey | hydrated | Used as supplied |
| Silica gel for chromatography | VWR | *Prolabo* 40-63 μm | Used as supplied |
| sodium periodate | Aldrich | ≥99.0% | Used as supplied |
| triphenylphosphine | Aldrich | 99% | Used as supplied |

The solvents employed (methanol, ethanol, toluene, petroleum ether 40-60º and methylene chloride) were of standard laboratory reagent grade. Solvents used for synthesis were dried and de-oxygenated using a Pure-SolvMD system from Innovative Technology UK.

Polypropylene substrates for adhesion testing were cut from injection moulded plaques of ICI Propathene® GWM101. Poly(methyl methacrylate) substrates were cut from Lucite International Perspex® Cast sheet.

## 2.2 **Synthesis.**

### 2.2.1 **Synthesis of monomers**

#### 2.2.1.1 ***Preparation of polyethylene acrylate macromonomer PE700Ac.***

Polyethylene mono-alcohol $M_n$ = 700 $gmol^{-1}$ (20.00 g, 28.56 mmol), sodium bicarbonate (3.60 g, 42.84 mmol, 1.5 equivalents) and anhydrous toluene (200 mL) were charged to a dry three-necked round-bottomed flask under a nitrogen atmosphere. The slurry was heated to 80 ºC and stirred for 30 minutes to allow the alcohol to dissolve. Acryloyl chloride (3.88 g, 42.84 mmol, 1.50 equivalents) was added dropwise *via* a syringe. The reaction mixture was heated to reflux (115 ºC) and stirred under a nitrogen atmosphere for 24 h. The temperature was reduced to 85 ºC and the reaction mixture was filtered to remove insoluble material using a pre-heated funnel and precipitated directly into methanol (800 mL). The resulting white precipitate was filtered off, washed with further methanol (200 mL) on the filter paper and dried at 40 ºC *in vacuo* to a constant mass (20.80 g, 27.58 mmol, 97%). $^1$H NMR ($d_8$-toluene, DPX400, 80 ºC, 400 MHz): δ 6.22 (dd, 1H, $^2J$ = 2 Hz, $^3J$ = 17 Hz), 5.95 (dd, 1H, $^3J_{CIS}$ = 10 Hz, $^3J_{TRANS}$ = 17 Hz), 5.33, (dd, 1H, $^2J$ = 2 Hz, $^3J$ = 10 Hz), 4.03 (t, 2H, $^3J$ = 7 Hz), 1.28—1.41, (br, m, 142.6H -C$H_2$-), 0.88, (t, 5.76H -C$H_3$); FT-IR $\nu_{max}/cm^{-1}$ 3144-2685 (broad), 1728 (s, ester C=O), 1637, 1472, 1408, 1272, 1195, 1061, 983, 964, 810, 731, 719. Elemental Microanalysis: Calculated for $C_{51}H_{100}O_2$: C, 82.18; H, 13.52; O, 4.29 Found: C, 81.68; H, 13.61; O, 4.71. MP: 99-104 °C.

#### 2.2.1.2 ***Preparation of polyethylene acrylate macromonomer PE460Ac.***

**PE460Ac** was prepared using an analogous procedure to **PE700Ac** and the following quantities of reactants; PE460-OH (20.00 g, 61.2 mmol), $NaHCO_3$ (5.51 g, 65.44 mmol), anhydrous toluene (200 mL) and acryloyl chloride (5.89 g, 65.24 mmol). The title product was isolated as a white solid (19.00 g, 36.96 mmol, 85%). $^1$H NMR ($d_8$-toluene, DPX400, 80 ºC, 400 MHz): δ 6.22 (dd, 1H, $^2J$ = 2 Hz, $^3J$ = 17 Hz ), 5.96 (dd, 1H, $^3J_{CIS}$ = 10 Hz, $^3J_{TRANS}$ = 17 Hz), 5.32, (dd, 1H, $^2J$ = 2 Hz, $^3J$ = 10 Hz), 4.04 (t, 2H, $^3J$ = 7 Hz), 1.47 (quintet, 2.7H, $^3J$ = 7 Hz) 1.15—1.41, (m, 103H -C$H_2$-),

0.88, (t, 5.27H -C*H*$_3$); FT-IR $\nu_{max}$/cm$^{-1}$ 3100-2700 (broad), 1729 (s, ester C=O), 1636, 1473, 1463, 1408, 1295, 1272, 1195, 1063, 984, 966, 810, 730, 720. Elemental Microanalysis: Calculated for $C_{34}H_{66}O_2$: C, 80.56; H, 13.12; O, 6.31 Found: C, 80.52; H, 13.40; O, 6.08. MP: 82-89 °C.

#### 2.2.1.3 *Preparation of polyethylene methacrylate macromonomer PE700MAc*

**PE700MAc** was prepared using an analogous procedure to **PE700Ac** and the following quantities of reactants; PE700-OH (20.00 g, 28.56 mmol), $NaHCO_3$ (3.60 g, 42.48 mmol), anhydrous toluene (200 mL) and methacryloyl chloride (4.48 g, 42.48 mmol). The title product was isolated as a white solid (20.20 g, 26.30 mmol, 92%). $^1$H NMR ($d_8$-toluene, DPX400, 80 ºC, 400 MHz): δ 6.05 (d, 1H, $^2J$ = 2 Hz,), 5.23 (d, 1H, $^2J$ = 2 Hz), 4.04 (t, 2H, $^3J$ = 7 Hz) 1.84 (s, 3H) 1.10—1.71, (br, m, 204H -C*H*$_2$-), 0.87, (t, 6.15H -C*H*$_3$); FT-IR $\nu_{max}$/cm$^{-1}$ 2917-2849 (broad), 1721 (s, ester C=O), 1639, 1473, 1463, 1323, 1297, 1167, 939, 815, 730, 720. Elemental Microanalysis: Calculated for $C_{52}H_{102}O_2$: C, 82.25; H, 13.54; O, 4.21 Found: C, 82.39; H, 13.82; O, 3.79. MP: 98-103 °C.

#### 2.2.1.4 *Preparation of polyethylene methacrylate macromonomer PE460MAc*

**PE460MAc** was prepared using an analogous procedure to **PE700Ac** and the following quantities of reactants; PE460-OH (20.00 g, 43.44 mmol), $NaHCO_3$ (5.48 g, 65.16 mmol), anhydrous toluene (200 mL) and methacryloyl chloride (6.81 g, 65.16 mmol). The title product was isolated as a white solid (18.20 g, 34.47 mmol, 79%). $^1$H NMR ($d_8$-toluene, DPX400, 80 ºC, 400 MHz): δ 6.04 (d, 1H, $^2J$ = 2 Hz,), 5.23 (d, 1H, $^2J$ = 2 Hz), 4.04 (t, 2H, $^3J$ = 7 Hz) 1.83 (s, 3H) 1.10—1.62, (br, m, 131H -C*H*$_2$-), 0.87, (t, 5.8H -C*H*$_3$); FT-IR $\nu_{max}$/cm$^{-1}$ 2917-2856 (broad), 1721 (s, ester C=O), 1639, 1473, 1463, 1322, 1297, 1167, 939, 815, 730, 720. Elemental Microanalysis: Calculated for $C_{35}H_{68}O_2$: C, 80.70; H, 13.16; O, 6.14 Found: C, 81.48; H, 13.50; O, 5.02. MP: 81-87 °C.

### 2.2.1.5 *Preparation of 2-hexadecylicosyl acrylate monomer B36Ac.*

2-Hexadecyl icosanol (20.00 g, 38.3 mmol), sodium bicarbonate (3.67 g, 45.9 mmol, 1.20 equivalents), DMAP (94 mg, 0.77 mmol) and anhydrous toluene (200 mL) were charged to a dry three-necked round-bottomed flask under a nitrogen atmosphere. Acryloyl chloride (4.16 g, 45.96 mmol, 1.20 equivalents) was added dropwise *via* a syringe to the stirred mixture at room temperature. The reaction mixture was stirred under a nitrogen atmosphere for 24 h at room temperature. The reaction mixture was filtered to remove insoluble material. The filtrate was washed with saturated sodium bicarbonate solution (2 x 100 mL), water (2 x 100 mL), dried over sodium sulfate and concentrated under reduced pressure at room temperature to provide the crude product as an off-white waxy solid. The crude product was dissolved in DCM (100 mL) and passed through a short plug of silica, eluting with further DCM. The eluant was concentrated under reduced pressure and dried at 40 ºC *in vacuo* to a constant mass to provide the title compound as a white solid (16.18 g, 28.1 mmol, 73%). $^{1}$H NMR ($CDCl_3$, DRX500, 27 ºC, 500 MHz): δ 6.39 (dd, 1H, $^{2}J$ = 1.5 Hz, $^{3}J$ = 18 Hz), 6.13 (dd, 1H, $^{3}J_{CIS}$ = 10 Hz, $^{3}J_{TRANS}$ = 18 Hz), 5.80, (dd, 1H, $^{2}J$ = 1.5 Hz, $^{3}J$ = 10 Hz), 4.06 (d, 2H, -O-C$H_2$-CH, $^{3}J$ = 5 Hz), 1.67 (m, 1H, -C*H*-, $^{3}J$ = 5 Hz) 1.10—1.50, (m, 64H, -C$H_2$-), 0.88, (t, 6H, -C$H_3$). $^{13}$C NMR ($CDCl_3$, DRX500, 27 ºC, 500 MHz): δ 166.34, 130.18, 128.73, 67.36, 31.95, 31.31, 30.10, 29.95, 29.85, 29.82, 29.73, 29.61, 29.57, 29.42, 29.39, 26.72, 22.70, 14.09. FT-IR $\nu_{max}/cm^{-1}$ 2913-2854 (broad), 1728 (s, ester C=O), 1637, 1620, 1471, 1407, 1295, 1271, 1190, 1053, 984, 966, 810, 719. Elemental Microanalysis: Calculated for $C_{39}H_{76}O_2$: C, 81.18; H, 13.28; O, 5.55 Found: C, 81.84; H, 13.65; O, 4.51. MP: 36.5-37.5 °C.

### 2.2.1.6 *Preparation of docosyl acrylate monomer DocAc.*

Docosyl acrylate (**DocAc**) was prepared using an analogous procedure to **B36Ac** (Section 2.2.1.5) and the following quantities of reactants; 1-docosanol (20.01 g, 61.2 mmol), $NaHCO_3$ (6.17 g, 73.44 mmol), anhydrous toluene (150 mL), DMAP (150 mg, 1.22 mmol) and acryloyl chloride (6.65 g, 73.44 mmol). The title product was isolated as a white waxy solid (16.44 g, 43.26 mmol, 71%). $^{1}$H NMR ($CDCl_3$, DRX500, 27ºC, 500 MHz): δ 6.41 (dd, 1H, $^{2}J$ = 1.5 Hz, $^{3}J$ = 17 Hz), 6.11 (dd, 1H,

$^{3}J_{CIS}$ = 10 Hz, $^{3}J_{TRANS}$ = 17 Hz), 5.80, (dd, 1H, $^{2}J$ = 1.5 Hz, $^{3}J$ = 10 Hz), 4.15 (t, 2H, -O-C$H_2$-$CH_2$-, $^{3}J$ = 6.5 Hz), 1.67 (quintet, 2H, -O-$CH_2$-C$H_2$-, $^{3}J$ = 6.5 Hz) 1.20—1.39, (m, 38H, -C$H_2$-), 0.88, (t, 3H, -C$H_3$). $^{13}$C NMR ($CDCl_3$, DRX500, 27ºC, 500 MHz): δ 166.27, 130.29, 128.68, 64.69, 31.93, 29.83, 29.80, 29.77, 29.71, 29.67, 29.61, 29.58, 29.52, 29.37, 29.26, 28.63, 25.93, 22.69, 14.09. FT-IR $\nu_{max}/cm^{-1}$ 2954-2849 (broad), 1728 (s, ester C=O), 1637, 1620, 1470, 1407, 1378, 1295, 1271, 1189, 1053, 984, 966, 810, 720. Elemental Microanalysis: Calculated for $C_{25}H_{48}O_2$: C, 78.88; H, 12.71; O, 8.41 Found: C, 78.79; H, 12.73; O, 8.48 MP: 49.1-50.1 °C.

### 2.2.2 Synthesis of copolymers

#### 2.2.2.1 *Preparation of the poly(methyl acrylate)-graft-polyethylene copolymers, PE700Ac/MA, PE460Ac/MA and DocAc/MA.*

**Preparation of PE700Ac/MA 1:5.0.**

PE700 acrylate (**PE700Ac**) (2.00 g, 2.65 mmol) was charged into a dry two-necked round-bottomed flask equipped with a reflux condenser under a nitrogen atmosphere and fitted to a Radleys six-position carousel reactor (the other positions were typically fitted with parallel reactions of different compositions, see Table 2.1) The solid was then de- gassed by nitrogen/vacuum purge cycling (6 times). Anhydrous toluene (15 mL) and purified and de-gassed methyl acrylate (9.94 g, 115.56 mmol) were then added. The reaction mixture was heated to 80 ºC with magnetic stirring for 20 minutes to dissolve the macromonomer. Re-crystallised AIBN (388.2 mg, 2.36 mmol, 2 mol%) was added to the reaction mixture under a nitrogen purge, the side-port was sealed and the flask was heated (80 ºC) with stirring for 20 h under nitrogen. The hot solution was precipitated into stirred methanol (150 mL), the resulting sticky white solid was filtered off and washed with further methanol (50 mL) and dried at 40 ºC *in vacuo* to a constant mass (8.36 g, 70%). $^{1}$H NMR ($d_8$-toluene, 80 ºC, AV400, 400 MHz): δ 4.10 (b, 2H, –C$H_2$–O– of the PE700Ac macromonomer), 3.37 (b, 173H, C$H_3$–O– of MA), 2.59 (b, 54H, PMA backbone hydrogens) 2.31 (b, 6H) 1.62 (b, 31H) 1.84 (b, 60H) 1.32 (b, 165H PE side chain -C$H_2$-), 0.89 (b, 5H side chain and residual non-functional PE terminal –C$H_3$).

An analogous procedure was followed for all of the copolymers prepared and the relevant feed and analytical data are shown in Tables 2.1—2.3.

**Table 2.1: PE700Ac/MA copolymer data.**

| Sample Name | Mass ratio | Feed masses /g | | | $^1$H NMR* | | Recovery | | HT-SEC data / g mol$^{-1}$ | | |
|---|---|---|---|---|---|---|---|---|---|---|---|
| | PE:A | DocAc | MA | AIBN | Mass ratio | Residual monomer | g | % | $M_w$ | $M_n$ | PDI |
| **PE700Ac/MA 1:9.0** | 1:10.0 | 1.000 | 8.962 | 0.346 | 1:10.5 | 1% | 6.27 | 63 | 28,450 | 8,860 | 3.2 |
| **PE700Ac/MA 1:5.0** | 1:5.5 | 2.000 | 9.938 | 0.388 | 1:6.4 | 1% | 8.36 | 70 | 30,800 | 7,380 | 4.2 |
| **PE700Ac/MA 1:0.99** | 1:1.1 | 2.000 | 1.988 | 0.085 | 1:1.4 | 1% | 3.53 | 88 | 14,000 | 4,530 | 3.1 |
| **PE700Ac/MA 1:0.50** | 1:0.6 | 3.000 | 1.490 | 0.070 | 1:0.68 | 1% | 4.13 | 92 | 22,900 | 4,020 | 5.6 |
| **PE700Ac/MA 1:0.10** | 1:0.1 | 3.000 | 0.298 | 0.024 | 1:0.14 | 7% | 3.19 | 97 | 9,560 | 3,020 | 3.2 |
| **PE700Ac/MA 1:0.05** | 1:0.1 | 3.000 | 0.149 | 0.019 | 1:0.08 | 10% | 3.09 | 98 | } Not measured | | |
| **PE700Ac/MA comb** | comb | 3.000 | 0.000 | 0.013 | ~ | 16% | 2.96 | 99 | | | |

* The amount of residual monomer was calculated from the resonances of vinyl protons in the $^1$H NMR spectrum of the polymer. The composition ratio was derived from the relative areas of the resonances corresponding to the -C$H_2$-O- hydrogen atoms due to each different monomer residue in the $^1$H NMR spectrum of the polymer.

**Table 2.2: PE460Ac/MA copolymer data.**

| Sample Name | Mass ratio | Feed masses /g | | | $^1$H NMR* | | Recovery | | HT-SEC data / g mol$^{-1}$ | | |
|---|---|---|---|---|---|---|---|---|---|---|---|
| | PE:A | DocAc | MA | AIBN | Mass ratio | Residual monomer | g | % | $M_w$ | $M_n$ | PDI |
| **PE460Ac/MA 1:8.4** | 1:10.0 | 1.000 | 8.401 | 0.327 | 1:11.3 | 1% | 6.37 | 68 | 31,800 | 7,850 | 4.0 |
| **PE460Ac/MA 1:4.7** | 1:5.6 | 2.000 | 9.460 | 0.374 | 1:6.0 | 1% | 9.76 | 85 | 33,350 | 6,860 | 4.8 |
| **PE460Ac/MA 1:0.95** | 1:1.1 | 5.000 | 4.730 | 0.213 | 1:1.1 | 1% | 8.48 | 87 | 16,550 | 2,120 | 7.8 |
| **PE460Ac/MA 1:0.47** | 1:0.6 | 2.000 | 0.946 | 0.049 | 1:0.48 | 2% | 2.24 | 76 | 11,100 | 3,020 | 3.7 |
| **PE460Ac/MA 1:0.095** | 1:0.1 | 3.000 | 0.284 | 0.030 | 1:0.10 | 7% | 2.91 | 88 | 7,670 | 1,980 | 4.0 |
| **PE460Ac/MA 1:0.047** | 1:0.1 | 3.000 | 0.142 | 0.025 | 1:0.05 | 10% | 2.76 | 88 | } Not measured | | |
| **PE460Ac comb** | Comb | 3.000 | 0.000 | 0.019 | ~ | 10% | 2.87 | 96 | | | |

* The amount of residual monomer was calculated from the resonances of vinyl protons in the $^1$H NMR spectrum of the polymer. The composition ratio was derived from the relative areas of the resonances corresponding to the -C$H_2$-O- hydrogen atoms due to each different monomer residue in the $^1$H NMR spectrum of the polymer.

**Table 2.3: DocAc/MA copolymer data.**

| Sample Name | Mass ratio | Feed masses /g | | | $^1$H NMR* | | Recovery | | HT-SEC data / g mol$^{-1}$ | | |
|---|---|---|---|---|---|---|---|---|---|---|---|
| | PE:A | DocAc | MA | AIBN | Mass ratio | Residual monomer | g | % | $M_w$ | $M_n$ | PDI |
| **DocAc/MA 1:7.5** | 1:10.0 | 2.000 | 15.035 | 0.592 | 1:8.1 | 1% | 18.5 | † | 85,400 | 29,050 | 3.0 |
| **DocAc/MA 1:3.8** | 1:5.0 | 2.000 | 7.517 | 0.305 | 1:4.3 | 1% | 9.95 | † | 66,550 | 23,200 | 2.9 |
| **DocAc/MA 1:0.75** | 1:1.0 | 2.000 | 1.503 | 0.076 | 1:0.8 | 1% | 3.09 | 88 | 39,750 | 16,100 | 2.4 |
| **DocAc/MA 1:0.38** | 1:0.5 | 2.000 | 0.752 | 0.047 | 1:0.4 | 1% | 2.39 | 87 | 28,300 | 8,500 | 3.3 |
| **DocAc/MA 1:0.075** | 1:0.1 | 2.000 | 0.150 | 0.024 | 1:0.1 | 2% | 1.90 | 88 | 19,900 | 10,600 | 1.9 |

* The amount of residual monomer was calculated from the resonances of vinyl protons in the $^1$H NMR spectrum of the polymer. The composition ratio was derived from the relative areas of the resonances corresponding to the -C$H_2$-O- hydrogen atoms due to each different monomer residue in the $^1$H NMR spectrum of the polymer.

† The reaction solvent (toluene) proved impossible to remove completely from these materials.

### 2.2.2.2 *Preparation of poly(methyl methacrylate)-g-polyethylene methacrylate copolymers, PE700MAc/MMA and PE460MAc/MMA.*

These were prepared essentially as before (Section 2.2.2.1). **PE700MAc /MMA 1:4.5:** $^1$H NMR ($d_8$-toluene, 80 ºC, AV400, 400 MHz): δ 3.99 (t, 2H, –C*H*$_2$–O– of the **PE700MAc** macromonomer), 3.42 (b, 134H, C*H*$_3$–O– of the MMA), 2.07—1.95 (br, m, 72H, PMMA backbone methyl groups) 1.35—1.06 (bm, 291H PE and PMMA backbone methylene groups) 1.32 (b, 165H, PE side chain and residual non-functional PE -C*H*$_2$-), 0.88 (t, 5H PE side chain and residual non-functional PE terminal –C*H*$_3$). See Tables 2.4 and 2.5.

**Table 2.4: PE460MAc/MMA copolymer data[*].**

| Sample Name | mass ratio | Feed masses / g | | | Recovery | |
|---|---|---|---|---|---|---|
| | PE:MA | PE700MAc | MMA | AIBN | g | % |
| **PE460MAc/MMA 1:4.5** | 1:5.6 | 2.000 | 9.091 | 0.311 | 8.87 | 80.0 |
| **PE460MAc/MMA 1:0.76** | 1:1:1 | 3.000 | 2.273 | 0.108 | 5.17 | 90.2 |
| **PE460MAc/MMA 1:0.38** | 1:0.5 | 3.000 | 1.136 | 0.063 | 4.10 | 94.0 |
| **PE460MAc/MMA 1:0.091** | 1:0.1 | 3.000 | 0.273 | 0.028 | 3.13 | 95.6 |
| **PE460MAc/MMA 1:0.045** | 1:0.1 | 3.000 | 0.136 | 0.023 | 2.96 | 94.4 |
| **PE460MAc/MMA comb** | Comb | 3.000 | 0.000 | 0.019 | 2.92 | 97.5 |

[*] NMR spectra were not recorded for these polymers.

**Table 2.5: PE700MAc/MMA copolymer data.**

| Sample Name | Mass ratio | Feed masses /g | | | $^1$H NMR data* | | Recovery | |
|---|---|---|---|---|---|---|---|---|
| | PE:MA | PE700MAc | MMA | AIBN | Mass ratio | Res. Mon. | g | % |
| **PE700MAc/MMA 1:8.8** | 1:10.0 | 1.000 | 8.776 | 0.292 | 1:8.6 | 1% | 8.23 | 84 |
| **PE700MAc/MMA 1:4.4** | 1:5.0 | 2.000 | 8.757 | 0.296 | 1:6.0 | 1% | 9.45 | 88 |
| **PE700MAc/MMA 1:0.88** | 1:1.0 | 4.000 | 3.503 | 0.132 | 1:1.3 | 1% | 6.84 | 91 |
| **PE700MAc/MMA 1:0.44** | 1:0.5 | 5.000 | 2.189 | 0.093 | 1:0.6 | 1% | 6.86 | 95 |

* The amount of residual monomer was calculated from the resonances of vinyl protons in the $^1$H NMR spectrum of the polymer. The composition ratio was derived from the relative areas of the resonances corresponding to the -C$H_2$-O- hydrogen atoms due to each different monomer residue in the $^1$H NMR spectrum of the polymer.

### 2.2.2.3 *Preparation of PE700Ac/MMA and PE700MAc/MA copolymers*

These were prepared essentially as before (Section 2.2.2.1). The reactions were carried out in parallel in a Radleys 6-position carousel and the relevant feed and analytical data are shown in Table 2.6. $^{1}$H NMR spectrum of **PE700MAc/MA 1:4.4** ($d^{8}$-toluene, 80 ºC, AV400, 400 MHz): δ 4.10 (b, 2H, –C$H_2$–O– of the macromonomer), 3.37 (b, 173H, C$H_3$– O– of MA), 2.59 (b, 54H, PMA backbone hydrogens) 2.31 (b, 6H) 1.62 (b, 31H)1.84 (b, 60H) 1.32 (b, 165H PE chain methylene groups), 0.89 (b, 5H).

**Table 2.6: 'Crossed' PE700MAc/MA and PE700Ac/MMA copolymer data**

| Sample Name | Mass ratio | Feed masses | | | $^{1}$H NMR data* | Recovery | |
|---|---|---|---|---|---|---|---|
| | PE:MA | PE700(M)Ac / g | (M)MA / g | AIBN / mg | Residual monomer | mass / g | % |
| **PE700MAc/MA 1:8.8** | 1:10 | 0.500 | 4.379 | 169.3 | 1% | 4.73 | 94 |
| **PE700MAc/MA 1:4.4** | 1:5 | 1.000 | 4.379 | 171.5 | 1% | 5.40 | 97 |
| **PE700MAc/MA 1:0.9** | 1:1 | 1.000 | 0.876 | 37.7 | 2% | 1.29 | 67 |
| **PE700Ac/MMA 1:9.0** | 1:10 | 0.500 | 4.481 | 149.3 | 1% | 5.01 | 98 |
| **PE700Ac/MMA 1:4.5** | 1:5 | 1.00 | 4.481 | 151.5 | 2% | 5.56 | 99 |

* The amount of residual monomer was calculated from the resonances of vinyl protons in the $^{1}$H NMR spectrum of the polymer.

### 2.2.2.4 *Preparation of PE700Ac/EHMA copolymers.*

These were prepared essentially as before (Section 2.2.2.1) and the relevant data are shown in Table 2.7. **PE700Ac/EHMA 1:12.1**: $^1$H NMR ($d_8$-toluene, 80 ºC, AV400, 400 MHz): [δ 6.07, 5.24 (vinyl hydrogens of residual monomer)] δ 4.20—3.90 (b, 4H, –C$H_2$–O– of the **PE700Ac** overlapping with the –C$H_2$–O– of the EHMA) 2.45—2.15 (b, 3.4H), 1.80—1.20 (b, 28.1H), 1.20—0.79 (b, 11.7H).

**Table 2.7: PE700Ac/EHMA copolymer data.**

| Sample Name | Mass ratio | Feed masses /g | | | Residual monomer* | Recovery | | DSC |
|---|---|---|---|---|---|---|---|---|
| | PE:A | PE700Ac | EHMA | AIBN | % | g | % | $T_m$ / °C |
| **PE700Ac/EHMA 1:24.1** | 1:10 | 1.000 | 24.112 | 0.435 | 2 | 20.4 | 81 | 101.5 |
| **PE700Ac/EHMA 1:19.3** | 1:8 | 0.250 | 4.822 | 0.087 | 1 | 5.00 | 84 | † |
| **PE700Ac/EHMA 1:16.9** | 1:7 | 0.250 | 4.220 | 0.076 | 1 | 4.46 | 98 | ‡ |
| **PE700Ac/EHMA 1:14.5** | 1:6 | 0.500 | 7.234 | 0.131 | 1 | 7.24 | 92 | ‡ |
| **PE700Ac/EHMA 1:12.1** | 1:5 | 1.000 | 12.056 | 0.219 | 1 | 10.7 | 82 | 104.3 |
| **PE700Ac/EHMA 1:9.6** | 1:4 | 0.500 | 4.822 | 0.088 | 1 | 5.39 | 99 | ‡ |
| **PE700Ac/EHMA 1:7.2** | 1:3 | 0.500 | 3.617 | 0.067 | 1 | 4.11 | 98 | ‡ |
| **PE700Ac/EHMA 1:2.4** | 1:1 | 2.000 | 4.822 | 0.095 | 1 | 6.5 | 95 | 105.6‡ |
| **PE700Ac/EHMA 1:1.2** | 1:0.5 | 2.000 | 2.411 | 0.051 | 1 | 4.2 | 96 | 106.1‡ |

* The amount of residual monomer was calculated from the resonances of vinyl protons in the $^1$H NMR spectrum of the polymer.
† Not measured
‡ Two melt transitions are observed for these polymers consistent with a block or graft copolymer structure, the higher of the two transitions is given here.

### 2.2.2.5 *Preparation of PE700MAc/EHMA copolymers.*

These were prepared essentially as before (Section 2.2.2.1) and the relevant data are shown in Table 2.8. **PE700MAc/EHMA 1:12.1:** $^1$H NMR ($d_8$-toluene, 80 ºC, AV400, 400 MHz): [δ 6.26, 6.07 and 5.24 (vinyl hydrogens of residual monomer)] δ 4.20—3.90 (b, 4H –C$H_2$–O– of the PE700MAc overlapping with the –C$H_2$–O– of the EHMA) 2.40—2.10 (b, 3.8H), 1.80—1.20 (b, 28.4H), 1.20—0.79 (b, 11.5H).

**Table 2.8: PE700MAc/EHMA copolymer data.**

| Sample Name | Mass ratio | Feed masses /g | | | Residual monomer* | Recovery | |
|---|---|---|---|---|---|---|---|
| | PE:Ac | PE700MAc | EHMA | AIBN | % | g | % |
| **PE700MAc/EHMA 1:24.1** | 1:10 | 1.000 | 24.112 | 0.434 | 1 | 24.91 | 99 |
| **PE700MAc/EHMA 1:12.1** | 1:5 | 1.000 | 12.056 | 0.219 | 1 | 13.01 | 99 |
| **PE700MAc/EHMA 1:2.4** | 1:1 | 2.000 | 4.822 | 0.095 | 1 | 6.49 | 95 |
| **PE700MAc/EHMA 1:1.2** | 1:0.5 | 2.000 | 2.411 | 0.051 | 1 | 4.16 | 94 |

* The amount of residual monomer was calculated from the resonances of vinyl protons in the $^1$H NMR spectrum of the polymer.

### 2.2.2.6 *Preparation of PE700MAc/EHA copolymers.*

These were prepared essentially as before (Section 2.2.2.1). **PE700MAc/EHMA 1:12.1:** $^{1}$H NMR ($d_8$-toluene, 80ºC, AV400, 400 MHz): [δ 6.20, 6.00 and 5.35 (vinyl hydrogens of residual monomer)] δ 4.35—3.90 (b, 4.0H –C*H*$_2$–O– of the PE700Ac overlapping with the –C*H*$_2$–O– of the EHA), 2.42—2.19 (b, 1.6H), 1.82—1.17 (b, 28.4H), 1.16—0.78 (b, 11.5H). See data in Table 2.9

**Table 2.9: PE700MAc/EHA copolymer data.**

| Sample Name | Mass ratio | Feed masses /g | | | Recovery | |
|---|---|---|---|---|---|---|
| | PE:Ac | PE700MAc | EHA | AIBN | g | % |
| **PE700MAc/EHA 1:24.1** | 1:10 | 0.500 | 12.056 | 0.434 | 12.17 | 97 |
| **PE700MAc/EHA 1:12.1** | 1:5 | 0.500 | 6.028 | 0.219 | 6.12 | 94 |
| **PE700MAc/EHA 1:2.4** | 1:1 | 2.000 | 4.822 | 0.095 | 6.17 | 90 |
| **PE700MAc/EHA 1:1.2** | 1:0.5 | 2.000 | 2.411 | 0.051 | 3.97 | 90 |

### 2.2.2.7 *Preparation of PE700Ac/EHA copolymers.*

These were prepared essentially as before (Section 2.2.2.1). **PE700Ac/EHA 1:2.4:** $^1$H NMR ($d_8$-toluene, 80ºC, AV400, 400 MHz): [δ 6.20, 6.00 and 5.35 (vinyl hydrogens of residual monomer)] δ 4.35—3.89 (b, 4.0H, –C$H_2$–O– of the PE700Ac overlapping with the –C$H_2$–O– of the EHA) 2.85—2.49 (b, 1.8H), 2.49—2.26 (b, 0.80H), 2.05—1.79 (b, 2.1H), 1.79—1.18 (b, 36.2H), 1.17—0.74 (b, 11.9H). See data in Table 2.10.

**Table 2.10: PE700Ac/EHA copolymer data.**

| Sample Name | Mass ratio | Feed masses /g | | | Recovery | |
|---|---|---|---|---|---|---|
| | PE:A | PE700Ac | EHA | AIBN | g | % |
| **PE700Ac/EHA 1:4.5** | 1:5 | 2.000 | 8.962 | 0.169 | 10.58 | 96 |
| **PE700Ac/EHA 1:2.4** | 1:1 | 2.000 | 4.822 | 0.095 | 6.18 | 91 |
| **PE700Ac/EHA 1:1.2** | 1:0.5 | 2.000 | 2.411 | 0.052 | 4.09 | 93 |
| **PE700Ac/EHA 1:0.24** | 1:0.1 | 3.000 | 0.723 | 0.026 | 3.58 | 96 |

### 2.2.2.8 *Preparation of PE700Ac/DMA copolymers.*

These were prepared essentially as before (Section 2.2.2.1). **PE700Ac/DMA 1:12.1**: $^1$H NMR ($d_8$-toluene, 80ºC, AV400, 400 MHz): [δ 6.07, 5.24 (vinyl hydrogens of residual monomer)] δ 4.25—3.93 (b, 4.0H –C$H_2$–O– of the PE700Ac overlapping with the –C$H_2$–O– of the DMA) 2.46—2.20 (b, 1.6H), 2.20—2.01 (b, 1.6H), 1.82—1.60 (b, 4.5H), 1.60—1.11 (b, 30.4H), 1.05—0.81 (b, 6.1H). See data in Table 2.11.

**Table 2.11: PE700Ac/DMA copolymer data.**

| Sample Name | Mass ratio | Feed masses /g | | | Residual monomer* | Recovery | |
|---|---|---|---|---|---|---|---|
| | PE:A | PE700Ac | DMA | AIBN | % | g | % |
| **PE700Ac/DMA 1:25.1** | 1:10 | 0.500 | 12.056 | 0.215 | 1 | 12.63 | 99 |
| **PE700Ac/DMA 1:12.1** | 1:5 | 1.000 | 12.056 | 0.219 | 1 | 12.58 | 95 |
| **PE700Ac/DMA 1:2.4** | 1:1 | 2.000 | 4.822 | 0.095 | 1 | 6.45 | 93 |
| **PE700Ac/DMA 1:1.2** | 1:0.5 | 2.000 | 2.411 | 0.052 | 1 | 4.18 | 94 |

* The amount of residual monomer was calculated from the resonances of vinyl protons in the $^1$H NMR spectrum of the polymer.

### 2.2.2.9 *Preparation of PE700Ac/BMA copolymers.*

These were prepared essentially as before (Section 2.2.2.1). **PE700Ac/BMA 1:9.0**: $^1$H NMR ($d_8$-toluene, 80ºC, AV400, 400 MHz): δ 4.18—3.90 (b, 4.0H, –C$H_2$–O– of the PE700Ac overlapping with the –C$H_2$–O– of the BMA) 2.40—2.15 (b, 1.6H), 2.15—2.00 (b, 1.6H), 1.72—1.49 (b, 4.6H), 1.49—1.15 (b, 12.3H), 1.00—0.78 (b, 5.9H). See data in Table 2.12.

**Table 2.12: PE700Ac/BMA copolymer data.**

| Sample Name | Mass ratio | Feed masses /g | | | Residual monomer* | Recovery | |
|---|---|---|---|---|---|---|---|
| | PE:Ac | PE700Ac | BMA | AIBN | % | g | % |
| **PE700Ac/BMA 1:9.0** | 1:10 | 0.500 | 4.481 | 0.173 | 1 | 6.76 | † |
| **PE700Ac/BMA 1:4.5** | 1:5 | 1.000 | 4.481 | 0.175 | 1 | 6.29 | † |
| **PE700Ac/BMA 1:0.90** | 1:1 | 2.000 | 1.792 | 0.077 | 1 | 3.98 | † |
| **PE700Ac/BMA 1:0.64** | 1:0.5 | 2.000 | 1.272 | 0.043 | 1 | 2.87 | 88 |

* The amount of residual monomer was calculated from the resonances of vinyl protons in the $^1$H NMR spectrum of the polymer.

† The reaction solvent (toluene) was impossible to completely remove from these polymers.

### 2.2.2.10 ***Preparation of DocAc/MA 1:3.8A copolymer ("high $M_w$")***

Docosyl acrylate (2.00 g, 5.25 mmol) was charged into a dry two-necked round-bottomed flask equipped with a reflux condenser under a nitrogen atmosphere and fitted to a Radleys six-position carousel reactor (the other positions were typically fitted with parallel reactions of different compositions (Table 2.13) The solid was then de-gassed by nitrogen/vacuum purge cycling (6 times). Anhydrous, oxygen-free toluene (15 mL), de-gassed methyl acrylate (7.52 g, 87.32 mmol) and re-crystallised AIBN (42.5 mg, 0.26 mmol, 0.5 wt%) were then added. The reaction mixture was heated (60 ºC) with stirring for 21 h under nitrogen. The hot solution was precipitated into stirred methanol (150 mL), the resulting sticky white solid was filtered off and washed with further methanol (50 mL) and dried at 40 ºC *in vacuo* to a constant mass (8.28 g, 87%). $^1$H NMR ($d_8$-toluene, 80ºC, DRX500, 500 MHz): δ 4.06 (b, 2H, –C*H*$_2$–O– of the macromonomer), 3.75 (b, 52H, C*H*$_3$–O– of MA), 2.39 (b, 98H, PMA backbone hydrogens) 1.73 (b, 18H) 1.32 (b, 45H alkyl chain methylene groups), 0.92 (b, 23H).

**Table 2.13: Data for the "high molecular weight" DocAc/MA copolymers**

| Sample Name | Ratio* PE: MA | Feed DocAc / g | Feed MA / g | Feed AIBN / mg | Residual monomer† / % | Recovery mass / g | Recovery % | SEC-MALLS data $M_n$ / g mol$^{-1}$ | SEC-MALLS data $M_w$ / g mol$^{-1}$ | PDI |
|---|---|---|---|---|---|---|---|---|---|---|
| **DocAc/MA 1:7.5A** | 1:10 | 1.000 | 7.517 | 42.5 | 1 | 7.45 | 87 | 124,700 | 220,500 | 1.8 |
| **DocAc/MA 1:3.8A** | 1:5 | 2.000 | 7.517 | 47.5 | 1 | 8.28 | 87 | 88,000 | 167,100 | 1.9 |
| **DocAc/MA 1:0.75A** | 1:1 | 2.000 | 1.503 | 17.5 | 1 | 2.92 | 83 | 32,400 | 67,900 | 2.1 |
| **DocAc/MA 1:0.38A** | 1:0.5 | 2.000 | 0.752 | 13.7 | 5 | 2.32 | 84 | 24,600 | 46,700 | 1.9 |
| **DocAc/MA 1:0.075A** | 1:0.1 | 2.000 | 0.150 | 10.7 | 59 | 1.59 | 73 | Not measured | | |

* This refers to the mass ratio of pendant docosyl chains to poly(acrylate) backbone chains in the final polymer.

† The amount of residual monomer was calculated from the resonances of vinyl protons in the $^1$H NMR spectrum of the polymer.

### 2.2.2.11 *Preparation of DocAc/MA 1:3.8 / 1:7.5 copolymers ("low $M_w$")*

With the addition of dodecane thiol (DDT) to the reaction mixture from the start, an analogous procedure to 2.2.2.10 was followed for the synthesis of these copolymers. The reactions were carried out in parallel in a Radleys 12-position carousel, 0.5 wt% of AIBN was used in each polymerisation and the relevant feed and analytical data are shown in Tables 2.14 and 2.15.

**Table 2.14: "Low molecular weight" DocAc/MA 1:3.8 C-G copolymer data**

| Ref | Ratio* | Feed masses | | | | Recovery | | SEC-MALLS data | | |
|---|---|---|---|---|---|---|---|---|---|---|
| | PE:MA | DocAc / g | MA / g | DDT mol% | DDT / mg | mass / g | % | $M_n$ / g mol$^{-1}$ | $M_w$ / g mol$^{-1}$ | PDI |
| **C** | 1:5 | 0.500 | 1.879 | 0.5 | 23.5 | 1.816 | 76 | 21,200 | 28,400 | 1.3 |
| **D** | 1:5 | 0.500 | 1.879 | 1.0 | 47.1 | 1.506 | 63 | 13,700 | 17,300 | 1.3 |
| **E** | 1:5 | 0.500 | 1.879 | 1.5 | 70.6 | 1.464 | 62 | 11,100 | 13,300 | 1.2 |
| **F** | 1:5 | 0.500 | 1.879 | 2.0 | 94.1 | 1.224 | 51 | 9,200 | 11,200 | 1.2 |
| **G** | 1:5 | 0.500 | 1.879 | 3.0 | 141.2 | 1.201 | 50 | 6,200 | 7,500 | 1.2 |

**Table 2.15: "Low molecular weight" DocAc/MA 1:7.5 C-G copolymer data**

| Ref | Ratio* | Feed masses | | | | Recovery | | SEC-MALLS data | | |
|---|---|---|---|---|---|---|---|---|---|---|
| | PE:MA | DocAc / g | MA / g | DDT mol% | DDT / mg | mass / g | % | $M_n$ / g mol$^{-1}$ | $M_w$ / g mol$^{-1}$ | PDI |
| **C** | 1:10 | 0.250 | 1.879 | 0.5 | 22.8 | 1.286 | 60 | 26,900 | 34,700 | 1.3 |
| **D** | 1:10 | 0.250 | 1.879 | 1.0 | 45.6 | 1.104 | 51 | 17,200 | 21,900 | 1.3 |
| **E** | 1:10 | 0.250 | 1.879 | 1.5 | 68.3 | 1.055 | 48 | 12,700 | 15,600 | 1.2 |
| **F** | 1:10 | 0.250 | 1.879 | 2.0 | 91.1 | 1.226 | 55 | 11,500 | 13,900 | 1.2 |
| **G** | 1:10 | 0.250 | 1.879 | 3.0 | 136.7 | 0.764 | 34 | 7,700 | 9,500 | 1.2 |

* This refers to the mass ratio of pendant docosyl chains to poly(acrylate) chains in the final polymer.

### 2.2.2.12 *Preparation of B36Ac/MA and PE700Ac/B36Ac/MA co- and ter-polymers.*

An analogous procedure to that in Section 2.2.2.1 was followed for the synthesis of these copolymers. The reactions were carried out in parallel in a Radleys 6-position carousel and the relevant feed and analytical data are shown in Table 2.16.

$^1$H NMR spectrum of **B36Ac/MA 1:4.2** ($CDCl_3$, 27 ºC, DRX500, 500 MHz): δ 3.94 (b, 2H, –C*H*$_2$–O– of B36 side-chain), 3.66 (b, 112H, C*H*$_3$–O– of MA), 2.59 (b, 1H), 2.31 (b, 36H), 1.93 (b, 16H), 1.67 (b, 39H), 1.51 (b, 20H), 1.25 (b, 88H), 0.87 (t, 8H).

$^1$H NMR spectrum of **PE700Ac/B36Ac/MA 1:2.2:14.5** ($d_8$-toluene, 80 ºC, DRX500, 500 MHz): δ 4.11 (b, 2H, –C*H*$_2$–O– of B36 and PE700 side-chains), 3.52 (b, 128H, C*H*$_3$–O– of MA), 2.59 (b, 42H), 1.82 (b, 46H), 1.62 (b, 22H), 1.34 (b, 97H), 0.91 (t, 7H).

**Table 2.16: B36Ac/MA and PE700Ac/B36Ac/MA copolymer data**

| Sample Name | Feed masses | | | | Res. Mon.* | Recovery | | SEC-MALLS data | | |
|---|---|---|---|---|---|---|---|---|---|---|
| | PE700Ac / g | B36Ac / g | MA / g | AIBN / mg | % | mass / g | % | $M_n$ / g mol$^{-1}$ | $M_w$ / g mol$^{-1}$ | PDI |
| **B36Ac/MA 1:8.4** | 0 | 1.000 | 8.426 | 328.1 | 1 | 9.38 | 96 | 14,500 | 73,500 | 5.1 |
| **B36Ac/MA 1:4.2** | 0 | 1.000 | 4.213 | 167.2 | 1 | 5.24 | 97 | 20,800 | 57,700 | 2.8 |
| **PE700Ac/B36Ac/MA 1:2.2:29.0** | 0.309 | 0.691 | 8.962 | 346.6 | 1 | 10.1 | 98 | Polymers were insoluble in THF and SEC-MALLS was not possible. | | |
| **PE700Ac/B36Ac/MA 1:2.2:14.5** | 0.309 | 0.691 | 4.481 | 175.5 | 1 | 5.61 | 99 | | | |

* The amount of residual monomer was calculated from the resonances of vinyl protons in the $^1$H NMR spectrum of the polymer ($d_8$-toluene, 80ºC, DRX500, 500 MHz).

### 2.2.3 **Synthesis of the MALDI-ToF MS substrate**

#### 2.2.3.1 ***Preparation of polyethylene bromide (PE700-Br)***

PE700-OH (1.489 g; 2.00 mmol) and toluene (10 mL) were charged into a two-necked round-bottomed flask equipped with a magnetic stir bar and a reflux condenser under a nitrogen atmosphere. The mixture was stirred at 80 °C for 30 minutes. $PBr_3$ (188 μL, 2.00 mmol) was then added dropwise *via* a syringe and the mixture was stirred at 80 °C for 5 hours under a nitrogen atmosphere. The hot reaction mixture was added slowly to cold, stirred MeOH (100 mL) and the off-white precipitate formed was filtered off and dried *in vacuo* to constant mass (1.238 g). The off-white solid was characterised by $^1$H NMR spectroscopy and the conversion of alcohol to bromide was found to be ~50%. The crude product was used without further purification. $^1$H NMR ($d_8$-toluene, AV400, 80 ºC, 400 MHz): δ 3.32 (t, 2H [-C$H_2$-Br]), 3.04 (t, 2H residual [-C$H_2$-OH]) 1.28—1.70 (m, 304H backbone [-C$H_2$-]), 0.93, (t, 10.6H [-C$H_3$]). FT-IR $\nu_{max}$/cm$^{-1}$ 2916 (s), 2849 (s), 1739 (weak), 1473 (s), 1463 (s), 1222 (b), 1007 (b), 730 (s), 720 (s). MP: 99-105 °C.

#### 2.2.3.2 ***Preparation of polyethylene phosphonium bromide (PE700-$PPh_3^+$ $Br^-$)***

Crude PE700-Br (0.529 g 0.69 mmol), toluene (10 mL) and $PPh_3$ (1.39 g, 5.30 mmol) were charged to a two-necked round-bottomed flask under a nitrogen atmosphere and stirred for 4 days at 110 °C. The reaction mixture was allowed to cool to around 80 °C and was added slowly to stirred petroleum ether 40-60° (0 °C). The yellow precipitate formed was washed into a cellulose extraction thimble and washed in a Soxhlet apparatus for 4 hours with petroleum ether 40-60° to remove excess $PPh_3$. The washed precipitate was dried *in vacuo* to provide a white solid (0.303 g), the conversion by $^1$H NMR spectroscopy was 63% relative to the starting material and no attempt was made to further purify the product. $^1$H NMR ($d_8$-toluene, AV400, 80 ºC, 400 MHz): δ 7.98 (b, 6H [Ar-*H*]), 7.35 (b, 9H [Ar-*H*]), 4.33 (b, 2H [-C$H_2$-$PPh_3$]), 1.70-1.10 (b, 321H backbone [-C$H_2$-]) 0.90 (t, 9.5H [-C$H_3$]) FT-IR $\nu_{max}$/cm$^{-1}$ 3375 (b), 2915 (b), 2848 (s), 2348 (b), 1473 (s), 1463 (s), 1439 (s), 1192 (b), 1115 (s), 997 (s), 720 (s), 691 (s), 536 (s), 509 (s). MP: 104-108 °C.

## 2.3 Molecular analytical procedures

### 2.3.1 NMR spectroscopy

$^{1}H$ and $^{13}C$ NMR spectra were recorded at 25ºC using $CDCl_3$ or 80ºC using $d_8$-toluene as the solvent in 5 mm NMR tubes on either a Bruker DPX-400 (400 MHz) or AV400 (400 MHz) or DRX-500 (500 MHz) using the residual solvent resonance as an internal reference, chemical shifts are given in ppm.

### 2.3.2 FT-IR spectroscopy

Fourier-transform infrared spectra were recorded on a Perkin Elmer Spectrum One FT-IR spectrometer using a Perkin Elmer SMS diamond compression cell. The sample was scanned over the range 4000-400 $cm^{-1}$ in transmission mode.

### 2.3.3 Elemental Microanalysis

Elemental microanalysis data were obtained from the University of Strathclyde microanalytical service. C, H and N analyses were carried out simultaneously using a Perkin Elmer 2400 series II analyser. Where applicable, bromine content was determined by a titration method.

### 2.3.4 SEC-MALLS analysis

The SEC-MALLS instrument comprised the following equipment; a solvent degasser (Jones Chromatography 760 series), an HPLC pump (Dionex Ultimate 3000), an autosampler (Jasco AS-950); a column oven (Shimadzu CTO-6A), one guard column (Polymer Labs PolyPore 5M, 7.5 x 75 mm) and two GPC columns (Polymer Labs PolyPore 5M, 7.5 x 300 mm). The two detectors, a multi-angle laser light scattering (MALLS) detector (Wyatt Technology mini-DAWN) and an interferometer refractometer detector (Wyatt Technology Optilab DSP) were connected in a serial configuration. The mobile phase was THF (HPLC grade, pre-filtered through a 0.2 μm polyamide membrane), the nominal flow rate was 1 mL/min and the column oven temperature was 40ºC.

Samples for SEC-MALLS analysis were prepared by adding a known mass of polymer (~15 mg) to 1.00 mL of THF and allowing the polymer to dissolve for at least 20 h at room temperature. The solution was filtered through a 0.2 μm syringe filter, (Acrodisc 13CR PTFE, ø13mm) into a 2 mL HPLC vial. The injection volume was 0.2 mL and data was collected for 40min. Data from the two detectors was processed using Wyatt Technology Astra software using a *dn/dc* value of 0.90 mL $g^{-1}$.

### 2.3.5 **HT-SEC analysis**

High-temperature size exclusion chromatography was carried out by Smithers RAPRA Ltd. The HT-SEC instrument used was a Polymer Laboratories (PL) GPC220, fitted with 2 PLgel Olexis 300 mm, 13 μm columns preceded by an Olexis guard column. The solvent used was 1,2,4-trichlorobenzene with anti-oxidant, the nominal flow-rate was 1.0 mL/min, the temperature was 160°C and the detectors used were refractive index (Polymer Labs) and differential pressure (Viscotek). The data was collected and analysed using Polymer Laboratories Cirrus software.

Samples for characterisation were prepared by adding 15 mL of cold 1,2,4-trichlorobenzene to 15 mg of polymer and heating at 190°C for 20 minutes, with shaking to dissolve. After cooling to 160°C, the sample solutions were transferred to glass autosampler sample vials without filtration. The vials were placed in the heated (160°C) autosampler compartment of the instrument and allowed to thermally equilibrate for thirty minutes before aliquots from each were automatically injected into the HT-SEC system in turn.

### 2.3.6 **PE700-OH Isocratic Liquid Adsorption Chromatography**

PE700-OH (3.050 g) was dissolved in 15.0 mL of toluene at 80 °C. The chromatography column was prepared by mixing silica gel (110 g) with toluene, charging the slurry to a water-jacketed column (270 mm long x 35 mm internal diameter) and pre-heating to 75 °C using a water circulator (Grant W6). The hot PE700-OH solution was charged to the top of the silica gel and the column was eluted with further hot toluene (~75 °C). When the initial eluate (~100 mL) started to

show signs of polymer precipitate on cooling, small fractions were collected (30 x 15 mL) until precipitation was no longer visible on cooling. The fractions were individually concentrated under reduced pressure at room temperature and finally dried *in vacuo* at 70 °C to constant mass. Each fraction was weighed and analysed by $^{1}$H NMR spectroscopy.

### 2.3.7 **MALDI-ToF Mass Spectrometry**

PE700-$PPh_3Br$ (1 mg) (see Section 2.2.3 for details of the synthetic procedure) was ground together with all-*trans*-retinoic acid (ATRA) (10 mg) in a mortar and pestle. A small amount of this paste was pressed onto the stainless steel MALDI target plate, removing any loose particles with a stream of compressed nitrogen. The samples were analysed using a Shimadzu Biotech Axima CFR MALDI-ToF mass spectrometer in reflectron mode, calibrated with protein standards.

## 2.4 **Copolymer physico-chemical characterisation**

### 2.4.1 **Transmission electron microscopy (TEM)**

Specimens for TEM characterisation were prepared by solvent casting a copolymer solution (100 mg in 0.5 mL) onto a PP substrate (10 x 10 mm), allowing the solvent to evaporate overnight at 110 °C and subsequently annealing at 70 °C under vacuum for 7 days. A small piece (~1 x 5 x 0.5 mm) was sliced from the copolymer film and embedded in hydrophobic methacrylate resin (Lowicryl HM20) in a cylindrical mould. The resin was cured under UV light at -40 °C for 7 days. This was then sectioned on an ultramicrotome, the thin sections were placed onto Au grids and stained overnight with either $OsO_4$ or $RuO_4$ vapours. Commercially available aqueous $OsO_4$ solution was used directly, whereas an aqueous solution of $RuO_4$ was freshly prepared according to the method of Li and co-workers[1]. $RuO_2$ (20 mg, mmol) and $NaIO_4$ (10 mg, mmol) were charged into a test tube. Saturated aqueous $NaIO_4$ (3 mL) was added, the test tube was sealed with a glass stopper and shaken gently. Dissolution of the $RuO_2$ accompanied by the appearance of a rich golden colour indicated the formation of $RuO_4$. Each sample was then imaged on a Zeiss 912 energy filtering transmission electron microscope operating in zero-loss mode at

120 kV. Images were acquired via a 2K Proscan camera using AnalySIS EsiVision software.

### 2.4.2 **ULAM ToF-SIMS**

Ultra-low-angle microtomy (ULAM) and subsequent time-of-flight secondary ion mass spectrometry (ToF-SIMS) characterisation of the adhesive joints were carried out at the University of Surrey. Specimens comprising of PP-adhesive and PMMA-adhesive sandwiches were prepared in an analogous way to adhesion test pieces but without any surface roughening of the commercial polymer substrates. The substrate size was 10 x 10 mm and the adhesive layer was angle-lapped from the surface using the ultra-low-angle microtomy (ULAM) methodology devised by Hinder and co-workers[2]. A schematic diagram of the ULAM apparatus as employed in the production of ultra-low-angle tapers is presented in Figure 2.1.

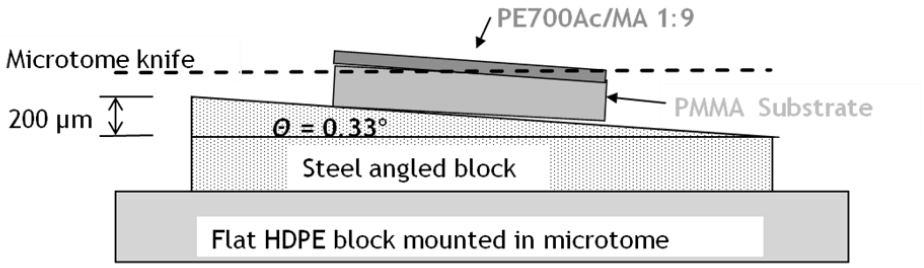


**Figure 2.1: Schematic diagram of the ULAM cross-sectioning methodology used.**

The ULAM processing of samples was carried out on a Microm HM355S motorised rotary microtome (Optech Scientific Instruments, Thame, UK) equipped with a standard specimen clamp and a tungsten carbide knife. The ultra-low-angle sectioning blocks (~3.5 $cm^2$ x 0.7 cm) were manufactured in-house from high-quality steel and had one 3.5 $cm^2$ tapered face raised by a 200 µm relative to the parallel edge of the tapered face (Figure 2.1), giving a taper angle of 0.33°. The following procedure was followed when processing adhesive samples by the ULAM technique.

i) A PE block (4 $cm^2$ x 2 cm) was placed in the microtome specimen clamp and trimmed (5 µm sections) with the knife until the sections comprised the complete PE

block face, this provided a surface which was parallel to the knife. The PE block was then retracted from the knife and double-sided adhesive tape applied to the freshly trimmed PE block face.

ii) The tapered face of an angled sectioning block was cleaned with acetone to ensure it was free of any contaminants. Double-sided adhesive tape was applied to the tapered face of the block and the specimen to be sectioned was applied to the adhesive tape at the centre of the block.

iii) The low-angle sectioning block was then secured to the PE block *via* the double-sided adhesive tape on the trimmed face of the PE block such that the specimen to be sectioned faced the microtome knife.

iv) The specimen was then presented to the knife and sectioned at a sectioning depth of between 1 and 5 μm depending on the thickness of the adhesive layer. Once the desired interface was revealed or the required depth of tapering obtained the sample was removed from the angled sectioning block for ToF-SIMS analysis.

ToF-SIMS analyses were carried out on an ION-TOF GmbH (Münster, Germany) TOF.SIMS 5 system. The instrument was equipped with a reflectron type analyser and microchannel plate detector with 20 kV post-acceleration capability. A bismuth liquid metal ion source was employed for mass data acquisition. The ToF-SIMS image data were acquired over a 500 x 500 $\mu m^2$ area at a resolution of 256 x 256 pixels. A 25 keV primary ion beam delivering 0.03 pA of current was employed. Imaging data were acquired at one cycle per pixel with a total of 126 scans. A cycle time of 200 μs was employed. Charge compensation was achieved using a pulsed electron flood source. Data acquisition and post-processing analyses were performed using the IonSpec version 4.5.0.0 and IonImage version 3.0.0.61 software products.

### 2.4.3 **'In-house' adhesion testing**

Discs of LDPE (with a nominal diameter of 29 mm) were cast from BDH LDPE powder using a film maker accessory and manual hydraulic press fitted with heated platens (Graseby Specac), at a thickness of 0.500 mm and a pressure of 3 tonnes. A digital thermometer (Testo 925) was used to accurately monitor the temperature of the film maker accessory. LDPE films were cast at ~112 ºC. Adhesive test pieces were constructed from a commercial PMMA substrate, LDPE or PP disc, a small amount of the polymer under investigation and a slip of aluminium foil to prevent the total adhesion of the two substrates (Figure 2.2).

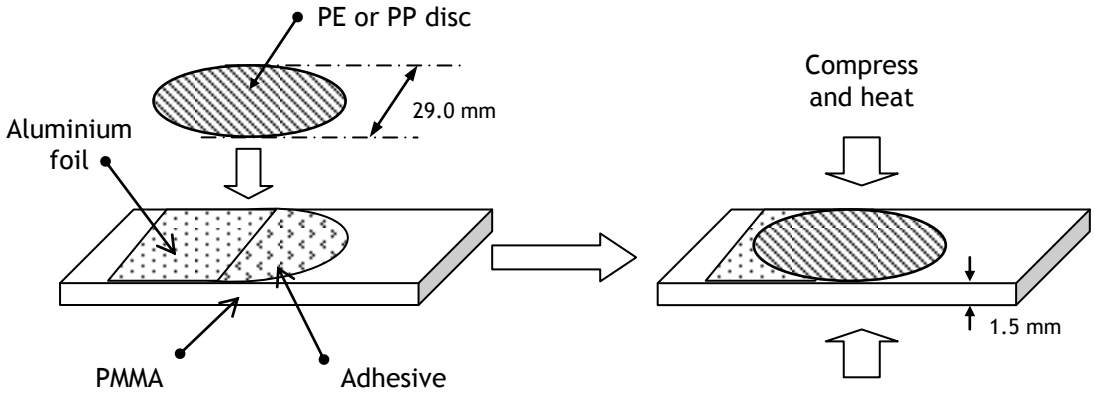


**Figure 2.2: Construction of an in-house adhesion test piece**

Each substrate-adhesive-substrate sandwich was then compressed and heated in the film maker accessory at temperatures of either 110ºC for LDPE or 160 ºC for PP substrates under a pressure of 200 kg for 5 minutes. The pressure was maintained until the test piece had cooled to room temperature. The test pieces were visually inspected to check that the adhesive had formed a coherent layer and two good replicates were tested manually by pulling the polymer substrates apart.

### 2.4.4 **ASTM adhesion testing**

Six replicate test specimens for each sample were prepared according to ASTM D1002-05[3] and D3163-1[4]. Each test specimen was made up from one PP substrate (25.4 x 97.0 x 2.8 mm) bonded to one PMMA substrate (25.4 x 105.0 x 1.5 mm) (Figure 2.3).

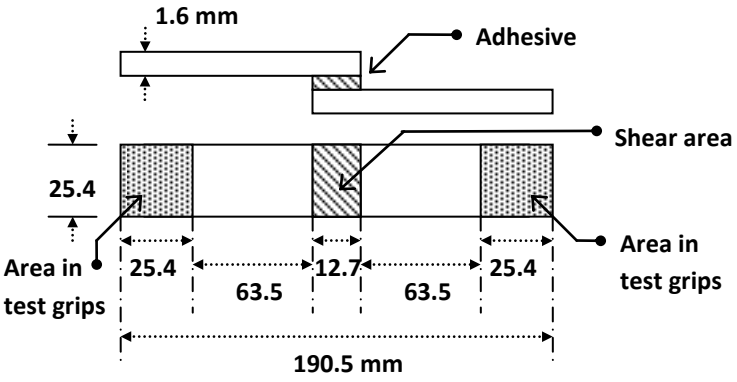


**Figure 2.3: A schematic representation of an ASTM D1002-05 tensile adhesion test specimen. All dimensions shown are in mm.**

The substrates were prepared by abrading the area to be bonded with wet-or-dry sandpaper (280 grade), degreasing with isopropanol and drying in a stream of compressed air. The copolymer was solution cast from a toluene solution (100 mg in 0.50 mL) onto the prepared end of the PP substrate to give an adhesive patch of approximately 12.7 x 25.4 mm. The solvent was evaporated overnight in an oven at 108 °C. The PMMA substrate was then aligned, pressed onto the adhesive and left compressed overnight at 108°C. Each test specimen was examined to check that a coherent and void free layer of adhesive was present. Five good replicates were tension tested on an Instron 1122 Dual Column Universal Materials Testing System at a free crosshead speed of 1 mm $min^{-1}$ using a 1 kN load cell. The average value for the failure load of all five test specimens was recorded.

## 2.5 References

(1) Li, J. X.; Ness, J. N.; Cheung, W. L. *J Appl Polym Sci* **1996**, *59*, 1733.

(2) (a) Hinder, S. J.; Watts, J. F.; Lowe, C. *Surf Interface Anal* **2004**, *36*, 1032 (b) Hinder, S. J.; Lowe, C.; Maxted, J. T.; Watts, J. F. *Surf. Interface Anal.* **2004**, *36*, 1575.

(3) D1005-05; ASTM International: West Conshohocken, PA, 2005.

(4) D3163-1; ASTM International: West Conshohocken, PA, 2001.

# Chapter 3

# Results and discussion

# 3 Results and discussion

## 3.1 Polyethylene mono-alcohol structural characterisation and purification

### 3.1.1 Introduction

By using $^{1}$H NMR spectroscopic analysis of the polyethylene alcohol starting materials (PE-OH) and HT-SEC of the copolymers derived from them, it was evident that the commercially sourced PE-OHs contained a fraction comprising a linear, non-functional polyethylene, confirming the information provided by the supplier. Therefore it was evident that the linear non-functional PE was not removed during any of the routine copolymer purification steps. This was likely to be as a result of the similar solubility and properties of the non-functional PE to the derived materials. Since the non-functional PE impurity was therefore present in the copolymers which were used as adhesives, it was desirable to determine what effect its presence had on adhesive performance. Therefore we wanted to devise a way to remove it from the copolymers at some stage of the synthesis. This was achieved in due course by using adsorption chromatography at an elevated temperature to resolve the PE-OH from the impurity.

The PE700-OH starting material was also characterised by MALDI-ToF mass spectrometry of a derivatised sample. This provided information on the molecular weight and molecular weight distribution.

### 3.1.2 Structural characterisation of the polyethylene mono-alcohols

#### 3.1.2.1 *Characterisation by $^{1}$H NMR spectroscopic analysis*

The macromonomers used in the present work were prepared from two commercially available polyethylene mono-alcohols. The alcohols are quoted by the supplier, Sigma-Aldrich, as being mono-terminated with –OH groups, having number averaged molecular weights of 460 ($T_m$ = 86°C) and 700 gmol$^{-1}$ ($T_m$ = 108°C) and polydispersity indices of 1.09. The supplier gives the purity of both materials as 15

to 20% of 'unreacted hydrocarbons' and this was taken to mean that linear, non-functional polyethylene of similar molecular weight was present. This could indeed be seen in the $^1$H NMR spectra of the products, with the integration of the terminal methyl hydrogens (δ = 0.90 ppm, triplet) being greater than the theoretical value derived from the integration of the resonance for the methylene hydrogens (δ = 3.37 ppm, triplet) adjacent to the hydroxyl group (Table 3.1).

**Table 3.1: $^1$H NMR spectral analysis of the PE-OH starting materials**

| PE-OH | Relative resonance area integrations derived from the $^1$H NMR spectra | | | | | | Purity | $M_n$* |
|---|---|---|---|---|---|---|---|---|
| | -C$H_2$-OH | | -CH$_2$-C$H_3$ | | -(-C$H_2$-)- | | % | g mol$^{-1}$ |
| | calc | found | calc† | found | calc‡ | found | | |
| '460' | 2 | 2.00 | 3 | 4.30 | ~63 | 85.92 | 82 | 540 |
| '700' | 2 | 2.00 | 3 | 5.56 | ~97 | 145.48 | 71 | 760 |

We believe that these materials are prepared by a degenerative transfer polymerisation of ethylene using a bis(imino)pyridine iron catalyst and triethylzinc as a co-catalyst[1]. This type of catalyst provides zinc-terminated PE chains which are insoluble in the reaction solvent (*o*-xylene) at a $M_n$ of over ~700 gmol$^{-1}$, which is the same as the $M_n$ quoted by the supplier. The zinc is then oxidised with air to provide Zn-O- end-groups which are subsequently hydrolysed *in situ* with HCl to the alcohol. The oxidation/hydrolysis step is not particularly efficient and results in some chains being capped by methyl groups, resulting in a non-functional PE impurity with a similar $M_n$.

Assuming that the number average degree of polymerisation of the PE-OH and the linear contaminant are equal (we believe this is reasonable in view of the likely

* Of the PE-OH, assuming that the molecular weight of the PE-OH and PE contaminant are equal

† The calculated values assume that all chains are linear

‡ These are based on the supplier's $M_n$ values for the PE-OH materials and assume 100% purity.

method of preparation of the precursor to the PE mono-alcohol) and that there is no branching, unsaturation or isomerism of either component, then the purity can be estimated from the $^1$H NMR spectrum. The resonances due to the –O*H* hydrogen were obscured by a solvent peak (residual C*H*$_3$- of toluene in $d^8$-toluene, $\delta$ = 2.09 ppm) in both spectra. There were no observed resonances in any of the $^1$H NMR spectra due to methine hydrogens that might have indicated the presence of branching. The molecular weight was estimated from the ratio of -(-C*H*$_2$-)- to -C*H*$_2$-OH, once the amount of alkyl hydrogens present from the linear PE had been subtracted. Data for the calculated purity and $M_n$ of the PE-OH 460 and 700 are shown in Table 3.1. The linear polyethylene impurities were therefore carried through and are present in all of the copolymers prepared using the two PE macromonomers.

The presence of the non-functional PE impurities has an unknown effect on the adhesive properties of the graft copolymers containing them. The presence of non-functional PE might enhance or diminish the adhesive performance of a given material. It was therefore desirable to be able to prepare copolymers which were free from the PE impurity to measure its effect on adhesion. In the **PE700Ac/MA 1:9.0 & 1:5.0** copolymers which gave the best results in adhesion testing (Section 3.5.7.3), only small proportions of macromonomer were used (~10-20%) so the amount (by mass) of non-functional PE present is relatively low in these materials (~2-4%).

#### 3.1.2.2 *Characterisation by MALDI-ToF mass spectrometry of derivatitised PE700-OH*

Another analytical technique capable of achieving high resolution of the molecular weights of organic oligomeric materials is MALDI-ToF mass spectrometry (MS) and we thought it would be valuable to generate some comparative data from such analysis. Unfortunately however consultation with the literature indicated that polyolefins are notoriously difficult to analyze by MALDI-ToF MS due to the ease with which they fragment under laser ablation, and hence require the sample to be dilute in the matrix (1 sample/10matrix) and the use of a low laser power[2]. All-*trans*-retinoic acid (ATRA) has however been shown to be a valuable matrix in the case of

polyolefins[3]. Preliminary in-house experiments with this matrix confirmed that neither the PE700-OH nor its non-functional PE impurity could be observed using MALDI-ToF MS. These molecules apparently fail to ionize at laser energies low enough to prevent excessive fragmentation. It was decided therefore to derivatise the PE700-OH with an ionic functionality and this was achieved *via* conversion of the terminal alcohol group to an alkyl bromide followed by reaction with triphenylphosphine to yield a terminal phosphonium bromide functionality, a procedure which has been used successfully by Lin-Gibson and co-workers to analyze hydroxy-functional PE by MALDI-ToF MS[3]. Though these reactions proceeded reasonably well using the as-supplied PE700-OH the conversions were not 100% (Scheme 3.1), and the final phophonated product was contaminated with starting material and bromo-intermediate.

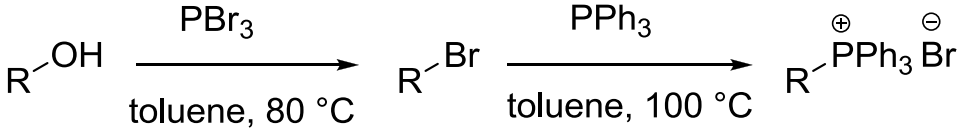


**Scheme 3.1: Derivatisation of the PE700-OH for MALDI-ToF mass spectrometry, R = PE700.**

From a MALDI-ToF MS perspective this was not a particular problem because only the phosphonated species was expected to undergo analysis in the MS. However, the $^{1}$H NMR spectrum of the phosphonated species was difficult to interpret quantitatively because of contamination with precursor materials. In addition it was not possible to deduce whether or not the PE700-OH had been derivatised statistically and that the molecular weight distribution of the final product reflected accurately that of the PE700-OH precursor. Nevertheless the phosphonated sample did undergo successful MALDI-ToF MS analysis from an all-*trans*-retinoic acid matrix and the molecular weight distribution obtained is shown in Figure 3.1. Adjusting the data to account for the presence of -$PPh_3^+Br^-$ in place of -OH, the molecular weight data for the PE700-OH precursor calculated from this mass spectrum are $M_n$ = 641 gmol$^{-1}$, $M_w$ = 676 gmol$^{-1}$ and *PDI* = 1.04. Each of these data

are lower than the corresponding data from our chromatographic analysis, with the lower *PDI* in particular probably reflecting the loss of some of the distribution during the derivatization steps. The lower values for $M_n$ and $M_w$ suggest that the loss is at the higher molecular weight end of the distribution, and it does not seem unreasonable that the chemical modification becomes less efficient as the chain length of the PE-OH increases. Bearing this in mind, and the potential loss of material at the low molecular weight end of the distribution in our chromatographic analysis (Section 3.1.3), the relative values of the respective $M_n$, $M_w$ and *PDI* parameters obtained from the two procedures are at least consistent with each other.

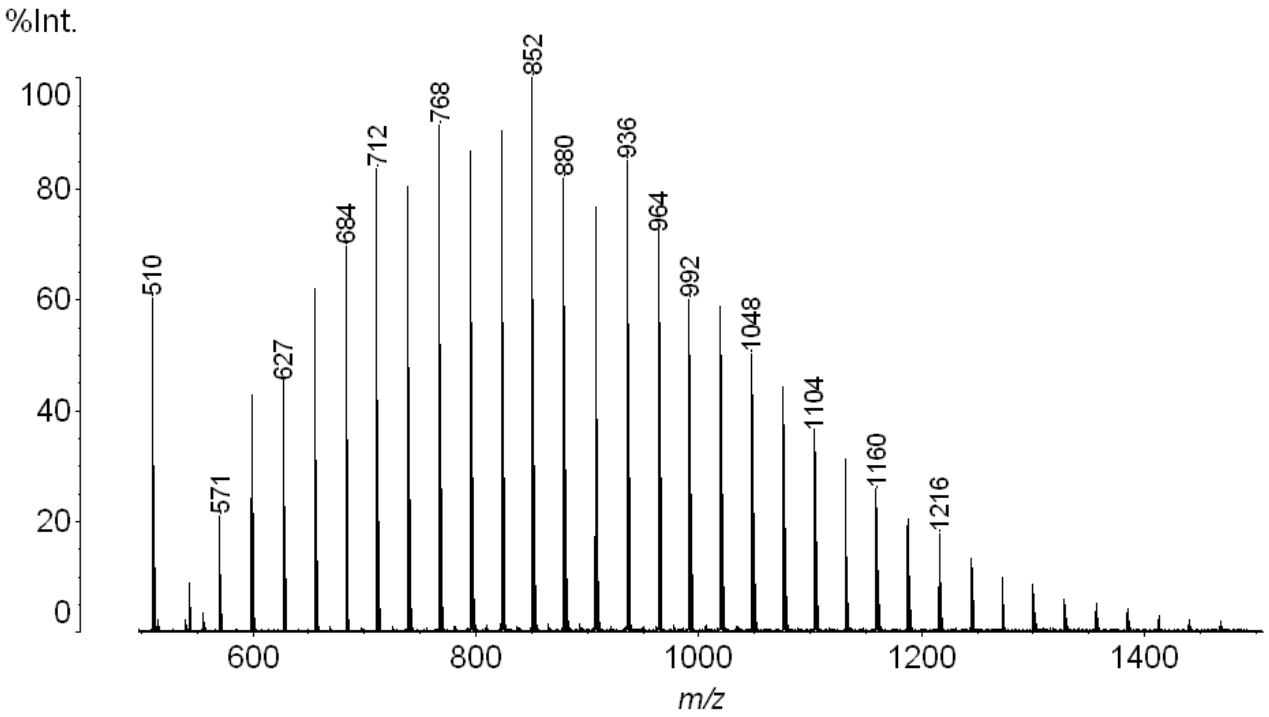


**Figure 3.1: The MALDI-ToF mass spectral molecular weight distribution for the PE-$PPh_3^+Br^-$ polymer. The peaks at m/z = 510 and 600 are due to a matrix adduct.**

### 3.1.3 **Purification of the PE700-OH starting material**

The chromatographic separation of polymeric materials is well known in the literature however to the best of our knowledge no examples exist which utilise the interaction of the polymer with the stationary phase as the sole means of resolution[4]. Most techniques rely on a combination of precipitation, sorption and/or size exclusion mechanisms, controlled by solvent polarity gradients and/or temperature gradients to achieve separation[5,6]. Meunker and Hudson showed that carboxy- and hydroxyl-functionalised polymers could be fractionated on silica gel according to their molar fraction of functionality using stepwise elution with solvent mixtures of progressively greater elution power[7]. In the present work we have found a polymer/stationary phase/solvent system that not only provides a facile means of purifying PE700-OH but in effect fractionates the end-functional polymer itself according to polarity and therefore molecular weight, as a result of the terminal group-stationary phase (SP) interaction being much greater than the polymer chain-SP interaction. Since the interaction is strong and the polymer has a relatively low molecular weight, we believe that any size exclusion effects are insignificant in this separation. Using end-group analysis by $^{1}$H NMR spectroscopy, the fractionation also serendipitously allowed us to evaluate the molar mass distribution of the polymer. The results were compared to the MALDI-ToF spectral distribution of the phosphonated polymer.

The polyethylene mono-alcohol, $M_n$ = 700 gmol$^{-1}$ (PE700-OH) was purified by isocratic column chromatography using silica gel in a water-jacketed column at 75 °C, and hot toluene as the eluant. The fractions collected were analysed by $^{1}$H NMR spectroscopy. The early ones were found to contain non-functional PE and only very low levels of PE-OH, whereas the later fractions seemingly contained high-purity PE-OH. The column separation was repeated with smaller (~ 15 mL) fractions being collected. These were evaporated to dryness, weighed and the residues were characterised by NMR spectroscopy. The proportion of the two components (PE-OH and non-functional PE) present in the fractions was calculated from their $^{1}$H NMR spectra in the same way as previously discussed, assuming that 1) no other components were present, 2) there was no branching of the PE chains and

3) the $\overline{DP}_n$ of the PE mono-alcohol and the PE impurity were the same. We believe that these materials are prepared by a degenerative transfer polymerisation[1b] (Section 3.1.2) with the terminal alcohol functionality generated by chemical modification of the chains attached to the initiator metal centre. The smaller non-functional fraction is believed to have the same $\overline{DP}_n$ as the terminally functional major fraction as a result of the polymerisation and the post-polymerisation chemistry.

The purity calculation was based on the ratio of the integrations (*R*) of the resonance due to the -C*H*$_2$-OH hydrogens present only in the PE700-OH at $\delta = 3.38$ and that of the -CH$_2$-C*H*$_3$ hydrogens which are present in both components (PE700-OH and PE impurity) at $\delta = 0.9$ as shown in Equation 3.1.

---

**Equation 3.1**

The mole fraction of PE impurity ($\chi_{PE}$) in the PE700-OH was then found from *R* using Equation 3.2.

---

**Equation 3.2**

The recovered total mass of each fraction was then split into the masses of each component present using mole ratios calculated from the $^1$H NMR spectra of each recovered fraction. The masses of both components were then plotted for all fractions (Figure 3.2).

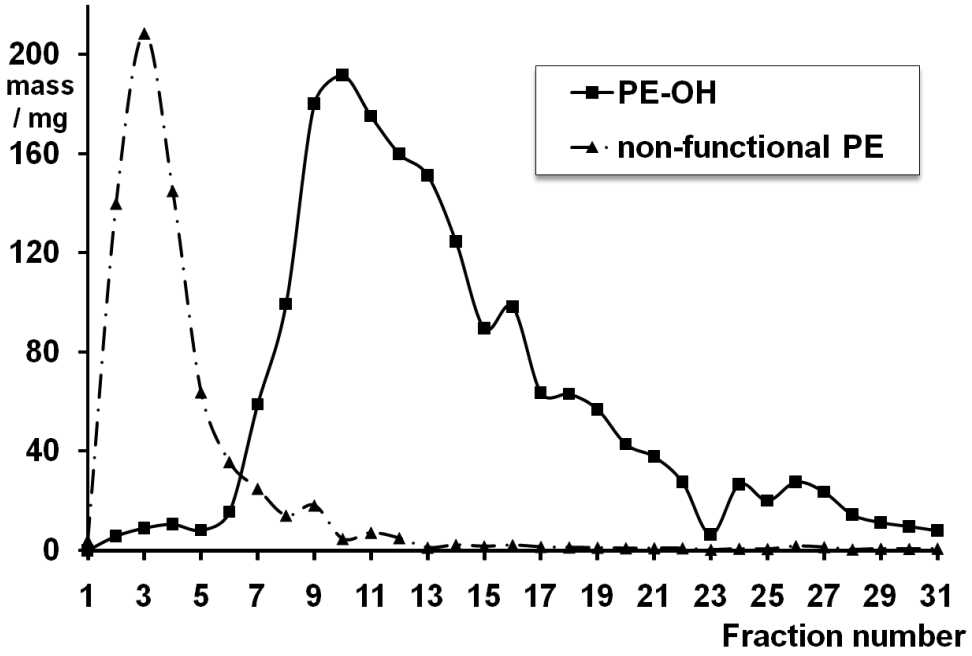


**Figure 3.2: Analysis of the column fractions by mass and $^{1}$H NMR spectroscopy.**

The non-polar linear PE impurity was eluted first, with fractions 0 to 6 containing the greatest proportion. From fraction 7 onwards the more polar PE700-OH becomes the main component. This was expected as the linear PE interacts less strongly with the polar silica stationary phase than the PE700-OH does.

By using the data derived from the $^{1}$H NMR spectra of each fraction along with the mass collected, it was possible to calculate the purity of the commercially available PE700-OH starting material. The purity was found to be 72.6% and this is in good agreement with the figure derived from the $^{1}$H NMR spectrum of the PE700-OH before column chromatography (71%) within experimental error. The agreement of these two figures suggests that the assumptions that the linear PE is the only impurity present and that this has the same $\overline{DP}_n$ as the PE700-OH are valid, and that the treatment of the data is correct.

Further manipulation of the $^{1}$H NMR data of the pure PE700-OH fractions also allowed the molecular weight of the PE700-OH in each fraction to be determined (Figure 3.3). The molar masses of the PE700-OH in fractions 1 to 6 were not plotted

as these fractions were made up predominantly of the non-functional PE impurity (Figure 3.2).

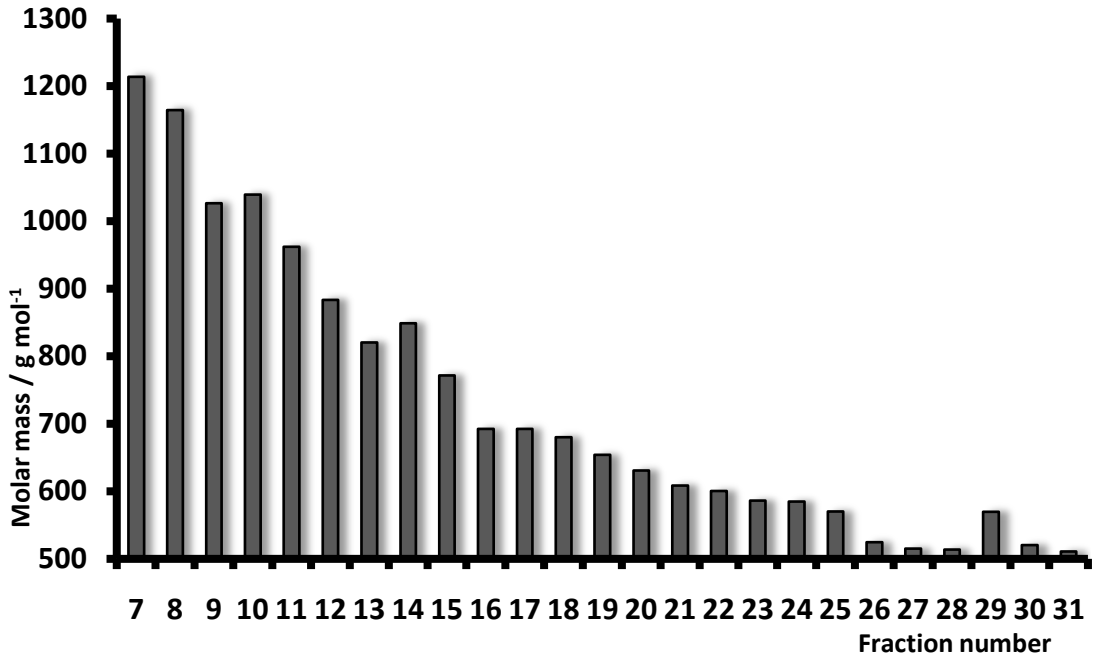


**Figure 3.3: The variation of molar mass of PE700-OH with column fraction, determined by $^{1}$H NMR spectroscopy for fractions 7 to 31.**

The molar mass of each fraction was found by comparing the peak area of the resonance due to the -C*H*$_2$-OH hydrogens to those due to the -C*H*$_2$- hydrogens of the PE chain, once any influence of the linear PE had been subtracted. Rather serendipitously the molecular weight was found to decrease with each fraction collected, the fractions presumably eluting differentially as a result of increasing polarity as the chain length decreases. In addition the molar mass distribution of the PE700-OH was established by plotting the mass fraction against the molar mass of fractions 7 to 31 (Figure 3.4).

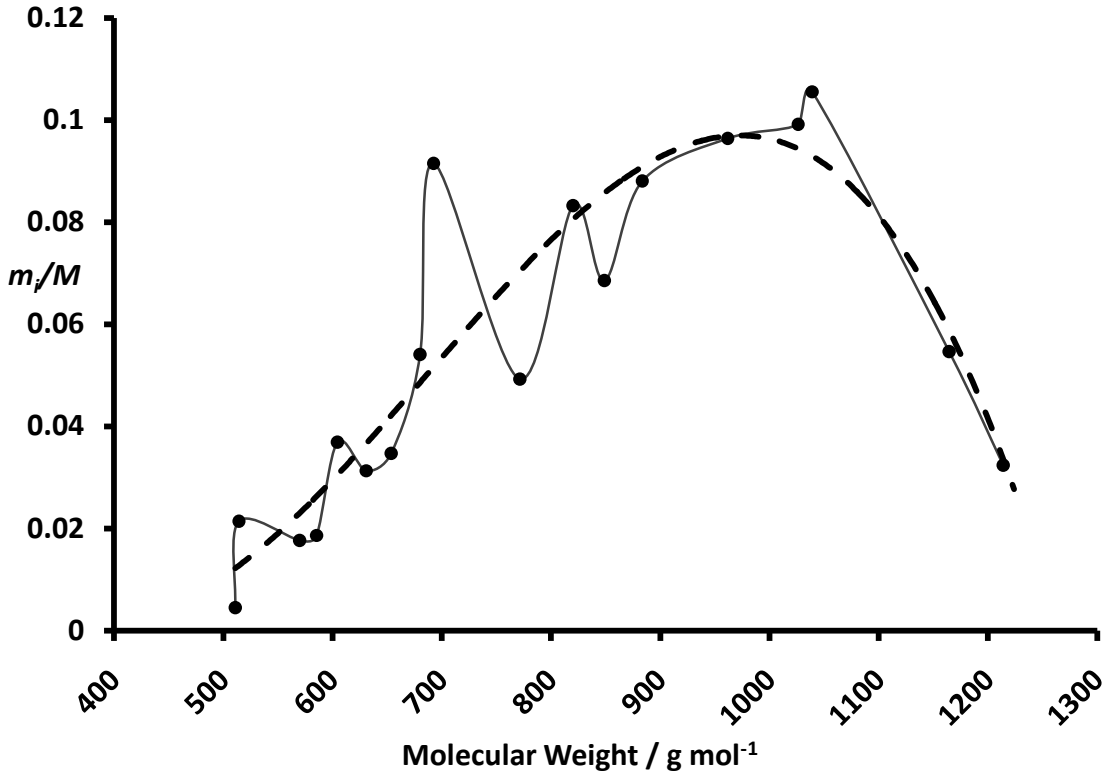


**Figure 3.4: The molecular weight distribution for the PE-OH polymer**

Subsequently the $M_w$, $M_n$ and *PDI* were calculated from the mass fraction and molecular weight data using Equations 1.3, 1.4 and 1.6 (Section 1.3.6). The $M_n$ = 816 gmol$^{-1}$, the $M_w$ = 859 gmol$^{-1}$ and the *PDI* = 1.05. The *PDI* is in reasonable agreement with the value of 1.09 from the supplier, whilst the $M_n$ is significantly higher. We assume that the quoted $M_n$ (700 gmol$^{-1}$ measured with calibrated SEC) and certainly the molecular weight measured by $^1$H NMR spectroscopy (760 gmol$^{-1}$, see Section 3.1.2.1) includes the molecular weight of the non-functional impurity which might well influence the overall $M_n$ of the mixture.

## 3.2 **Monomer synthesis and molecular structure determination.**

### 3.2.1 **Introduction**

In the present work several acrylate and methacrylate monomers were prepared by the esterification of three different long-chain alkyl alcohols (1-docosanol, PE460-OH and PE700-OH) with acryloyl or methacryloyl chloride (Scheme 3.2). The synthesis, purity and purification of the two polyethylene mono-alcohol starting materials have already been discussed (Section 3.1). We chose commercially available high-purity (*ca* 97%) 1-docosanol to prepare an acrylate monomer which would be as similar as possible to those derived from the two PE-OH starting materials, thus providing us with a model system. 1-Docosanol or behenyl alcohol can be prepared by reduction of behenic acid, a natural product extracted from *Moringa Oleifera*, or Ben-oil tree[8]. The main advantages of using 1-docosanol were that the monomers and copolymers derived from it were soluble at room temperature in a few solvents (e.g. toluene or THF) and that it was essentially free from any non-functional alkyl chains. This allowed not only facile characterisation the docosanol-derived products by SEC-MALLS and NMR spectroscopy but also provided copolymers which had a well defined molecular composition, allowing us to rationalise any structure/property relationships with greater certainty.

Esterifications of the type used in the present work between an acid chloride and an alcohol are long established and well-known reactions for preparing methacrylates and acrylates[9]. Acryloyl or methacryloyl chloride can themselves be prepared by heating methacrylic or acrylic acid with benzoyl chloride in the presence of hydroquinone to prevent polymerisation[10]. Although the acid chlorides used in this reaction are moisture-sensitive and tend to be toxic, lachrymatory and corrosive, they are readily available, inexpensive and were found to provide relatively clean reactions with high yield. The presence of a base is essential to activate the reaction and to neutralise the acid by-product produced. If the acid generated is not neutralised it can catalyse hydrolysis of the ester and may add across the double bond of the methacrylate or acrylate. Stoichiometric amounts of base are required, with

tertiary amines such as pyridine or inorganic bases like sodium bicarbonate being common choices.

### 3.2.2 **Polyethylene-based and docosyl monomers.**

The PE macromonomers and docosyl acrylate were prepared in high yield by esterification of the two polyethylene mono-alcohols (nominal $M_n$ = 460 and $M_n$ = 700 gmol$^{-1}$) and docosanol with either acryloyl chloride or methacryloyl chloride (Scheme 3.2).

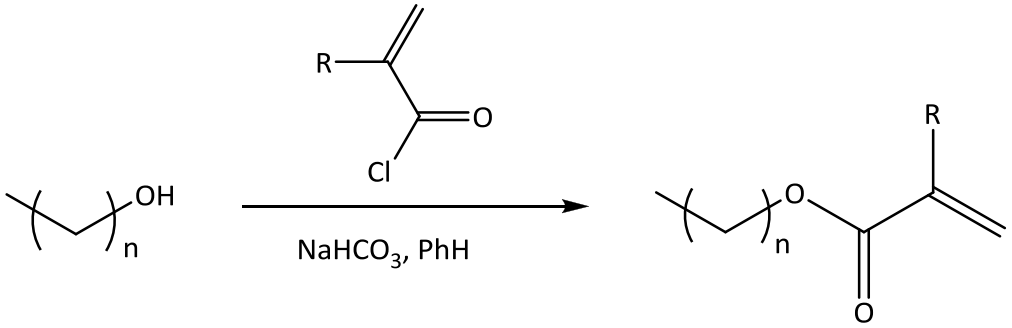


**Scheme 3.2: PE Macromonomer synthesis *via* esterification. R = H or $CH_3$. n = 21, ~31, or ~48.**

The esterification reactions were stirred at 112 °C for 4 hours in toluene under a nitrogen atmosphere. The polyethylene macromonomers (**PE700Ac, PE700MAc**, **PE460Ac** and **PE460MAc**) were isolated by adding the hot reaction mixture into cold methanol and the resulting white precipitate was collected by filtration and dried under reduced pressure at 40 ºC to a constant mass. Further purification (e.g. either aqueous washes or chromatography to remove inhibitors) was problematic due to the insolubility of all of the PE-based macromonomers in any solvent at ambient temperatures, requiring hot aromatic solvents (e.g. toluene at 75 °C). However, since high conversions were observed for all of these reactions by $^1$H NMR spectroscopy (at high temperatures for PE-based materials), further purification was not necessary. Since docosanol and docosyl acrylate (DocAc) were found to dissolve in toluene at room temperature, the product of this reaction was isolated by washing a dilute toluene solution of the reaction mixture with brine, drying the organic layer over

sodium sulfate and removing the solvent under reduced pressure. The product was further purified to remove the inhibitor (methoxyhydroquinone, present in the acryloyl chloride at 5 ppm) by dissolving it in toluene and passing the resulting solution through a short column of neutral alumina, eluting with toluene. The eluant was concentrated under reduced pressure to provide a white solid (this step significantly reduced the yield presumably due to losses on the column). The esterification reactions were first attempted on a 5 g scale and once found to be successful this was subsequently increased to 20 g and 30 g for the **PE700Ac** and **PE460Ac**. Macromonomer data are shown in Table 3.2

**Table 3.2: Data for the acrylate and methacrylate macromonomers prepared.**

| Sample | alcohol mass / g mol$^{-1}$ | Isolated Yield / % |
|---|---|---|
| **DocAc** | 326 (docosyl) | 67 |
| **PE460Ac (1)** | ~460 | 85 |
| **PE460Ac (2)** | ~460 | 82 |
| **PE700Ac (1)** | ~700 | 97 |
| **PE700Ac (2)** | ~700 | 95 |
| **PE700Ac (3)** | ~700 | 90 |
| **PE460MAc (1)** | ~460 | 79 |
| **PE460MAc (2)** | ~460 | 78 |
| **PE700MAc** | ~700 | 92 |

The macromonomers were characterised by $^{1}$H NMR and FT-IR spectroscopy. The polyethylene acrylate and methacrylate NMR spectra were recorded in $d_8$-toluene at 80 ºC to keep the polymers in solution. Comparison of the corresponding spectra of the PE-OH starting material and reaction product (PE-(M)Ac) clearly showed the shifted resonance for the methylene protons next to the oxygen (PE-OH: -C$H_2$-OH at δ 3.3 ppm vs. PE-(M)Ac: -C$H_2$-OCO- at δ 3.9 ppm ) and the additional resonances due to the vinyl protons of the monomer. In the spectra recorded for the polyethylene mono-alcohols the -$CH_2$-O*H* proton resonance was obscured by the resonance due to the residual Ar-$CH_3$ protons from the NMR solvent, toluene.

Recording the $^{1}$H NMR spectrum of docosanol in $CDCl_3$ allowed this resonance to be seen, but both polyethylene alcohols were insoluble in this solvent necessitating the use of $d_8$-toluene.

There was no evidence from $^{1}$H NMR spectra of polymerisation in any of the esterification reactions, this may have been a problem as the acrylates and methacrylates are known to polymerise thermally. Presumably the inhibitors present in the methacryloyl and acryloyl chlorides were sufficient to prevent polymerisation. If there was any sign of polymerisation then a small amount of additional inhibitor (e.g. 2 mg of hydroquinone) could have been added at any stage where the monomers were heated. The lack of any observed polymerisation during the esterification reactions suggests that the macromonomers are relatively stable (compared to MMA or MA for example). This seemingly low reactivity compared to essentially isoelectronic monomers can be explained by the 'diluting' effect of the long alkyl chain, a phenomenon which was also observed when the macromonomers were (co)polymerised (see Section 3.3.1).

When the FT-IR spectrum of the polyethylene alcohol was compared to that of both the methacrylate and acrylate monomers, the disappearance of the broad –OH peak (3341 $cm^{-1}$) and the appearance of peaks due to a conjugated alkene (1635 $cm^{-1}$) clearly show the successful progress of both reactions. The carbonyl peaks, present in the acrylate and methacrylate (1729 $cm^{-1}$) are diagnostic of an ester, although these do overlap with another peak in the starting material.

### 3.2.3 **Branched alkyl acrylate monomer, 2-hexadecyl icosanyl acrylate; B36Ac.**

The novel branched monomer, 2-hexadecyl icosanyl acrylate (**B36Ac**) was prepared by esterification of the commercially available Guerbert alcohol[11] 2-hexadecyl icosanol with acryloyl chloride (Scheme 3.3). We reasoned that a copolymer derived from this branched co-monomer might reduce the degree of crystallinity or number of any hydrocarbon domains, and hence reduce the mechanical strength whilst possessing a similar alkyl side-chain content to a corresponding copolymer derived from **PE460Ac**. In addition copolymers derived from **B36Ac** might have better solubility compared to linear **PE460Ac/PE700Ac** derived copolymers not only as the

side chains cannot pack so efficiently but also since they are essentially free from non-functional alkyl impurities. The **B36Ac** monomer and copolymers derived from it (Section 3.3.7) were indeed soluble at room temperature in some solvents (e.g. THF, $CHCl_3$, or toluene) allowing facile characterisation and were studied in our structure/property evaluation (Section 3.5.9).

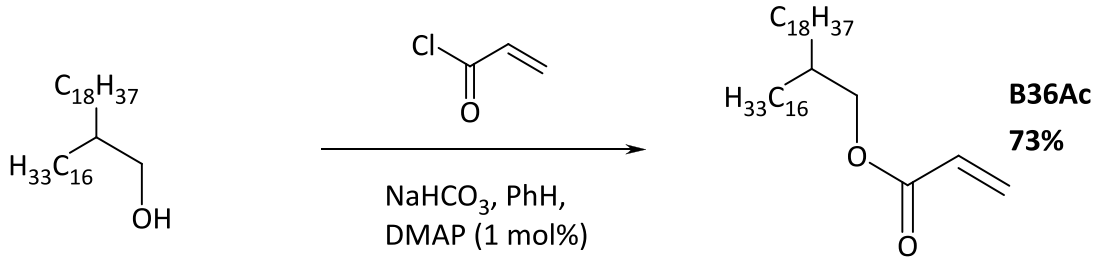


**Scheme 3.3: The synthesis of the 2-hexadecyl icosanyl acrylate monomer 'B36Ac'.**

Using the catalyst dimethylaminopyridine (DMAP) allowed the reaction to proceed at a lower temperature with quantitative conversion indicated by $^1$H NMR spectroscopy. The crude product was purified by column chromatography, isolated in good yield (73%) and was stable. The product was soluble in toluene and chloroform under ambient conditions unlike the **PE700Ac** and **PE460Ac** which were only soluble in hot toluene.

## 3.3 Polymer synthesis and characterisation

### 3.3.1 Copolymerisation of the PE460(M)Ac and PE700(M)Ac macromonomers with MA or MMA.

Following a previous study by the author[12] where the same polymerisation was optimised to provide high conversion which was measured by $^1$H NMR spectroscopy, the polymerisation reactions were carried out in a Radleys Carousel 6-position reactor at 90 °C in toluene under nitrogen, with 2 mol% of the initiator AIBN added. Each of the six 250 mL carousel flasks was charged with a different ratio of co-monomers (Scheme 3.4) and oxygen was excluded by sparging with nitrogen. The total reaction time was 24 h and the products were isolated by either precipitation of the hot reaction mixture into methanol (10 times the volume) or by removing the solvent under reduced pressure when the copolymer would not precipitate. The polymers were dried at 40 °C under vacuum to constant mass and were recovered in high yield (Sections 2.2.2.1 and 2.2.2.2). They were characterised where possible by $^1$H NMR spectroscopy (400 or 500 MHz, 80 ºC, 128 scans with $d^8$-toluene as the solvent) and DSC. None of the copolymers prepared from monomers derived from the polyethylene alcohols were sufficiently soluble in THF to perform SEC-MALLS analysis, however some of the most technologically interesting materials were characterised by intrinsic viscosity measurements and subsequently by HT-SEC in trichlorobenzene at 160 °C (Section 3.4).

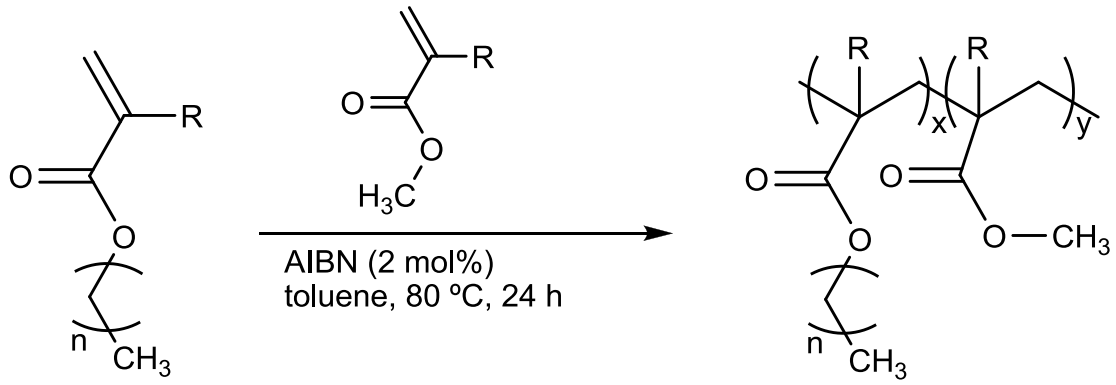


**Scheme 3.4: Copolymerisation of macromonomers. R = H or $CH_3$, n = 21, ~31, ~48.**

**Table 3.3: MA-*co*-docosyl acrylate copolymers.**

| Sample Name | Mass Ratio* | Feed Masses / g | | Recovery | |
|---|---|---|---|---|---|
| | PE:MA | DocAc | MA | mass / g | % |
| **DocAc/MA 1:7.5** | 1:10 | 2.000 | 15.035 | 18.51 | 105† |
| **DocAc/MA 1:3.8** | 1:5.0 | 2.000 | 7.517 | 9.95 | 102† |
| **DocAc/MA 1:0.75** | 1:1.0 | 2.000 | 1.503 | 3.09 | 88 |
| **DocAc/MA 1:0.38** | 1:0.5 | 2.000 | 0.752 | 2.39 | 87 |
| **DocAc/MA 1:0.075** | 1:0.1 | 2.000 | 0.150 | 1.90 | 88 |

**Table 3.4: MA-*co*-PE460Ac copolymers.**

| Sample | Mass Ratio* | Feed Masses / g | | Recovery | |
|---|---|---|---|---|---|
| | PE:MA | PE460Ac | MA | mass / g | % |
| **PE460Ac/MA 1:8.4** | 1:10 | 1.000 | 8.401 | 6.37 | 68 |
| **PE460Ac/MA 1:4.7** | 1:5.6 | 2.000 | 9.460 | 9.76 | 85 |
| **PE460Ac/MA 1:0.95** | 1:1.1 | 5.000 | 4.730 | 8.48 | 87 |
| **PE460Ac/MA 1:0.47** | 1:0.6 | 2.000 | 0.946 | 2.24 | 76 |
| **PE460Ac/MA 1:0.095** | 1:0.1 | 3.000 | 0.284 | 2.91 | 88 |
| **PE460Ac/MA 1:0.047** | 1:0.1 | 3.000 | 0.142 | 2.76 | 88 |
| **PE460Ac comb**‡ | Comb | 3.000 | 0.000 | 2.87 | 96 |

* This refers to the mass ratio of pendant PE chains to poly[(meth) acrylate] chains in the final polymer.
† The reaction solvent proved impossible to remove completely from these materials.
‡ i.e. a homopolymer of PE460Ac.

**Table 3.5: MA-*co*-PE700Ac copolymers.**

| Sample | Mass Ratio* | Feed Masses / g | | Recovery | |
|---|---|---|---|---|---|
| | PE:MA | PE700Ac | MA | mass / g | % |
| **PE700Ac/MA 1:9.0** | 1:10 | 1.000 | 8.962 | 6.27 | 63 |
| **PE700Ac/MA 1:5.0** | 1:5.5 | 2.000 | 9.938 | 8.36 | 70 |
| **PE700Ac/MA 1:0.99** | 1:1.1 | 2.000 | 1.988 | 3.53 | 88 |
| **PE700Ac/MA 1:0.50** | 1:0.6 | 3.000 | 1.490 | 4.13 | 92 |
| **PE700Ac/MA 1:0.10** | 1:0.1 | 3.000 | 0.298 | 3.19 | 97 |
| **PE700Ac/MA 1:0.05** | 1:0.1 | 3.000 | 0.149 | 3.09 | 98 |
| **PE700Ac comb**† | Comb | 3.000 | 0.000 | 2.96 | 99 |

**Table 3.6: MMA-*co*-PE460MAc copolymers.**

| Sample | Mass Ratio* | Feed Masses / g | | Recovery | |
|---|---|---|---|---|---|
| | PE:MMA | PE460MAc | MMA | mass / g | % |
| **PE460MAc/MMA 1:4.5** | 1:5.6 | 2.000 | 9.091 | 8.87 | 80 |
| **PE460MAc/MMA 1:0.76** | 1:1.1 | 3.000 | 2.273 | 5.17 | 90 |
| **PE460MAc/MMA 1:0.38** | 1:0.5 | 3.000 | 1.136 | 4.10 | 94 |
| **PE460MAc/MMA 1:0.091** | 1:0.1 | 3.000 | 0.273 | 3.13 | 96 |
| **PE460MAc/MMA 1:0.045** | 1:0.1 | 3.000 | 0.136 | 2.96 | 94 |
| **PE460MAc comb**‡ | Comb | 3.000 | 0.000 | 2.92 | 98 |

* This refers to the mass ratio of pendant PE chains to poly[(meth) acrylate] chains in the final polymer.
† i.e. a homopolymer of PE700Ac.
‡ i.e. a homopolymer of PE460MAc.

**Table 3.7: MMA-co-PE700MAc copolymers.**

| Sample | Mass Ratio* | Feed Masses / g | | Recovery | |
|---|---|---|---|---|---|
| | PE:MMA | PE700MAc | MMA | mass / g | % |
| **PE700MAc/MMA 1:8.8** | 1:10 | 1.000 | 8.776 | 8.23 | 84 |
| **PE700MAc/MMA 1:4.4** | 1:5 | 2.000 | 8.757 | 9.45 | 88 |
| **PE700MAc/MMA 1:0.88** | 1:1 | 4.000 | 3.503 | 6.84 | 91 |
| **PE700MAc/MMA 1:0.44** | 1:0.5 | 5.000 | 2.189 | 6.86 | 95 |

### 3.3.2 **"Crossed acrylate/methacrylate" copolymers**

"Crossed acrylate/methacrylate" **PE700Ac/MMA** and **PE700MAc/MA** copolymers were prepared and then characterised by $^{1}$H NMR spectroscopy. These were made by the same methodology and in the same monomer ratios as the **PE700Ac/MA** and **PE700MAc/MMA** materials which are discussed in section 3.3.1. Although molecular weight data could not be collected due to the lack of solubility in THF, the $^{1}$H NMR spectra of the copolymers showed high conversion (Table 3.8).

**Table 3.8: Crossed acrylate/methacrylate copolymer data.**

| Sample | Mass Ratio* | Feed masses | | recovery | |
|---|---|---|---|---|---|
| | PE:MA | PE700(M)Ac / g | (M)MA / g | mass / g | % |
| **PE700MAc/MA 1:8.8** | 1:10 | 0.500 | 4.379 | 4.73 | 94 |
| **PE700MAc/MA 1:4.4** | 1:5 | 1.000 | 4.379 | 5.40 | 97 |
| **PE700MAc/MA 1:0.9** | 1:1 | 1.000 | 0.876 | 1.29 | 67 |
| **PE700Ac/MMA 1:9.0** | 1:10 | 0.500 | 4.481 | 5.01 | 98 |
| **PE700Ac/MMA 1:4.5** | 1:5 | 1.000 | 4.481 | 5.56 | 99 |

* This refers to the mass ratio of pendant PE chains to poly[(meth) acrylate] chains in the final polymer.

### 3.3.3 Co-polymerisation of the macromonomers with 2-ethylhexyl (meth)acrylates.

Working on the assumption that having a high $T_g$ was responsible for the poor mechanical properties (see Section 3.5.3) of the all-methacrylate (**PE700MAc/MMA** and **PE460MAc/MMA**) copolymers (Section 3.3.1), new comonomers were sought that would allow the polymer backbone to be methacrylate-based whilst still possessing a lower $T_g$. Using either 2-ethylhexyl methacrylate (**EHMA**) or 2-ethylhexyl acrylate co-monomers along with a PE-based acrylate or methacrylate macromonomer (**PE700MAc**, **PE700Ac** or **PE460Ac**), a series of polymers were prepared with various combinations and ratios of monomers (Scheme 3.5). The copolymers were prepared by free-radical polymerisation using the same method as previous examples using the Radleys six-position parallel carousel reactor and again were recovered in high yield. They were characterised by $^1$H NMR spectroscopy and DSC where possible but were insoluble in THF preventing SEC-MALLS analysis. The mass ratio specified in the tables refers to the projected final mass ratio of PE segments to P(M)MA backbone content in the final product, however this ratio could not be confirmed with $^1$H NMR spectroscopy as the resonances due to the -C*H*$_2$O- protons from both monomers overlapped.

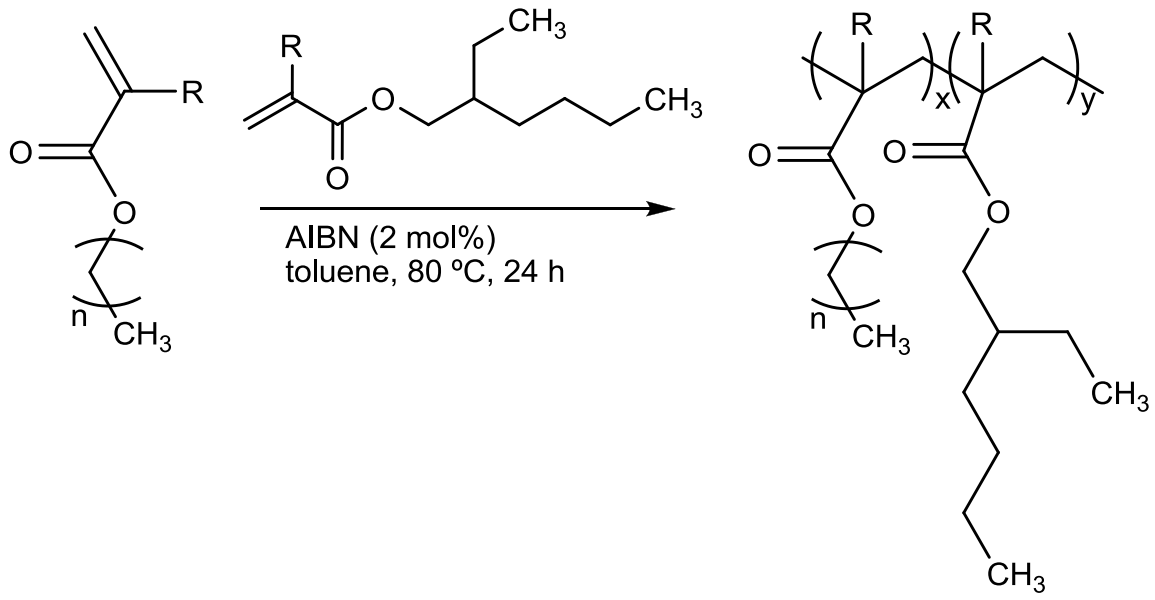


**Scheme 3.5: The copolymerisation of polyethylene macromonomers with 2-EH(M)A. R = H or $CH_3$, n = 21, ~31, ~48.**

In the case of a copolymerisation involving acrylate and methacrylate comonomers, it is possible that composition drift may occur due to the difference in reactivity ratios of the two co-monomers. For example, for the **PE700Ac/EHMA** copolymers this would result in a copolymer architecture where, statistically, the polymer chains from early in the reaction are methacrylate-rich (i.e. 'PMMA'-rich) as the methacrylate monomer has higher reactivity towards the propagating radical while chains generated later in the reaction when the methacrylate is at a lower concentration would be acrylate-rich. Unfortunately this effect could not be measured from the characterisation techniques used. **EHMA** is also more non-polar than **MMA** so incorporating it may also have contributed toward making the copolymer more compatible with polyolefin surfaces. Relevant data for all of the **EHA** and **EHMA** copolymers are shown in Tables 3.9—3.13.

**Table 3.9: EHMA-*co*-PE700MAc copolymer data.**

| Sample | Mass ratio* | Feed masses / g | | Recovery | |
|---|---|---|---|---|---|
| | PE:MA | PE700MAc | EMHA | mass / g | % |
| **PE700MAc/EHMA 1:24.1** | 1:10 | 1.000 | 24.112 | 24.91 | 99 |
| **PE700MAc/EHMA 1:12.1** | 1:5 | 1.000 | 12.056 | 13.01 | 99 |
| **PE700MAc/EHMA 1:2.4** | 1:1 | 2.000 | 4.822 | 6.49 | 95 |
| **PE700MAc/EHMA 1:1.2** | 1:0.5 | 2.000 | 2.411 | 4.16 | 94 |

**Table 3.10: EHMA-*co*-PE700Ac copolymer data**

| Sample | Mass ratio* | Feed masses / g | | Recovery | |
|---|---|---|---|---|---|
| | PE:A | PE700Ac | EHMA | mass / g | % |
| **PE700Ac/EHMA 1:24.1** | 1:10 | 1.000 | 24.112 | 20.37 | 81 |
| **PE700Ac/EHMA 1:19.3** | 1:8 | 0.250 | 4.822 | 5.00 | 84 |
| **PE700Ac/EHMA 1:16.9** | 1:7 | 0.250 | 4.220 | 4.46 | 98 |
| **PE700Ac/EHMA 1:14.5** | 1:6 | 0.500 | 7.234 | 7.24 | 92 |
| **PE700Ac/EHMA 1:12.1** | 1:5 | 1.000 | 12.056 | 10.74 | 82 |
| **PE700Ac/EHMA 1:9.6** | 1:4 | 0.500 | 4.822 | 5.39 | 99 |
| **PE700Ac/EHMA 1:7.2** | 1:3 | 0.500 | 3.617 | 4.11 | 98 |
| **PE700Ac/EHMA 1:2.4** | 1:1 | 2.000 | 4.822 | 6.46 | 95 |
| **PE700Ac/EHMA 1:1.2** | 1:0.5 | 2.000 | 2.411 | 4.24 | 96 |

* This refers to the mass ratio of pendant PE chains to poly[(meth) acrylate] chains in the final polymer.

**Table 3.11: EHA-*co*-PE700Ac copolymer data**

| Sample | Mass ratio* | Feed masses / g | | Recovery | |
|---|---|---|---|---|---|
| | PE:A | PE700Ac | EHA | mass / g | % |
| **PE700Ac/EHA 1:4.5** | 1:5 | 2.000 | 8.962 | 10.58 | 96 |
| **PE700Ac/EHA 1:2.2** | 1:1 | 2.000 | 4.822 | 6.18 | 91 |
| **PE700Ac/EHA 1:1.1** | 1:0.5 | 2.000 | 2.411 | 4.09 | 93 |
| **PE700Ac/EHA 1:0.24** | 1:0.1 | 3.000 | 0.723 | 3.58 | 96 |

**Table 3.12: EHA-*co*-PE700MAc copolymer data**

| Sample | Mass ratio* | Feed masses / g | | Recovery | |
|---|---|---|---|---|---|
| | PE:MA | PE700MAc | EHA | mass / g | % |
| **PE700MAc/EHA 1:4.5** | 1:10 | 0.500 | 12.056 | 12.17 | 97 |
| **PE700MAc/EHA 1:2.2** | 1:5 | 0.500 | 6.028 | 6.12 | 94 |
| **PE700MAc/EHA 1:1.1** | 1:1 | 2.000 | 4.822 | 6.17 | 90 |
| **PE700MAc/EHA 1:0.24** | 1:0.5 | 2.000 | 2.411 | 3.97 | 90 |

* This refers to the mass ratio of pendant PE chains to poly[(meth) acrylate] chains in the final polymer.

### 3.3.4 **Copolymerisation of the PE700Ac with linear alkyl methacrylates.**

A further two series of copolymers were derived from the **PE700Ac** monomer, this time using the comonomers dodecyl and butyl methacrylate, using similar synthetic conditions. We reasoned that copolymers derived from there monomers would, like those incorporating 2-ethylhexyl side-chains, have lower glass transition temperatures than the corresponding **PE700MAc/MMA** copolymers whilst having a poly(methacrylate) backbone (Tables 3.14 and 3.15).

**Table 3.13: Dodecyl methacrylate-*co*-700acrylate copolymer data**

| Sample | Mass ratio* | Feed masses / g | | Recovery | |
|---|---|---|---|---|---|
| | PE:MA | PE700Ac | DMA | mass / g | % |
| **PE700Ac/DMA 1:25.1** | 1:10 | 0.500 | 12.056 | 12.63 | 99 |
| **PE700Ac/DMA 1:12.1** | 1:5 | 1.000 | 12.056 | 12.58 | 95 |
| **PE700Ac/DMA 1:2.4** | 1:1 | 2.000 | 4.822 | 6.45 | 93 |
| **PE700Ac/DMA 1:1.2** | 1:0.5 | 2.000 | 2.411 | 4.18 | 94 |

**Table 3.14: Butyl methacrylate-*co*-700acrylate copolymer data**

| Sample | Mass ratio* | Feed masses / g | | Recovery | |
|---|---|---|---|---|---|
| | PE:MA | PE700Ac | BMA | mass / g | % |
| **PE700Ac/BMA 1:9.0** | 1:10 | 0.500 | 4.481 | 6.76 | † |
| **PE700Ac/BMA 1:4.5** | 1:5 | 1.000 | 4.481 | 6.29 | † |
| **PE700Ac/BMA 1:0.90** | 1:1 | 2.000 | 1.792 | 3.98 | † |
| **PE700Ac/BMA 1:0.64** | 1:0.5 | 2.000 | 1.272 | 2.87 | 88 |

* This refers to the mass ratio of pendant PE chains to poly[(meth) acrylate] chains in the final polymer.

† Reaction solvent (toluene) proved impossible to remove completely.

### 3.3.5 DocAc/MA copolymers; increasing the molecular weight

A further series of **DocAc/MA** copolymers were prepared under modified synthetic conditions in order to increase the molecular weight obtained relative to those already in-hand (Section 3.2.2). We reasoned that having copolymers of the same composition but with different molecular weights would allow us to study the effect of $M_w$ on apparent adhesive strength. The copolymers were characterised by $^1$H NMR spectroscopy and SEC-MALLS analysis. A molecular weight increase was accomplished by lowering the initiator concentration from 2 mol% to 0.5 wt%, increasing the reaction time (from 24 to 48 h) and decreasing the temperature (from 80 to 60 °C). A comparison of the reaction conditions and analytical data of the two series of **DocAc/MA** copolymers is shown in Table 3.15.

**Table 3.15: Comparison of high (A) and low (B) molecular weight DocAc copolymers**

| Sample | Ratio* | Feed masses | | Recovery | | SEC-MALLS data | | |
|---|---|---|---|---|---|---|---|---|
| | PE:MA | DocAc / g | MA / g | mass / g | % | $M_n$ / g mol$^{-1}$ | $M_w$ / g mol$^{-1}$ | PDI |
| **DocAc/MA 1:7.5B** | 1:10 | 2.000 | 15.035 | 18.51 | 105† | 10,700 | 80,500 | 7.5 |
| ***DocAc/MA 1:7.5A*** | | *1.000* | *7.517* | *7.45* | *87* | *124,700* | *220,500* | *1.8* |
| **DocAc/MA 1:3.8B** | 1:5.0 | 2.000 | 7.517 | 9.95 | 102† | 12,300 | 58,600 | 4.8 |
| ***DocAc/MA 1:3.8A*** | | *2.000* | *7.517* | *8.28* | *87* | *88,000* | *167,100* | *1.9* |
| **DocAc/MA 1:0.75B** | 1:1.0 | 2.000 | 1.503 | 3.09 | 88 | 18,300 | 41,100 | 2.3 |
| ***DocAc/MA 1:0.75A*** | | *2.000* | *1.503* | *2.92* | *83* | *32,400* | *67,900* | *2.1* |
| **DocAc/MA 1:0.38B** | 1:0.5 | 2.000 | 0.752 | 2.39 | 87 | 13,500 | 27,800 | 2.1 |
| ***DocAc/MA 1:0.38A*** | | *2.000* | *0.752* | *2.32* | *84* | *24,600* | *46,700* | *1.9* |
| **DocAc/MA 1:0.075B** | 1:0.1 | 2.000 | 0.150 | 1.90 | 88 | 9,700 | 15,700 | 1.6 |
| ***DocAc/MA 1:0.075A*** | | *2.000* | *0.150* | *1.586* | *73* | Not Measured‡ | | |

* This refers to the mass ratio of pendant PE chains to poly(acrylate) chains
† Reaction solvent (toluene) proved impossible to remove completely.
‡ Not measured due to low conversion

All of the new copolymers, shown in italics, were formed in high yield and high conversion (by $^{1}$H NMR spectroscopy) except **DocAc/MA 1:0.075A** (41%) (Table 3.15), and indeed as targeted these were systematically of higher molecular weight than the first series. The low conversion of this last example is likely to be a result of the reaction mixture being too dilute. Since the reaction conditions used to prepare the initial, lower molecular weight copolymers had been chosen to improve the conversion of the macromonomer-rich systems, this was therefore not an unexpected result. A general trend can be seen where molecular weight ($M_n$ or $M_w$) decreases as the fraction of macromonomer increases. The reason for this is likely to be the decreasing concentration of polymerisable double bonds as more macromonomer is added since the alkyl chain and the reaction solvent both dilute the reaction mixture.

### 3.3.6 DocAc/MA copolymers; decreasing the molecular weight

To fully investigate the effect of molecular weight on adhesive strength it was necessary to prepare, characterise and evaluate the adhesive strength of low and high molecular weight copolymers. The **DocAc/MA 1:3.8** and **1.7.5** copolymers were chosen as they performed reasonably well in the ASTM adhesive tests and have the advantage (over the **PE700Ac** or **PE460Ac**-based materials) of being soluble in THF which allowed their molecular weight to be determined by SEC-MALLS. The preparation of high molecular weight DocAc/MA copolymers has been already been discussed (Section 3.3.5)

In order to reduce the degree of polymerisation the chain transfer agent dodecanethiol (DDT) was used. This was added in increasing concentration to a series of five copolymerisation reactions which had the same concentration of monomers and initiator. The process was repeated for both the **DocAc/MA 1:1.38** (Table 3.16) and **DocAc/MA 1:7.5** (Table 3.17) copolymers and all of the polymerisations were carried out at 60 °C.

**Table 3.16: Data for DocAc/MA 1:3.8 copolymerisations with added chain transfer agent**

| Sample | Ratio* PE:MA | DDT mol%† | Recovery mass / g | Recovery % | SEC-MALLS data $M_n$ / g mol$^{-1}$ | SEC-MALLS data $M_w$ / g mol$^{-1}$ | PDI |
|---|---|---|---|---|---|---|---|
| **DocAc/MA 1:3.8C** | 1:5 | 0.5 | 1.816 | 76 | 21,200 | 28,400 | 1.3 |
| **DocAc/MA 1:3.8D** | 1:5 | 1.0 | 1.506 | 63 | 13,700 | 17,300 | 1.3 |
| **DocAc/MA 1:3.8E** | 1:5 | 1.5 | 1.464 | 62 | 11,100 | 13,300 | 1.2 |
| **DocAc/MA 1:3.8F** | 1:5 | 2.0 | 1.224 | 51 | 9,200 | 11,200 | 1.2 |
| **DocAc/MA 1:3.8G** | 1:5 | 3.0 | 1.201 | 50 | 6,200 | 7,500 | 1.2 |

**Table 3.17: Data for DocAc/MA 1:7.5 copolymerisations with added chain transfer agent**

| Sample | Ratio* PE:MA | DDT mol%† | Recovery mass / g | Recovery % | SEC-MALLS data $M_n$ / g mol$^{-1}$ | SEC-MALLS data $M_w$ / g mol$^{-1}$ | PDI |
|---|---|---|---|---|---|---|---|
| **DocAc/MA 1:7.5C** | 1:10 | 0.5 | 1.286 | 60 | 26,900 | 34,700 | 1.3 |
| **DocAc/MA 1:7.5D** | 1:10 | 1.0 | 1.104 | 51 | 17,200 | 21,900 | 1.3 |
| **DocAc/MA 1:7.5E** | 1:10 | 1.5 | 1.055 | 48 | 12,700 | 15,600 | 1.2 |
| **DocAc/MA 1:7.5F** | 1:10 | 2.0 | 1.226 | 55 | 11,500 | 13,900 | 1.2 |
| **DocAc/MA 1:7.5G** | 1:10 | 3.0 | 0.764 | 34 | 7,700 | 9,500 | 1.2 |

Again as targeted these were all of lower molecular weight than the first series of copolymers. Indeed the data from these two series of polymerisations allowed the chain transfer constant for DDT to be calculated for each composition using a Mayo plot (Figure 3.5). There is also a trend of decreasing recovery with decreasing molecular weight; this is likely to be a result of soluble oligomer formation in the

* This refers to the mass ratio of pendant alkyl chains to poly(acrylate) chains in the final polymer.

† The mol% of DDT was based on the number of moles of polymerisable double bonds in the initial comonomer mixture.

presence of the CTA, since high conversions were observed in all cases. Oligomeric or low molecular weight polymeric species which are soluble in the non-solvent used during purification will be removed at this stage. Since the addition of DDT lowers the molecular weight average, the amount of low molecular weight species increases as the concentration of the CTA increases which decreases the recovery.

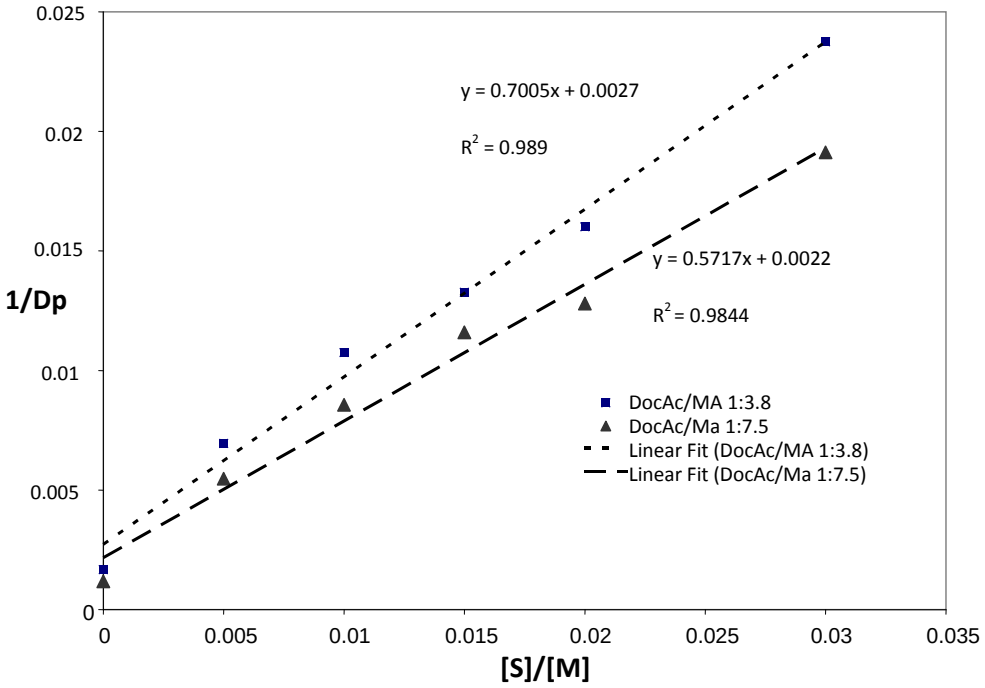


**Figure 3.5: Mayo plots for the DocAc/MA 1:3.8 and DocAc/MA 1:7.5 copolymers**

The Mayo plot for each series of polymerisations was found to be linear and the two values for the chain transfer constant (CTC) for both were ~0.6-0.7, which is indicative of efficient chain transfer for both compositions. Although specific data is not available in the literature for this copolymerisation, CTC values for similar monomers with DDT compare favourably to those found in this work, for example methyl methacrylate polymerised in the presence of 1-dodecanethiol has a CTC of 0.7 at 60 °C[13].

### 3.3.7 Preparation of the B36Ac/MA and PE700Ac/B36Ac/MA branched side chain co- and ter-polymers

To investigate the effect on adhesive strength of side-chain branching in the polyalkane graft chains four novel copolymers were prepared using the monomer **B36Ac**. Since PE:MA composition ratios of 1:10 and 1:5 had previously been shown to be favourable for good adhesion, these were chosen for the new copolymers. Two copolymers, **B36Ac/MA 1:4.2** and **B36Ac/MA 1:8.4,** were prepared, characterised (by $^{1}$H NMR spectroscopy and SEC-MALLS analysis) and evaluated in ASTM adhesion tests. A further two terpolymers, **PE700Ac/B36Ac/MA 1:2.2:29.0** and **PE700Ac/B36Ac/MA 1:2.2:14.5** were also prepared and characterised by $^{1}$H NMR spectroscopy (insolubility in THF prevented SEC-MALLS analysis). All four polymers were formed with high conversion and isolated in excellent yields (Table 3.18).

**Table 3.18: Data for co- and ter-polymers prepared from the B36Ac monomer**

| Sample | Feed masses / g | | | Recovery | SEC-MALLS data | | |
|---|---|---|---|---|---|---|---|
| | PE700Ac | B36Ac | MA | % | $M_n$ / g mol$^{-1}$ | $M_w$ / g mol$^{-1}$ | PDI |
| **B36Ac/MA 1:8.4** | 0 | 1.000 | 8.426 | 96 | 14,500 | 73,500 | 5.1 |
| **B36Ac/MA 1:4.2** | 0 | 1.000 | 4.213 | 97 | 20,800 | 57,700 | 2.8 |
| **PE700Ac/B36Ac/ MA 1:2.2:29.0** | 0.309 | 0.691 | 8.962 | 98 | Polymers were insoluble in THF; SEC-MALLS analysis was not possible. | | |
| **PE700Ac/B36Ac/ MA 1:2.2:14.5** | 0.309 | 0.691 | 4.481 | 99 | | | |

It was interesting to note that the two **B36Ac/MA** copolymers were freely soluble in THF whilst the corresponding **PE460Ac/MA** materials, with a similar alkyl chain length, were not. The branched side chain **B36Ac/MA** is likely to disrupt packing and hence lower the crystallinity of the copolymer, improving solubility. The presence of linear, non-functional PE impurities (Section 3.1) in the **PE700Ac/MA** and **PE460Ac/MA** copolymers also seems to have a detrimental effect on their

solubility. It seems likely that the presence of the non-functional PE certainly increases the crystallinity and probably worsens solubility compared to pure copolymers. It is also likely that the non-functional impurities themselves have poor solubility compared to that of the copolymers derived from the PE-OH starting materials.

## 3.4 Molecular weight determination of the copolymers

### 3.4.1 Introduction

The most interesting copolymers in terms of their adhesion performance were derived from either **PE700Ac** or **PE460Ac** and these were found to be insoluble in THF and hence could not be analysed on our in-house SEC-MALLS instrument. It was imperative that the molecular weight and molecular weight distributions were determined for these materials in particular as differences could affect the mechanical and adhesive properties and render any structure/property comparisons invalid. Two approaches to determining the molecular weight data of these materials were undertaken: i) intrinsic viscosity (IV) measurements and ii) high-temperature size exclusion chromatography (HT-SEC-viscosity and HT-SEC-calibrated). IV measurements were extremely time-consuming and so were limited to four of the **PE700Ac/MA** series of copolymers. The number of samples which could be characterised by HT-SEC was limited to 20 as the service was out-sourced.

### 3.4.2 Intrinsic viscosity measurements

The **PE700Ac/MA** series of copolymers were analysed by dilute solution viscometry to compare their intrinsic viscosity, $[\eta]$, which gives an indication of their molecular weight relative to one another, a phenomenon first observed by Staudinger[14]. With the copolymers being novel however, values were not known for the two Mark-Houwink-Sakurada[15] (MHS) constants, which would have allowed the molecular weight to be calculated. The measurements were carried out in replicates of six for each dilution at 40°C in *m*-cresol using a size 0B Ubbelohde viscometer and the values for $[\eta]$ are presented in Table 3.19.

**Table 3.19: IV measurement data for the PE700Ac/MA copolymers**

| Material | Mass ratio PE:MA | $[\eta]$ / mL $g^{-1}$ | Comments |
|---|---|---|---|
| **PE700Ac/MA 1:9.0** | 1:10 | **41.0** | soluble at 2 wt% |
| **PE700Ac/MA 1:5.0** | 1:5.5 | **36.0** | soluble at 2 wt% |
| **PE700Ac/MA 1:0.99** | 1.1:1 | **20.0** | Only isotropic in dilute conditions (> 1 wt %)* |
| **PE700Ac/MA 1:0.50** | 1:0.5 | **10.0** | Only isotropic in dilute conditions (> 1 wt %)* |

The intrinsic viscosity values appear to show decreasing molecular weight for increasing PE content in the copolymers. It may not however be acceptable to compare the $[\eta]$ values to one another as the copolymers have a grafted architecture and therefore a might behave differently in solution according to their composition, i.e. the values of the two MHS constants, *K* and *a*, could vary with monomer ratio. For a given molecular weight they may have higher or lower intrinsic viscosity depending on the degree of grafting. Copolymers with a higher PE content have more grafts than those with less and it is possible that this is reflected in the values of $[\eta]$ measured. It is possible however that the MA-rich copolymers simply have larger molecular weights and the effect of the degree of grafting on viscosity is small in comparison. However the effect of grafting seems to be small as the results corresponded well to the $M_w$ averages obtained subsequently by HT-SEC-viscosity analysis of the same series of copolymers (Section 3.4.3). In addition, the observed trend of decreasing intrinsic viscosity with increasing PE content is consistent with the observed decreasing molecular weight of the **DocAc/MA** copolymers, made under the same reaction conditions, with increasing PE content (Table 3.15).

* During the IV measurements the solution appeared to be slightly cloudy and this seemed to show that the polymer was not fully soluble in the solvent even at this very low concentration. The data collected was however used in the calculation of $[\eta]$ as otherwise there would not have been enough points on the graph.

### 3.4.3 High Temperature SEC

Fifteen samples were submitted to RAPRA for high-temperature size-exclusion chromatography (HT-SEC). The samples chosen for analysis were from the all-acrylate series of copolymers as they represent the most interesting materials and have a broad range of adhesive performance. The **PE700Ac/MA** and **PE460Ac/MA** copolymers, which are insoluble in THF preventing their analysis on our in-house SEC-MALLS instrument, were analysed alongside the analogous **DocAc/MA** series which we had previously characterised in-house to allow comparison of the data from the different chromatographic methods. The HT-SEC results seem to give a good estimation of the $M_w$ for these copolymers however the $M_n$ and polydispersity were not so reliable. Refractive indices for the copolymers analysed by HT-SEC-viscosity were back calculated, assuming 100% mass recovery. A comparison (Section 3.4.5; Table 3.23) of results from our SEC-MALLS and the two high-temperature SEC techniques (viscosity and calibrated) employed by RAPRA aims to show the limitations of each technique in characterising these copolymers.

### 3.4.4 Copolymer synthesis and molecular weight distributions by HT-SEC

**Table 3.20: DocAc/MA copolymer data**

| Sample | Ratio* | Feed masses / g | | Recovery | HT-SEC data / g mol$^{-1}$ | | |
|---|---|---|---|---|---|---|---|
| | Doc:PMA | DocAc | MA | % | $M_w$ | $M_n$ | PDI |
| **DocAc/MA 1:7.5** | 1:10 | 2.000 | 15.035 | † | 85,400 | 29,050 | 3.0 |
| **DocAc/MA 1:3.8** | 1:5.0 | 2.000 | 7.517 | † | 66,550 | 23,200 | 2.9 |
| **DocAc/MA 1:0.75** | 1:1.0 | 2.000 | 1.503 | 88 | 39,750 | 16,100 | 2.4 |
| **DocAc/MA 1:0.38** | 1:0.5 | 2.000 | 0.752 | 87 | 28,300 | 8,500 | 3.3 |
| **DocAc/MA 1:0.075** | 1:0.1 | 2.000 | 0.150 | 88 | 19,900 | 10,600 | 1.9 |

The **DocAc/MA** series of copolymers exhibited a decreasing molecular weight as the concentration of **DocAc** monomer was increased. The PDI values and the molecular

* This refers to the mass ratio of pendant docosyl chains to poly(methyl acrylate) chains in the final polymer.
† Recovery over 100% as the reaction solvent was impossible to completely remove.

weight distributions (Figure 3.6) show that the copolymers are relatively polydisperse. With the exception of **DocAc/MA 1:0.075** which has a low molecular weight all of the other copolymer molecular weight distributions appear to be slightly irregular (*i.e.* not gaussian) and perhaps bimodal. This is likely to be as a result of the high concentration of initiator used.

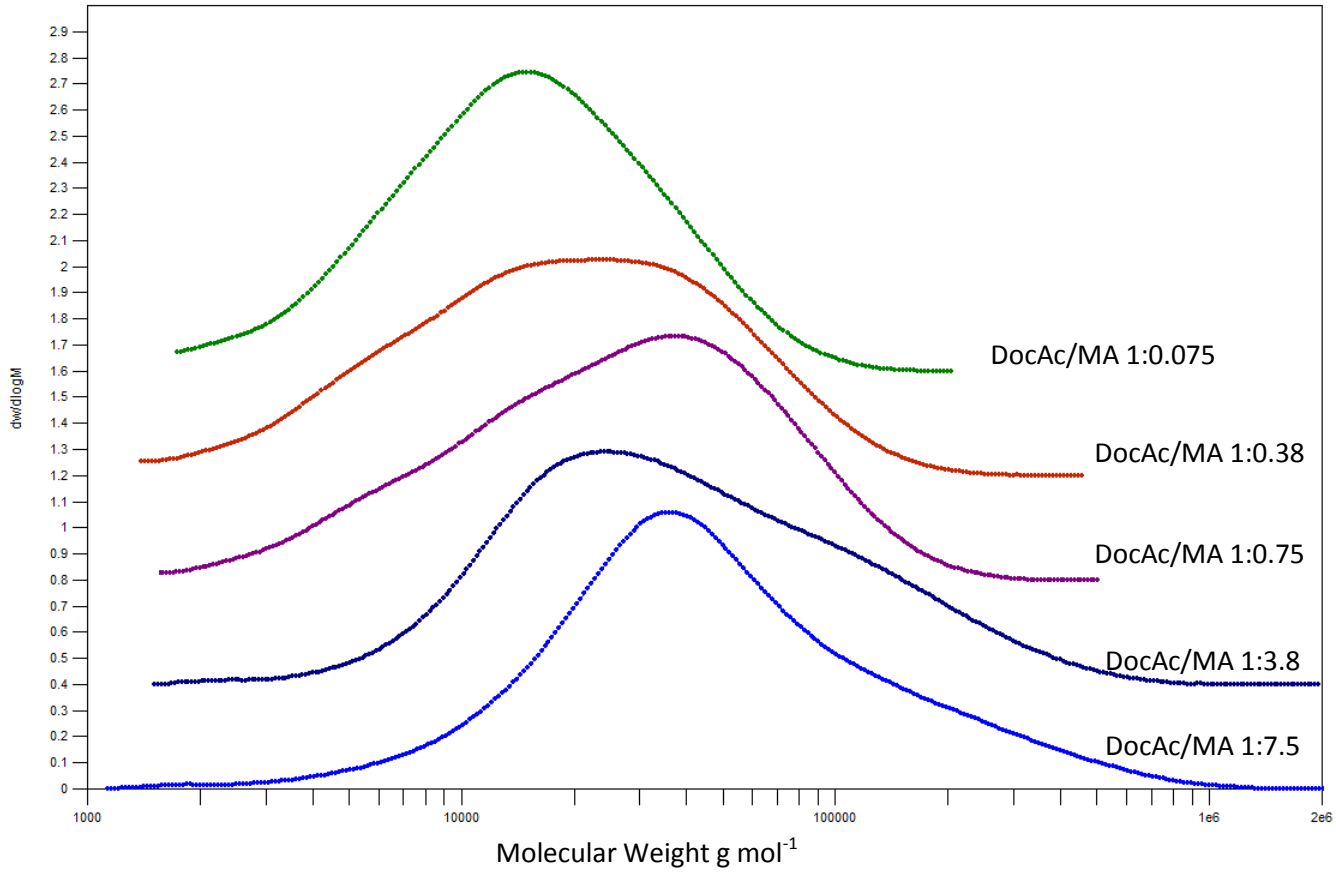


**Figure 3.6: Molecular weight distributions of the DocAc/MA series of copolymers, the distributions have normalised areas.**

**Table 3.21: PE460Ac/MA copolymer data**

| Sample | Ratio* | Feed masses / g | | Recovery | HT-SEC data / g mol$^{-1}$ | | |
|---|---|---|---|---|---|---|---|
| | PE:PMA | PE460Ac | MA | % | $M_w$ | $M_n$ | PDI |
| **PE460Ac/MA 1:8.4** | 1:10 | 1.000 | 8.401 | 68 | 31,800 | 7,850 | 4.0 |
| **PE460Ac/MA 1:4.7** | 1:5.6 | 2.000 | 9.460 | 85 | 33,350 | 6,860 | 4.8 |
| **PE460Ac/MA 1:0.95** | 1:1.1 | 5.000 | 4.730 | 87 | 16,550 | 2,120 | 7.8 |
| **PE460Ac/MA 1:0.47** | 1:0.6 | 2.000 | 0.946 | 76 | 11,100 | 3,020 | 3.7 |
| **PE460Ac/MA 1:0.095** | 1:0.1 | 3.000 | 0.284 | 88 | 7,670 | 1,980 | 4.0 |

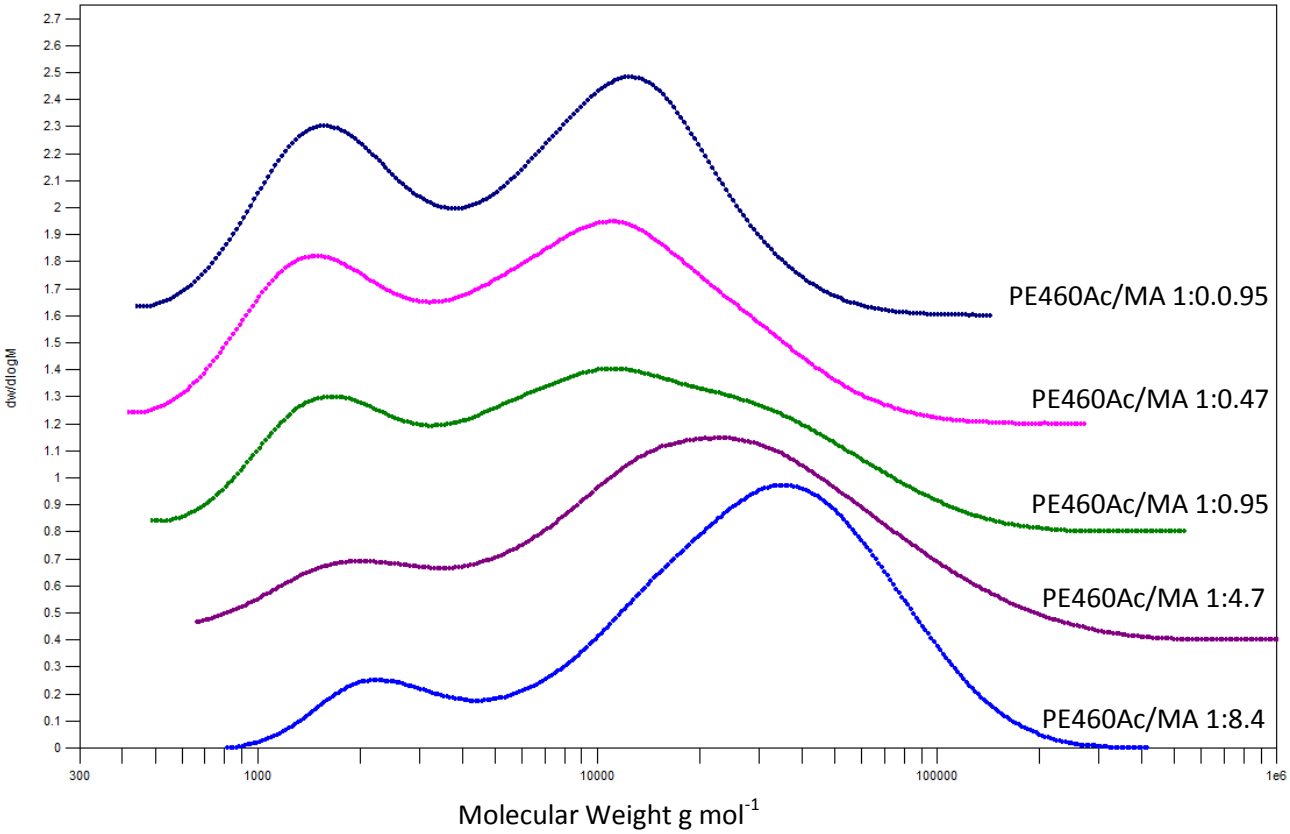


**Figure 3.7: Molecular weight distributions of the PE460Ac/MA series of copolymers, the distributions have normalised areas.**

The distributions for the PE460-based copolymers are bimodal, with the lower molecular weight shoulder or fraction (which appears at around ~1000 g mol$^{-1}$)

* This refers to the mass ratio of pendant PE chains to poly(methyl acrylate) chains in the final polymer.

highly likely to be the linear non-functional PE contaminant, which can be seen to increase as the amount of **PE460Ac** monomer in the feed was increased. Apart from the shoulder at ~1000 g $mol^{-1}$ the distributions for the **PE460Ac/MA 1:8.4, PE460Ac/MA 1:4.7, PE460Ac/MA 1:0.47** and **PE460Ac/MA 1:0.095** copolymers appear to unimodal. The **PE460Ac/MA 1:0.95** copolymer has a slight shoulder toward the high molecular weight end, similar to those seen with some of the **DocAc/MA,** which may again be due to the relatively high concentration of initiator used.

**Table 3.22: PE700Ac/MA copolymer data**

| Sample | Ratio* | Feed masses / g | | Recovery | HT-SEC data / g $mol^{-1}$ | | |
|---|---|---|---|---|---|---|---|
| | PE:PMA | PE700Ac | MA | % | $M_w$ | $M_n$ | PDI |
| **PE700Ac/MA 1:9.0** | 1:10 | 1.000 | 8.962 | 63 | 28,450 | 8,860 | 3.2 |
| **PE700Ac/MA 1:5.0** | 1:5.5 | 2.000 | 9.938 | 70 | 30,800 | 7,380 | 4.2 |
| **PE700Ac/MA 1:0.99** | 1:1.1 | 2.000 | 1.988 | 88 | 14,000 | 4,530 | 3.1 |
| **PE700Ac/MA 1:0.50** | 1:0.6 | 3.000 | 1.490 | 92 | 22,900 | 4,020 | 5.6 |
| **PE700Ac/MA 1:0.10** | 1:0.1 | 3.000 | 0.298 | 97 | 9,560 | 3,020 | 3.2 |

* This refers to the mass ratio of pendant PE chains to poly(methyl acrylate) chains in the final polymer.

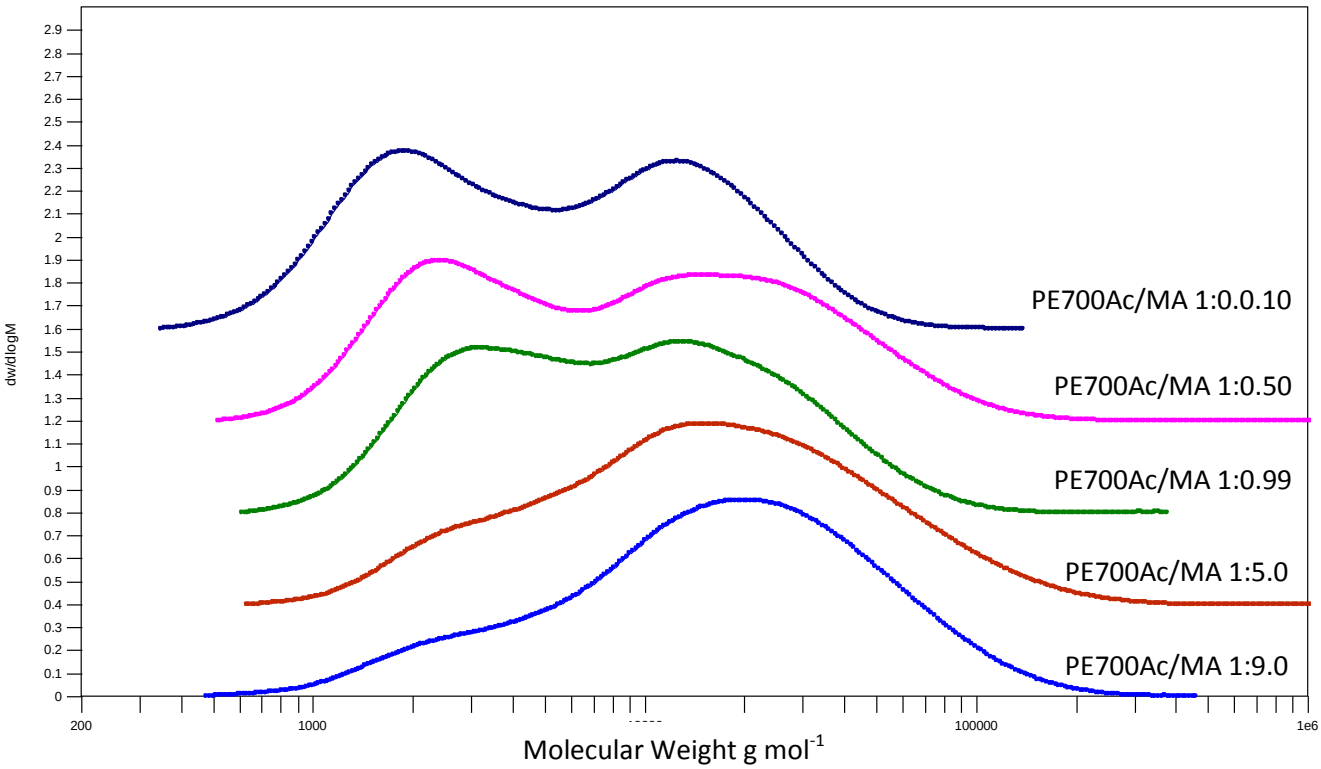


**Figure 3.8: Molecular weight distributions of the PE700Ac/MA series of copolymers, the distributions have normalised areas.**

As with the **DocAc/MA** and **PE460Ac/MA** series of copolymers, the distributions for the **PE700Ac**-based copolymers are bimodal, with the lower molecular weight shoulder or fraction which appears at ~1200 g $mol^{-1}$ is the non-functional PE contaminant, which can be seen to increase as the amount of **PE700Ac** monomer in the feed was increased. The HT-SEC characterisation highlights the need for a more comprehensive optimisation of the copolymerisation reaction. This was not undertaken during the present work as there was no regular access to a high-temperature SEC instrument. The over-estimation of the $M_w$ of the linear non-functional PE contaminant in the analyses of both PE-based copolymer series is likely to be as a result of its molecular structural differences to the main copolymer component.

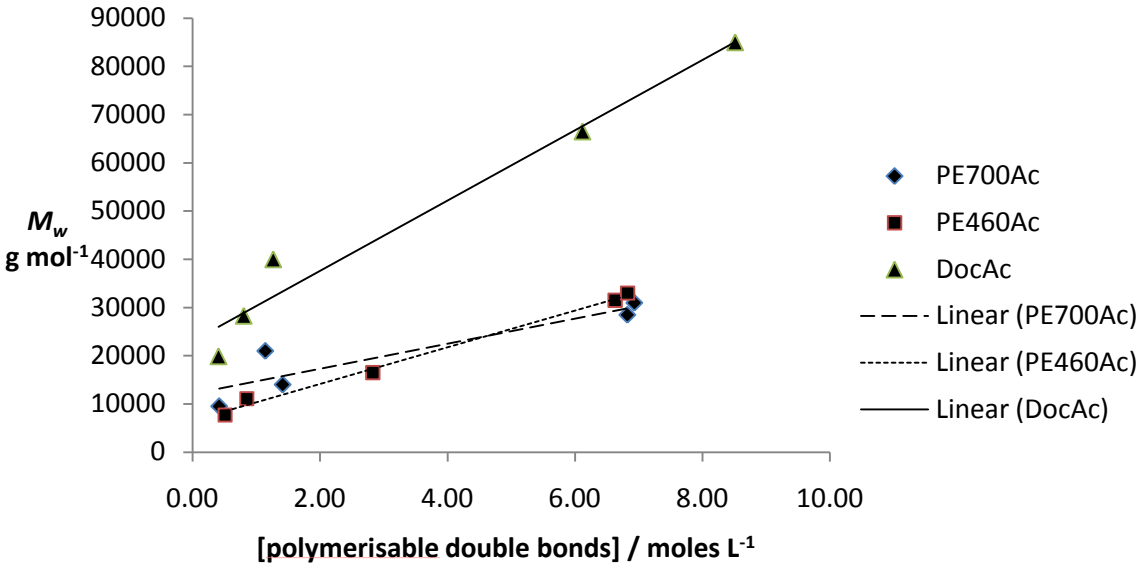


**Figure 3.9: $M_w$ vs concentration of polymerisable groups [M]. for the PE700Ac/MA, PE460Ac/MA and DocAc/MA copolymer series. $M_w$ data was derived from the HT-SEC-viscosity characterisation.**

All three series of copolymers **DocAc/MA** (Table 3.20), **PE460Ac/MA** (Table 3.21) and **PE700Ac/MA** (Table 3.22) show the same trend in $M_w$, the latter increasing as the proportion of MA in each copolymer increases. These data are expressed in terms of the concentration of polymerisable groups, [M], in the copolymer synthesis and are plotted in Figure 3.9. The effect is almost certainly due in part to the lower reactivity of each macromonomer, **DocAc**, **PE460Ac** and **PE700Ac**, relative to MA, and to the experimental fact that as the ratio of macromonomer rises the concentration of double bonds is reduced, and hence the rate of polymerisation and the $DP_n$ both likewise reduced.

Along with the molecular weight distributions, this phenomenon underscores the difficulty encountered when trying to polymerise the macromonomers due to their low reactivity.

### 3.4.5 Comparison of the different SEC techniques in the analysis of the DocAc/MA copolymer series

**Table 3.23: Comparison of the in-house SEC-MALLS and HT-SEC data (from RAPRA) for the DocAc/MA series of copolymers. The calibration was performed using polyethylene standards. Where a second set of data are given for a sample these represent a replicate chromatographic analysis on the same sample.**

| Sample | SEC-MALLS / g mol$^{-1}$ in THF | | | HT-SEC-viscosity / g mol$^{-1}$ in TCB | | | HT-SEC-calibrated / g mol$^{-1}$ in TCB | | |
|---|---|---|---|---|---|---|---|---|---|
| | $M_w$ | $M_n$ | PDI | $M_w$ | $M_n$ | PDI | $M_w$ | $M_n$ | PDI |
| **DocAc/MA** | 80,500 | 10,700 | 7.5 | 82,400 | 28,200 | 2.9 | 42,200 | 11,700 | 3.6 |
| **1:7.5** | | | | 88,400 | 29,900 | 3.0 | 44,900 | 12,100 | 3.7 |
| **DocAc/MA** | 58,600 | 12,300 | 4.8 | 66,200 | 24,000 | 2.8 | 33,500 | 8,740 | 3.8 |
| **1:3.8** | | | | 66,900 | 22,400 | 3.0 | 33,800 | 8,890 | 3.8 |
| **DocAc/MA** | 41,100 | 18,300 | 2.3 | 38,200 | 15,200 | 2.5 | 18,500 | 5,030 | 3.7 |
| **1:0.75** | | | | 41,300 | 17,000 | 2.4 | 18,200 | 4,970 | 3.7 |
| **DocAc/MA** | 27,800 | 13,500 | 2.1 | 28,300 | 8,500 | 3.3 | 12,100 | 4,100 | 3.0 |
| **1:0.38** | | | | | | | 12,600 | 4,140 | 3.0 |
| **DocAc/MA** | 15,700 | 9,700 | 1.6 | 19,900 | 10,600 | 1.9 | 6,610 | 3,220 | 2.1 |
| **1:0.075** | | | | | | | | | |

The $M_w$ values obtained from the high-temperature SEC-viscosity analysis agree quite well to those derived for the same **DocAc/MA** copolymers analysed on our own SEC-MALLS system, which is more or less expected for these absolute methods of molecular weight evaluation (Table 3.23). However the $M_n$ values, and hence the polydispersity indices are less certain than $M_w$ values, particularly for the combined SEC-viscosity technique and indeed some do have large differences depending on the copolymer composition. This molecular weight comparison using the model **DocAc/MA** copolymer series is very important since the 'agreement' between the in-house SEC-MALLS and HT-SEC-viscosity (RAPRA) data in effect helped to validate the reliability of the HT-SEC-viscosity derived $M_w$ values for the

two PE-based copolymer series which being insoluble in THF could not be analysed by the in-house SEC-MALLS instrumentation. The results for both $M_w$ and $M_n$ derived from the calibrated system are however much lower than those derived from both of the other techniques, this is most likely to be due to the lack of structural similarity between the copolymers and the calibration standards used, which were linear polyethylenes. The opposite effect to this can be seen with the underestimation of the mass of the non-functional PE contaminant in the distributions of the two PE-based copolymer series (Figures 3.7 and 3.8).

## 3.5 Adhesion testing

### 3.5.1 Introduction

Since the ultimate technological objective of the present work was to find new materials to use as adhesives, methods of measuring the relative adhesive strength of different materials were devised. Two types of adhesion testing were used; an 'in-house' method and a modified ASTM protocol for lap-shear tensile testing. The 'in-house' method provided a quick and easy but purely subjective test whereas the more time consuming ASTM method provided values for the shear strength of the adhesives which could be compared to one another.

### 3.5.2 The 'in-house' adhesion test.

The acrylate and methacrylate copolymers were tested as an adhesive layer between cast films of low-density poly(ethylene) (LDPE) and commercially available non-surface treated poly(methyl methacrylate) (PMMA) sheet. Thin film discs (0.500 x 30 mm) of LDPE were melt cast at ~112 °C. A sandwich of PMMA-copolymer adhesive-LDPE was then placed in a film press. The sandwich consisted of a disc of PMMA, which was half covered by aluminium foil and half covered by the copolymer adhesive being tested in powder form (Figure 3.10). An LDPE disc was positioned on top of this and the entire sandwich was annealed in the hot-press at 110 ºC, which was the $T_g$ of the PMMA and above the melt temperature of the copolymer, for 10 minutes under a pressure of 200 kg. This temperature was chosen as it allowed the test specimen to be made without any distortion of the PMMA substrate, whilst still allowing the PMMA to soften slightly to maximise the chance of any diffusion of the adhesive into the substrate and *vice versa*. Figure 3.11 shows a photograph of a complete adhesion test piece before testing whilst a detailed description of the equipment and methods employed is given in Section 2.4.3.

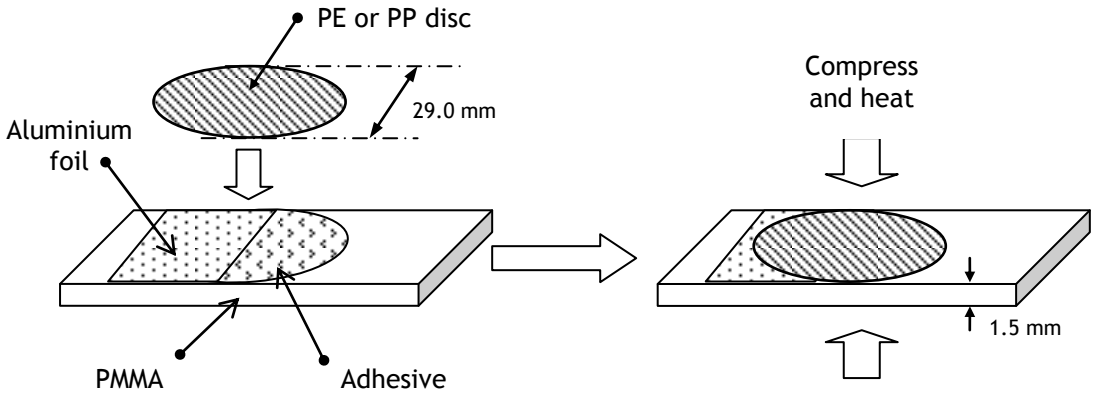


**Figure 3.10: Construction of an 'in-house' adhesion testing sample, polyolefin discs were 0.50 mm thick.**

Promising materials from this initial test were then re-tested with polypropylene (PP) sheet instead of LDPE using a similar method. When polypropylene substrates were used only the lower platen, which was in contact with the PP, was heated to prevent the PMMA sheet from being badly deformed. The PP-copolymer adhesive-PMMA samples were annealed close to the melting point of the PP at 160 °C instead of 110 °C and this was found to greatly improve adhesion. This was presumably as a result of the PP substrate melting or softening slightly, perhaps allowing the PE component of the adhesive to bond to a greater extent with the substrate. Since the preparation temperature was also well above the $T_g$ of the PMMA substrate, the surface in contact with the adhesive would have presumably been highly mobile and able to diffuse together with the adhesive.

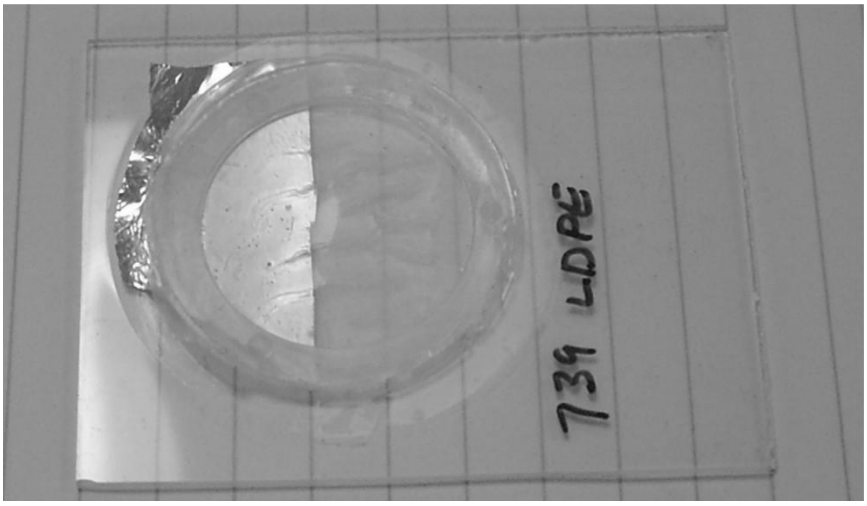


**Figure 3.11: A photograph of an annealed PMMA/LDPE 'in-house' adhesion test piece.**

The approach of bonding only half of the LDPE disc to the PMMA sheet allowed the two parts which had been separated by foil to be used as 'handles' to apply a force manually in order to test the adhesive shear strength (Figure 3.12).

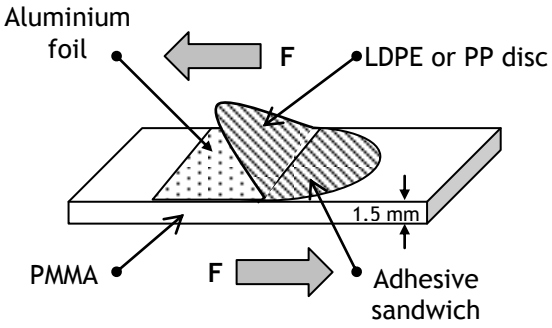


**Figure 3.12: An annealed 'in-house' adhesion testing sample. F = Force applied by hand to test adhesive strength.**

### 3.5.3 Copolymers of the macromonomers with MA or MMA

Data from the preliminary testing of acrylate based materials is shown in Tables 3.25, 3.26 and 3.27.

**Table 3.24: DocAc/MA copolymer in-house adhesion test results.**

| Sample | Mass ratio* PE:MA | Adhesion LDPE/PMMA |
|---|---|---|
| **DocAc/MA 1:7.5** | 1:10.0 | Good |
| **DocAc/MA 1:3.8** | 1:5.0 | Good |
| **DocAc/MA 1:0.75** | 1:1.0 | Poor |
| **DocAc/MA 1:0.38** | 1:0.5 | Poor |
| **DocAc/MA 1:0.075** | 1:0.1 | Poor |

**Table 3.25: PE460Ac/MA copolymer in-house adhesion test results.**

| Sample | Mass ratio* PE:MA | Adhesion LDPE/PMMA |
|---|---|---|
| **PE460Ac/MA 1:8.4** | 1:10.0 | Good |
| **PE460Ac/MA 1:4.7** | 1:5.6 | Good |
| **PE460Ac/MA 1:0.95** | 1:1.1 | Good |
| **PE460Ac/MA 1:0.47** | 1:0.6 | Poor |
| **PE460Ac/MA 1:0.095** | 1:0.1 | Poor |
| **PE460Ac/MA 1:0.047** | 1:0.1 | Poor |
| **PE460Ac comb** | comb | Poor |

* This refers to the mass ratio of pendant PE chains to poly[(meth) acrylate] chains in the final polymer.

**Table 3.26: PE700Ac/MA copolymer series in-house adhesion test results.**

| Sample | mass ratio* | Adhesion | |
|---|---|---|---|
| | PE:MA | LDPE/PMMA | PP/PMMA |
| **PE700Ac/MA 1:9.0** | 1:10 | Very good | Poor |
| **PE700Ac/MA 1:5.0** | 1:5.5 | Very good | Poor |
| **PE700Ac/MA 1:0.99** | 1:1.1 | Good | Poor |
| **PE700Ac/MA 1:0.50** | 1:0.6 | Poor | not tested |
| **PE700Ac/MA 1:0.10** | 1:0.1 | Poor | not tested |
| **PE700Ac/MA 1:0.05** | 1:0.1 | Poor | not tested |
| **PE700Ac/MA comb** | comb | Poor | not tested |

Before commencing the preliminary adhesion testing our thoughts included the idea that perhaps a graft copolymer involving ~50 mass% PE and ~50 mass% PMMA might yield the best adhesion performance. We were therefore rather surprised to find that low PE content materials were the most encouraging. In particular in the case of all three series of copolymers mass ratios of PE:MA of ~1:10 and ~1:5 performed well (Tables 3.25—3.27) in LDPE/ PMMA adhesion tests.

Additional adhesion tests were carried out using the best materials (**PE700Ac/MA 1:5.0** & **PE700Ac/MA 1:9.0**) with PP/PMMA substrates (Table 3.26 Using PP/PMMA substrates only sample **PE700Ac/MA 1:5.0** exhibited some limited adhesion, with adhesive failure occurring between the copolymer and the PP. *As a control commercially available poly(methyl acrylate) (PMA) was tested as the adhesive between LDPE and PMMA using the same heat and pressure sealing conditions. Adhesion was found to be minimal, with an adhesive failure occurring between the LDPE and the PMA.* The PE component in the copolymers was therefore essential in developing their adhesion properties.

* This refers to the mass ratio of pendant PE chains to poly[(meth) acrylate] chains in the final polymer.

**Table 3.27: PE460Mac/MMA copolymer in-house adhesion test results.**

| Sample | Mass ratio* PE:MMA | Adhesion LDPE/PMMA |
|---|---|---|
| **PE460MAc/MMA 1:4.5** | 1:5.6 | Poor |
| **PE460MAc/MMA 1:0.76** | 1:1:1 | Poor |
| **PE460MAc/MMA 1:0.38** | 1:0.5 | Poor |
| **PE460MAc/MMA 1:0.091** | 1:0.1 | Poor |
| **PE460MAc/MMA 1:0.045** | 1:0.1 | Poor |
| **PE460MAc/MMA** | comb | Poor |

**Table 3.28: PE700Mac/MMA copolymer preliminary adhesion test results.**

| Sample | Mass ratio* PE:MMA | Adhesion LDPE/PMMA |
|---|---|---|
| **PE700MAc/MMA 1:8.8** | 1:10.0 | Poor |
| **PE700MAc/MMA 1:4.4** | 1:5.0 | Poor |
| **PE700MAc/MMA 1:0.88** | 1:1.0 | Poor |
| **PE700MAc/MMA 1:0.44** | 1:0.5 | Poor |

Copolymers containing a methyl methacrylate block (**PE460MAc/MMA** and **PE700MAc/MMA**) were expected to show stronger binding to PMMA than the corresponding poly(methyl acrylate). However this proved not to be the case as shown by the data in Tables 3.28 and 3.29. This result may be due to the methacrylate polymers having a higher glass transition temperature and the associated brittleness. The in-house adhesion testing results (Tables 3.25 to 3.29) also illustrated a definite qualitative trend towards the longer PE chain length co-polymers having better adhesion than those of the shorter ones, as well as the acrylate polymers showing better performance than their methacrylate counterparts.

* This refers to the mass ratio of pendant PE chains to poly[(meth) acrylate] chains in the final polymer.

In summary therefore it seemed that a relatively small amount of PE content (~10-20%) in the acrylate copolymers greatly enhanced their interfacial and mechanical adhesive properties. Longer PE grafts in the methyl acrylate copolymer also seemed to impart better adhesive properties than shorter grafts and finally methacrylate based polymers seemed to offer poorer adhesion presumably as a result of having a higher $T_g$ in the methacrylate component.

As an additional control experiment, methyl acrylate was polymerised in the presence of PE700-OH in the same molar ratio to determine the effect of having a PE component present but not covalently grafted onto the PMA backbone. The control materials were adhesion tested in the LDPE/PMMA sandwich and the results are shown in Table 3.29.

**Table 3.29: Control experiments, in-house adhesion test results using compositions involving the PE700 mono-alcohol.**

| Sample | Mass ratio PE:MA | Adhesion LDPE/PMMA |
|---|---|---|
| **PE700OH/MA 1:10** | 1:10 | Poor |
| **PE700OH/MA 1:5** | 1:5 | Poor |
| **PE700OH/MA 1:1** | 1:1 | Poor |
| **PE700OH/MA 1:0.5** | 1:0.5 | Poor |
| **PE700OH/MA 1:0.1** | 1:0.1 | Poor |
| **blend** | 1:5 | Poor |

It was quite clear from these data that the PE component had to be grafted to the polyacrylate mainchains to develop the adhesion properties required.

### 3.5.4 **Copolymers containing ethyl hexyl side chains**

Though macromonomer copolymers with methyl acrylate were showing promising adhesion results it was felt important to assess the behaviour of copolymers prepared with other (meth)acrylate monomers, particularly with more hydrophobic species and indeed potentially with more polar species. 2-Ethylhexyl acrylate (EHA) and 2-ethylhexyl methacrylate (EHMA) are both inexpensive and readily available monomers and copolymers involving these were examined first. We were also conscious that homopolymers of these had low $T_g$ values and this seemed to be a potentially important factor to evaluate in our PE graft copolymers. The longer chain macromonomers PE700Ac and PE700MAc were used to produce four groups of copolymers PE700MAc/EHMA, PE700Ac/EHA, PE700MAc/EHA and PE700Ac/EHMA. The results of our 'in-house' adhesion tests using these copolymers are shown in Tables 3.31 to 3.34.

**Table 3.30: PE700MAc/EHMA copolymer in-house adhesion test results.**

| Sample | Mass ratio | Adhesion | |
|---|---|---|---|
| | PE:MMA | LDPE/PMMA | PP/PMMA |
| **PE700MAc/EHMA 1:24.1** | 1:10 | Good | Not tested |
| **PE700MAc/EHMA 1:12.1** | 1:5 | Good | Poor |
| **PE700MAc/EHMA 1:2.4** | 1:1 | Poor | Not tested |
| **PE700MAc/EHMA 1:1.2** | 1:0.5 | Poor | Not tested |

**Table 3.31: PE700Ac/EHA copolymer in-house adhesion test results.**

| Sample | Mass ratio | Adhesion |
|---|---|---|
| | PE:MA | LDPE/PMMA |
| **PE700Ac/EHA 1:4.5** | 1:5 | Poor |
| **PE700Ac/EHA 1:2.4** | 1:1 | Poor |
| **PE700Ac/EHA 1:1.2** | 1:0.5 | Poor |
| **PE700Ac/EHA 1:0.24** | 1:0.1 | Poor |

**Table 3.32: PE700MAc/EHA copolymer in-house adhesion test results.**

| Sample | Mass ratio PE:MA | Adhesion LDPE/PMMA |
|---|---|---|
| **PE700MAc/EHA 1:24.1** | 1:10 | Poor |
| **PE700MAc/EHA 1:12.1** | 1:5 | Poor |
| **PE700MAc/EHA 1:2.4** | 1:1 | Poor |
| **PE700MAc/EHA 1:1.2** | 1:0.5 | Poor |

**Table 3.33: PE700Ac/EHMA copolymer in-house adhesion test results.**

| Sample | Mass ratio PE:MMA | Adhesion LDPE/PMMA | Adhesion PP/PMMA |
|---|---|---|---|
| **PE700Ac/EHMA 1:24.1** | 1:10 | Good | Not tested |
| **PE700Ac/EHMA 1:12.1** | 1:5 | Excellent | Excellent |
| **PE700Ac/EHMA 1:2.4** | 1:1 | Poor | Not tested |
| **PE700Ac/EHMA 1:1.2** | 1:0.5 | Poor | Not tested |

The all-methacrylate copolymers of **PE700MAc** and **2-EHMA** (Table 3.30) did adhere well to the LDPE and PMMA substrates but overall they did not perform well, they were very soft and tacky and appeared to slip even under a small tensile load. These copolymers had low shear strength and tended to undergo cohesive failure.

The 2-EHA based copolymers, with both **PE700Ac** (Table 3.31) or **PE700MAc** (Table 3.32), were too soft and tended to flow easily under stress and were therefore not particularly good as adhesives in much the same way as the all-methacrylate copolymers (Table 3.30).

Using 2-EHMA or 2-EHA as the comonomer had however allowed the incorporation of the methacrylate macromonomer **PE700MAc** into the copolymer backbone without imparting a high $T_g$ and the associated brittleness which had been observed earlier with the **PE700MAc/MMA** copolymers. Interestingly the copolymers of

**PE700Ac** and **2-EHMA** seemed to be mechanically tougher than any of the other copolymers, as well as giving good adhesion of PMMA to the two different substrates (LDPE and PP) (Table 3.33). After assessing the adhesive strength of all the **2-EHA** and **2-EHMA** copolymers, **PE700Ac/EHMA 1:12.1,** with a PE content of around 20% seemed to give the best results. Further polymerisations were therefore carried out using these two monomers, but this time the ratio of PE to backbone was 'fine-tuned' around the best performing material (Table 3.34).

**Table 3.34: Fine-tuned PE700Ac/EHMA copolymers preliminary adhesion test results**

| Sample | Mass ratio* PE:MA | Adhesion LDPE/PMMA |
|---|---|---|
| **PE700Ac/EHMA 1:19.3** | 1:8 | Good |
| **PE700Ac/EHMA 1:16.9** | 1:7 | Good |
| **PE700Ac/EHMA 1:14.5** | 1:6 | Good |
| **PE700Ac/EHMA 1:9.6** | 1:4 | Good |
| **PE700Ac/EHMA 1:7.2** | 1:3 | Good |

None of the new copolymers (Table 3.34) seemed to perform quite as well as the **PE700Ac/EHMA 1:12.1** material in preliminary tests with LDPE/PMMA sandwiches. However as these are very subjective in-house tests full testing using the ASTM method (Section 3.5) would be required for a more realistic evaluation. These results also highlight the need for molecular weight data for all the products, as an accurate comparison of two or more materials would require them to have similar $M_w$ values. If the $M_w$ for a particular polymer is below the critical mass for entanglement then the mechanical strength of that polymer will be reduced.

### 3.5.5 Copolymers of macromonomers with BMA and DMA

Copolymers derived from the **PE700A**c macromonomer with the linear alkyl monomers dodecyl methacrylate (**DMA**) (Table 3.35) or butyl methacrylate (**BMA**) (Table 3.36) were prepared on the grounds that these may have had similar or

intermediate physical-chemical properties relative to the copolymers with **MMA** and those with **2-EHMA**. In the event the dodecyl copolymers (Table 3.35) were soft and sticky materials which were less effective as adhesives than the copolymers with **2-EHMA**.

**Table 3.35: PE700Ac/DMA copolymer preliminary adhesion test results**

| Sample | Mass ratio PE:MA | Adhesion LDPE/PMMA |
|---|---|---|
| **PE700Ac/DMA 1:25.1** | 1:10 | Poor |
| **PE700Ac/DMA 1:12.1** | 1:5 | Poor |
| **PE700Ac/DMA 1:2.4** | 1:1 | Good |
| **PE700Ac/DMA 1:1.2** | 1:0.5 | Poor |

However the **PE700Ac/BMA** copolymers were much stronger materials than the **PE700Ac/DMA** materials and gave good results during adhesive evaluation (Table 3.36). Indeed the performance of the original best **PE700Ac/MA** copolymer (Table 3.26) and the best **PE700Ac/BMA** copolymer (Table 3.36) were very similar. Clearly the incorporation of the butyl groups in BMA with **PE700Ac** rather than with **PE700MAc** considerably reduces the brittleness relative to the earlier **PE700MAc/MMA** copolymers (Table 3.28). This also suggested that examination of other 'crossed' acrylate/methacrylate copolymers might be worthwhile. It is worth noting as well that all of the PE700Ac/BMA materials tested gave good adhesion with the exception of the 1:0.90 material. This may indicate a molecular weight effect, i.e. **PE700Ac/BMA 1:0.90** may have a much lower $M_w$ than the other butyl methacrylate copolymers prepared and this potential dependence needed further investigation.

**Table 3.36: PE700Ac/BMA copolymer preliminary adhesion test results**

| Sample | Mass ratio PE:MA | Adhesion LDPE/PMMA |
|---|---|---|
| **PE700Ac/BMA 1:9.0** | 1:10 | Good |
| **PE700Ac/BMA 1:4.5** | 1:5 | Good |
| **PE700Ac/BMA 1:0.90** | 1:1 | Poor |
| **PE700Ac/BMA 1:0.64** | 1:0.5 | Good |

### 3.5.6 Crossed acrylate/methacrylate copolymers and DuPont Vamac in-house adhesion tests.

To complete the matrix of copolymers studied the "crossed" acrylate/methacrylate copolymers **PE700MAc/MA** and **PE700Ac/MMA** were prepared (Section 3.3.2) and along with samples of commercially available DuPont *Vamac*® resins, these were evaluated using the in-house adhesion test (Table 3.37). The DuPont resins were selected for testing as they were thought to have similar compositions to the polyethylene-poly(methyl acrylate) graft copolymers which have been prepared and evaluated in the present work. Vamac® DP is an "ethylene acrylic copolymer elastomer", Vamac® DHC is a "copolymer of ethylene and methyl acrylate" whilst Vamac® G is a "terpolymer of ethylene, methyl acrylate, and a cure site monomer." The compositions of the crossed acrylate/methacrylate materials chosen were low in the PE component.

**Table 3.37: In-house adhesion testing data for the crossed acrylate/methacrylate PE graft copolymers and the DuPont *Vamac*® adhesives.**

| Sample | Mass ratio PE:M(M)A | Adhesion LDPE/PMMA | Comments |
|---|---|---|---|
| **PE700MAc/MA 1:8.7** | 1:10 | Good | These behaved similarly to the corresponding PE700Ac/MA copolymers. |
| **PE700MAc/MA 1:4.4** | 1:5 | Good | |
| **PE700MAc/MA 1:0.87** | 1:1 | Poor | |
| **PE700Ac/MMA 1:9.0** | 1:10 | Poor | Both were brittle, similar to the PE700Mac/MMA materials |
| **PE700Ac/MMA 1:4.5** | 1:5 | Poor | |
| DuPont *Vamac® G* | ~ | Poor | Adhesive failure at the LDPE substrate in all three tests |
| DuPont *Vamac® DHC* | ~ | Poor | |
| DuPont *Vamac® DP* | ~ | Poor | |

As might have been predicted, the **PE700MAc/MA** copolymers had similar good adhesive performance to the earlier **PE700Ac/MA** materials, with a corresponding composition that had been previously tested. This is likely to be as a result of the analogous structures of each copolymer, with the exchange of small mole amounts of methacrylate macromonomer for acrylate macromonomer and hence methacrylate and acrylate segments in the backbone having a negligible effect on mechanical properties and presumably on the $T_g$.

Similarly the poor adhesive behaviour of the corresponding **PE700Ac/MMA** and **PE700MAc/MMA** copolymers is comparable. Again the addition of small amounts of acrylate to the methacrylate in the backbone has a negligible effect on the mechanical properties of these brittle copolymers. Interestingly these two observations also seem to indicate that the relative reactivities of the **PE700Ac** and **PE700MAc** monomers are comparable. Normally the structurally equivalent methacrylate of an acrylate monomer is more reactive, however, in the present case the large PE700 ester presumably attenuates and dominates the reactivity of both.

The three DuPont materials tested were regarded as potential commercially available competitors to our copolymers. However these were sticky and rubbery and none adhered well to the PE substrate under the test conditions.

### 3.5.7 **Industry standard (ASTM) adhesion testing**

#### 3.5.7.1 ***Introduction***

Copolymers that had displayed favourable adhesion characteristics were re-tested according to the latest available American Society for Testing and Materials (ASTM) standards D1002[16] and D3163[17]. The need for the preparation and analysis of replica samples and the time required to carry out a single test on the tensile testing instrument meant that all the samples previously tested using the 'in-house' procedure could not be assessed with the ASTM procedure. Hence the limitation to copolymers that had displayed favourable behaviour and a few comparative materials. ASTM D1002 refers to apparent shear stress measurements for adhesively bonded substrates, while D3163 is a modification of the first method to allow the use of plastic substrates. These methods were employed as they would provide a relatively cheap and simple comparison of the adhesive strength of the copolymers. They do not provide an absolute measurement of the shear stress; rather they can allow the comparison of the strength of different adhesives and substrate combinations. This is due to the nature of the test.

The test method stipulates that the failure type should be stated along with the shear strength for any materials tested. The failure type is judged by looking at the adhesive area post-testing and deciding if the adhesive became unstuck from one of the substrates (adhesive failure, AF) or if the adhesive material failed itself (cohesive failure, CF). A third classification involves failure of one of the adherands (substrate failure, SF). Sometimes the failure was a combination of two or more failure types, in these cases the area of each type of failure on the end of the substrate was estimated and the fraction of each type was expressed as a percentage.

The sample preparation technique, which follows the ASTM method, had to be optimised to allow the use of the new adhesive copolymers. The adhesive sandwich could not be prepared in the hot press as this was found to distort the substrates (adherands). Any distortion meant that the adhesive area would have been different from the specification, with the adherands also being thinned (and therefore

weakened) as they were compressed. Since the strength of the adherands contribute to the results of the tension test, their integrity was crucial. Since improved adhesion between PMMA and PP is more technologically interesting and more challenging to achieve, PP was selected instead of PE for the ASTM testing (Figure 3.13). Using temperatures over 110 °C during sample preparation was also impossible as this also tended to distort the adherands. Instead the samples were prepared in an oven set to 108 °C. For each test, six PMMA-adhesive-PP samples were aligned and compressed with a weight (3.3 kg) in the oven overnight at 108 °C, the samples were allowed to cool then were tensile tested in an Instron according to the ASTM method (Section 2.4.4).

Both the PMMA and the PP substrates were cut to 25.4 mm by 101.6 mm in size, with an overlap of 25.4 mm by 12.7 mm (an area of 322.58 $mm^2$) being filled with the adhesive. In all tests the area of the substrate to be bonded was first roughened with wet-or-dry sandpaper (240 grit), degreased with isopropanol (IPA) and dried under a stream of compressed air.

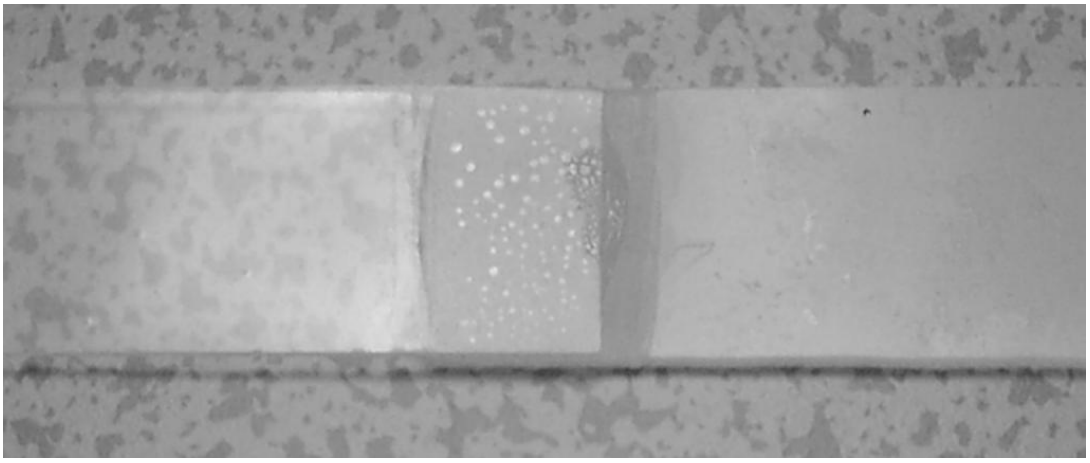

**Figure 3.13: A photograph showing details of a prepared ASTM adhesive lap joint between PMMA (left) and PP (right) substrates. The adhesive shown here (PE700Ac/MA 1:9.0) has voids present and this test piece was not used for a shear strength measurement.**

### 3.5.7.2 *Sample preparation optimisation*

Using one of the best materials from the preliminary testing, **PE700Ac/EHMA 1:12.1**, three adhesion tests were performed to compare different methods for sample preparation. One set of six replicate samples had the adhesive melt cast onto the PP substrate at 108 °C, a second set was solution cast from *n*-hexane (100 mg in 0.5 mL) and the last was solution cast from toluene (100 mg in 0.5 mL). The solution cast adhesive samples were allowed to dry on the PP substrates at 108 °C for 4 hours before the PMMA substrates were aligned and pressed into place overnight. Maximum load at failure and breaking strain values were averaged over all of the samples tested (Table 3.38). The failure type was worked out by looking at the substrates after testing and assessing the area still covered by adhesive.

**Table 3.38: A comparison of different adhesive application methods for the PE700Ac/EHMA 1:12.1 copolymer bonding PMMA with PP. Solutions were 100 mg in 0.5 mL.**

| Casting method / solvent | Shear strength / MPa | Max load at failure / kN | Failure Type |
|---|---|---|---|
| hexane solution | 2.23 | 0.72 | ~100% CF |
| melt cast | 2.08 | 0.67 | ~100% CF |
| toluene solution | 1.61 | 0.52 | ~90% CF |

From the data comparing casting method, it was decided that *n*-hexane solutions should be used to apply the adhesive. It seems that the toluene may not have been removed fully, weakening the adhesive layer. When it was necessary for solubility reasons to use toluene the adhesive solution was allowed to dry overnight rather than for 4 hours. The *n*-hexane-cast solutions seemed to give comparable or slightly better results to melt casting. Also solution casting was much easier to achieve in practice than melt casting, with more uniform adhesive films being formed. There was also the possibility that the use of solvent might allow the adhesive an opportunity to align with its PE segments at the PP surface by enhancing its mobility.

### 3.5.7.3 *Effect of composition on adhesive strength*

To compare the effect of varying the copolymer composition on the adhesive strength, two more **PE700Ac/EHMA** copolymers (1:10 and 1:1) were tested. The two compositions chosen were the closest available (at that time) to the 1:5 which had previously been tested. The comparison of these results is shown in Table 3.39.

**Table 3.39: EHMA-*co*-700A copolymer lap-shear test data. Copolymers were solution cast from an *n*-hexane solution (100 mg in 0.5 mL) onto the PP substrate.**

| Copolymer | Mass ratio PE:EHMA | Shear strength / MPa | Max load at failure / kN | Failure Type |
|---|---|---|---|---|
| **PE700Ac/EHMA 1:24.1** | 1:10 | 1.49 | 0.48 | ~100% AF* |
| **PE700Ac/EHMA 1:12.1** | 1:5 | 2.23 | 0.72 | ~100% CF† |
| **PE700Ac/EHMA 1:2.4** | 1:1 | 1.08 | 0.35 | ~100% CF† |

These three copolymers seemed to show that a small amount of PE in the copolymer (around 20%) greatly improves adhesion, but too much (~50%) starts to have a detrimental effect. In the case of too little PE (**PE700Ac/EHMA 1:24.1**), the copolymer was quite soft and weak and this is reflected in the lower shear strength relative to **PE700Ac/EHMA 1:12.1**. These results mirror the preliminary adhesion tests where **PE700Ac/EHMA 1:12.1** performed best (Section 3.5.2)

A second set of adhesives were tested, these were the **PE700Ac/MA** copolymers which had shown some promise during preliminary testing. The copolymers were solution cast from toluene (100 mg in 0.5 mL) as they were found to be insoluble in *n*-hexane, even at temperatures close to the boiling point of the solvent. The copolymers were cast onto roughened and de-greased PP substrates as before,

* 'AF' denotes an adhesive failure
† 'CF' denotes a cohesive failure

allowed to dry overnight at 108 °C and tested using the same protocols as before (Table 3.40).

**Table 3.40: PE700Ac/MA copolymer lap-shear test data. Copolymers were solution cast from a toluene solution (100 mg in 0.5 mL) onto the PP substrate.**

| Copolymer | Mass ratio PE:MA | Shear strength / MPa | Max load at failure / kN | Failure Type |
|---|---|---|---|---|
| **PE700Ac/MA 1:9.0** | 1:10 | 2.70 | 0.87 | ~50% AF*, ~50% SF† |
| **PE700Ac/MA 1:5.0** | 1:5.5 | 2.48 | 0.80 | ~50% AF*, ~50% SF† |
| **PE700Ac/MA 1:0.99** | 1.1:1 | 1.46 | 0.47 | ~100% CF‡ |
| **PE700Ac/MA 1:0.50** | 1:0.5 | 0.74 | 0.24 | ~100% CF‡ |

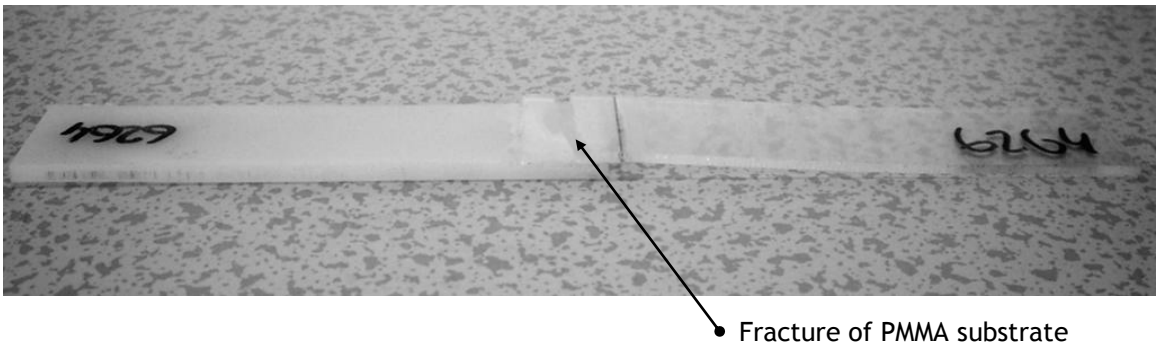


**Figure 3.14: A post-test ASTM PP/PMMA test piece for a PE700Ac/MA 1:9.0 copolymer showing a PMMA substrate failure.**

* 'AF' denotes an adhesive failure
† 'SF' denotes a substrate failure
‡ 'CF denotes a cohesive failure

With two of the copolymers tested (**PE700Ac/MA 1:9.0** and **PE700Ac/MA 1:5.0**) the PMMA substrate broke off about halfway through the adhesive joint in all replicates, with part of the substrate remaining bonded to the polypropylene. It seemed that the sudden failure of the adhesive may have caused the PMMA substrate to shatter. Thicker PMMA substrates (the present ones were 1.50 mm thick) may be needed to get more accurate results, although this would require a review of all previous tests. When the composition is compared to the breaking strain a trend can be seen which is similar to that for the **PE700Ac/EHMA** copolymers. Here 10-20% of PE in the copolymer seemed to give the best performance, and larger proportions (50% and over) had a detrimental effect.

During this ASTM testing the all-acrylate materials **PE700Ac/MA 1:9.0** and **PE700Ac/MA 1:5.0** outperformed the **PE700Ac/EHMA 1:12.1,** which is the opposite of the results from test samples made on the hot press, where the adhesion with **PE700Ac/MA 1:9.0** and **PE700Ac/MA 1:5.0** with PP was poor. This apparent anomaly may possibly be a result of different sample preparation; the samples in the ASTM tests were heat-sealed at a lower temperature (108 °C instead of 160 °C), the substrates were also roughened and the adhesive sandwich was left overnight at 108 °C. It may be that if the **PE700Ac/EHMA 1:12.1** ASTM test pieces could have been prepared at 160 °C they would have performed much better. It is quite clear however that some PE component is needed in adhesives and the amount of PE in the copolymer needs to be relatively low (10-20%) to give good adhesive properties; this trend can be seen here for two different copolymers, although further synthesis and testing is needed to complete the picture.

As a comparison, the all-methacrylate copolymer **PE700MAc/EHMA 1:12.1** was also tested (Table 3.41). This material was soft and sticky and did not perform well in preliminary ‘in-house’ adhesion testing. In the ASTM test after yielding at a relatively low tensile load the adhesive was seen to slip, allowing the substrates to move past one another.

**Table 3.41: PE700MAc/EHMA copolymer lap-shear test data. Copolymers were solution cast from an n-hexane solution (100 mg in 0.5 mL) onto the PP substrate.**

| Copolymer | Mass ratio* PE:MMA | Shear strength / MPa | Max load at failure / kN | Failure Type |
|---|---|---|---|---|
| **PE700MAc/EHMA 1:12.1** | 1:5 | 1.12 | 0.36 | 100% CF* Adhesive slips after yielding |

### 3.5.8 Effect of PE side chain length

The **PE460Ac/MA** (~31 carbon atom chain) (Table 3.42) and **DocAc/MA** (22 carbon atom chain) copolymers (Table 3.43) were adhesion tested using the ASTM method. The results of these tests were compared to those of the corresponding **PE700Ac/MA** (~48 carbon atom chain) copolymers to ascertain the influence of side-chain length on adhesive strength.

**Table 3.42: PE460Ac/MA copolymer lap-shear test data. Copolymers were solution cast from a toluene solution (100 mg in 0.5 mL) onto the PP substrate.**

| Material | Mass ratio PE:MA | Shear strength / MPa | Max load at failure / kN | Failure Type |
|---|---|---|---|---|
| **PE460Ac/MA 1:9.0** | 1:10 | 2.48 | 0.80 | ~50% AF†, ~50% SF‡ |
| **PE460Ac/MA 1:5.0** | 1:5.6 | 2.42 | 0.78 | ~50% AF†, ~50% SF‡ |
| **PE460Ac/MA 1:0.99** | 1.1:1 | 0.56 | 0.18 | ~100% CF* |

* 'CF' denotes an adhesive failure
† 'AF' denotes an adhesive failure
‡ 'SF' denotes a substrate failure

**Table 3.43: DocAc/MA copolymer lap-shear test data. Copolymers were solution cast from a toluene solution (100 mg in 0.5 mL) onto the PP substrate.**

| Material | Mass ratio PE:MA | Shear strength / MPa | Max load at failure / kN | Failure Type |
|---|---|---|---|---|
| **DocAc/MA 1:7.5** | 1:10 | 1.08 | 0.35 | ~100% CF* |
| **DocAc/MA 1:3.8** | 1:5 | 1.27 | 0.41 | ~100% CF* |
| **DocAc/MA 1:0.99** | 1.1 | 0.81 | 0.26 | ~100% CF* |

The **PE460Ac/MA** materials had similar adhesive strength in this test to the **PE700Ac/MA** materials previously tested, whereas the adhesive strength of the **DocAc/MA** copolymers was significantly lower. A graphical comparison of the data for the shear strength of copolymers with similar compositions is shown in Figure 3.15.

* 'CF' denotes a cohesive failure

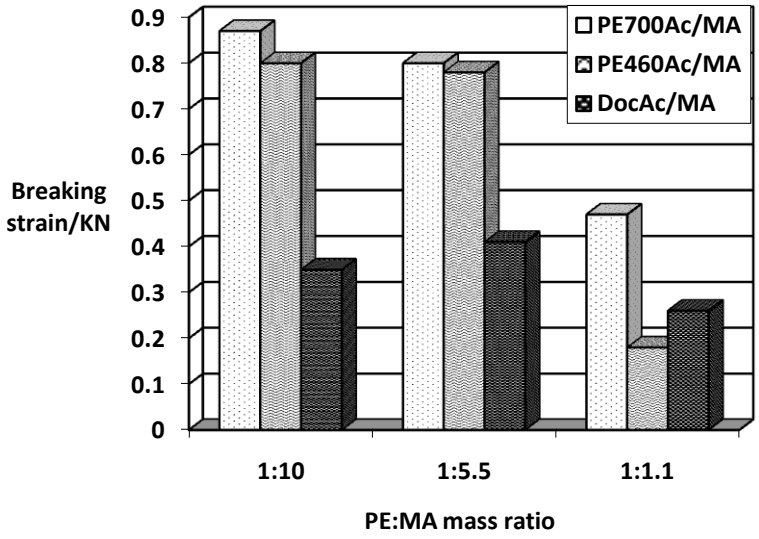


**Figure 3.15: The effect of alkyl side-chain length on shear strength for the PE-PMA graft copolymers.**

Substrate failure occurred for both the **PE700Ac/MA** and the **PE460Ac/MA** materials (composition ratios of 1:10 and 1:5.5) at similar load, therefore the ASTM sample preparation/dimensions used might not have allowed a distinction to be seen between these materials. This could be improved by using stronger a PMMA substrate or by using a smaller adhesive overlap, however any changes to the substrate dimensions or sample preparation would invalidate the comparison of the results to those of the earlier tests. The **DocAc/MA** copolymers achieved significantly lower values for the breaking strain and displayed cohesive failure. This was somewhat surprising given that the **PE460Ac/MA** copolymers have only an extra ~10 carbon atoms in the side chain. The improved adhesive strength might also have been a result of the presence of the non-functional PE impurity in the **PE460Ac/MA** and **PE700Ac/MA** materials. Interestingly the observed adhesive performance of the **PE460Ac/MA 1:0.95** copolymer was lower than would be expected, indeed it was lower than that of the corresponding **DocAc/MA** copolymer. This seems likely to be due to the low $M_w$ of the **PE460Ac/MA 1:0.95** copolymer relative to that of the **DocAc/MA 1:0.99** (~16,000 *vs*. ~39,000 g $mol^{-1}$) (see Section 3.4.3).

### 3.5.9 **Effect of side-chain branching on dhesion**

The branched side-chain acrylates (**B36Ac/MA 1:8.4** and **B36Ac/MA 1:4.2**) were adhesion tested and compared to data for analogous linear materials, which are shown in italics in Table 3.44.

**Table 3.44: Linear and branched alkyl side-chain acrylate comparison data**

| Sample | Ratio* | ASTM data | | |
|---|---|---|---|---|
| | PE:MA | Shear strength / MPa | Max load at failure / kN | Failure Type |
| **B36Ac/MA 1:8.4** | 1:10 | 1.30 | 0.42 | ~100% CF† |
| ***PE460Ac/MA 1:9.0*** | *1:10* | *2.48* | *0.80* | *~50%AF‡* *~50%SF§* |
| ***PE700Ac/MA 1:9.0*** | *1:10* | *2.70* | *0.87* | *~50%AF‡* *~50%SF§* |
| **B36Ac/MA 1:4.2** | 1:5.0 | 1.30 | 0.42 | ~100% CF |
| ***PE460Ac/MA 1:5.0*** | *1:5.0* | *2.42* | *0.78* | *~50%AF‡* *~50%SF§* |
| ***PE700Ac/MA 1:5.0*** | *1:5.5* | *2.48* | *0.80* | *~50%AF‡* *~50%SF§* |

The data show clearly that the branched side-chain copolymers perform significantly more poorly than the linear side-chain species with a similar alkyl group content and 'PE' chain length.

* This refers to the mass ratio of pendant PE chains to poly(acrylate) chains in the final polymer.
† 'CF' denotes a cohesive failure
‡ 'AF' denotes an adhesive failure
§ 'SF' denotes a substrate failure

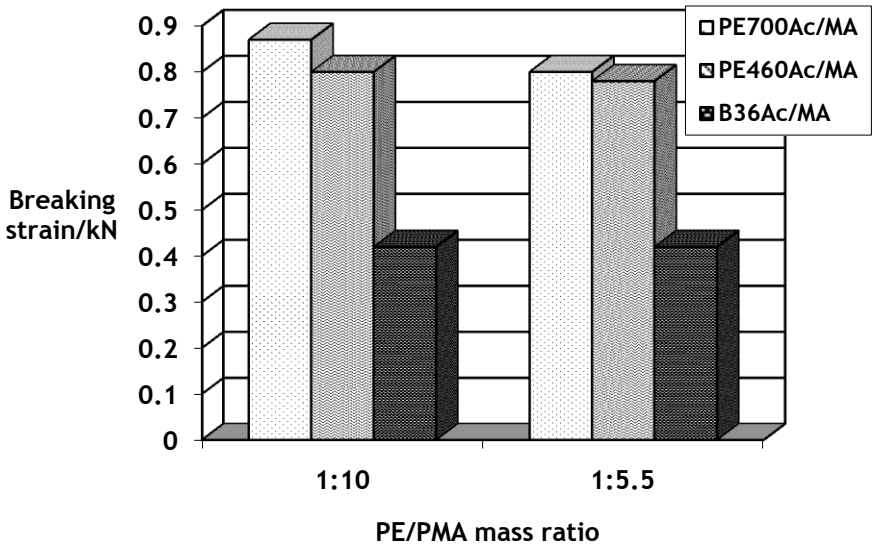


**Figure 3.16: Graphical comparison of the adhesion properties of linear and branched alkyl side-chain acrylate copolymers.**

One possible explanation for this is that the crystallinity of the alkane domains may have a strong effect on the adhesive and mechanical properties (Figure 3.16). The **PE460Ac** has a PE side chain comprising 31 carbons on average, whilst the B36Ac has a well-defined branched 36-carbon chain. Having branched side chains is likely to lower the crystallinity to some extent and the effect on adhesion performance is significant. Again, as was the case in the comparison with the **DocAc/MA** copolymers, the **PE460Ac/MA** and the **PE700Ac/MA** copolymers contain some non-functional PE impurities derived from the precursors **PE460-OH** and **PE700-OH**, and the presence of these might significantly improve the crystallinity, adhesive and mechanical properties. Some experiments were therefore designed to investigate this possible effect i.e. the blending of a low molecular weight PE into the **B36Ac/MA** or **DocAc/MA** copolymers in hand followed by adhesion testing or the preparation of **PE460Ac/MA** and **PE700Ac/MA** copolymers which are free from their PE impurities, then blending with linear PE at different ratios and subsequent adhesive evaluation.

### 3.5.10 **Blending experiments**

#### 3.5.10.1 ***DocAc/MA and B36Ac/MA copolymers***

In order to further investigate the possible effects of non-functional PE impurities present in the PE-OH starting materials and polymers derived from them, a low-molecular weight PE was blended with the **DocAc/MA 1:3.8A** and the **B36Ac/MA 1:4.2** copolymers and the resulting blends were adhesion tested using the ASTM method (Table 3.45). The amount of PE added was equivalent to the amount indicated to be present by the supplier in the PE-OH precursors (*i.e.* ~20% in the PE-OH precursors) divided by the ratio of PE macromonomer used to prepare the corresponding **PE700Ac/MA** copolymer. From subsequent further investigation of these precursor materials it now seems likely that this figure is around 29% and 18% for the **PE700-OH** and **PE460-OH** respectively (Section 3.1). However the PE additive used here has a higher molecular weight ($M_n$ = 1,700 g mol$^{-1}$) than the non-functional PE impurity found in either the **PE700Ac/MA** (impurity $M_n$ = 700 g mol$^{-1}$) or that found in the **PE460Ac/MA** (impurity $M_n$ = 460 g mol$^{-1}$).

**Table 3.45: Effect on adhesion of blending a non-functional PE into the DocAc/MA 1:3.8 and B36Ac/MA 1:4.2 copolymers**

| sample | | Blend / wt % | | ASTM | | |
|---|---|---|---|---|---|---|
| | | Co-polymer | PE | Shear strength / MPa | Max load at failure / kN | Failure Type |
| **DocAc/MA 1:3.8A** | Pure | 100 | 0 | 1.55 | **0.50** | ~100% CF* |
| **DocAc/MA 1:3.8A** | Blend | 96.0 | 4.0 | 1.83 | **0.59** | ~100% CF |
| **B36Ac/MA 1:4.2** | Pure | 100 | 0 | 1.30 | **0.42** | ~100% CF |
| **B36Ac/MA 1:4.2** | Blend | 95.3 | 4.7 | 1.49 | **0.48** | ~100% CF |

* 'CF' denotes a cohesive failure

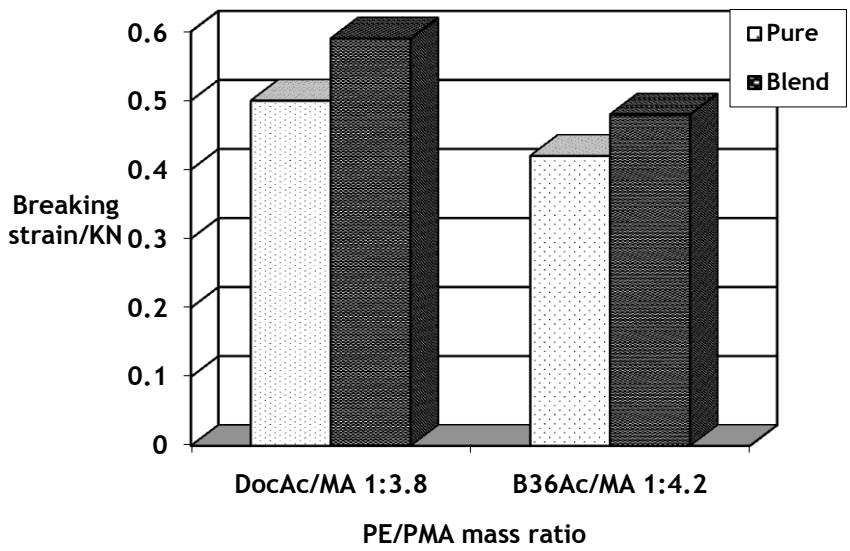


**Figure 3.17: Effect of blending a non-functional PE on adhesion for the DocAc/MA 1:3.8 and B36Ac/MA 1:4.2 copolymers**

A relatively small but consistent increase in adhesive strength can be seen from the data in Figure 3.17 for both blends relative to the corresponding pure copolymers, although the breaking strain is still well below that of the best performing materials. It does seem possible therefore that the low molecular weight PE additive does increase the degree of crystallinity (*i.e.* the amount of and/or size of crystalline domains) and hence improves the mechanical strength of the blend, which in turn improves the cohesive strength and the hence performance in the ASTM test. Indeed the strengthening effect of crystallites within an amorphous matrix is well known and these domains might be considered as acting like thermally labile cross-links[18].

### 3.5.10.2 *PE700Ac/MA copolymers derived from purified PE700-OH*

Using PE700-OH which had been purified by column chromatography to remove most of the non-functional PE impurity, an acrylate monomer and subsequently two new copolymers were prepared. These copolymers were similar in composition to the most technologically interesting copolymers already in-hand (**PE700Ac/MA 1:9.0** and **PE700Ac/MA 1:5.0**), but with most of the non-functional PE impurity removed (Table 3.46).

**Table 3.46: Comparison of the ASTM adhesion test data for PE700Ac/MA copolymers prepared with the original non-functional PE content present, and with this substantially reduced.**

| Sample | Non-functional PE content | Mass ratio* PE:PMA | ASTM data | | |
|---|---|---|---|---|---|
| | | | Shear strength / MPa | Max load at failure / kN | Failure Type† |
| **PE700Ac/MA 1:9.0 Purified** | ~0.6% | 1:10 | 2.35 | 0.76 | ~85%AF, ~15%SF |
| **PE700Ac/MA 1:9.0 Original** | ~2% | 1:10 | 2.69 | 0.87 | ~50%AF, ~50%SF |
| **PE700Ac/MA 1:5.0 Purified** | ~1.2% | 1:5.5 | 2.17 | 0.70 | ~50%AF, ~50%SF |
| **PE700Ac/MA 1:5.0 Original** | ~4% | 1:5.5 | 2.48 | 0.80 | ~50%AF, ~50%SF |

At both of these compositional ratios, the presence of a low concentration of the non-functional PE impurity seemed to improve the apparent adhesive shear strength. This observation correlates well with the results of blending low molecular weight PE into the **DocAc/MA** and **B36Ac/MA** copolymers, when the apparent adhesive strength was also improved relative to the copolymer alone (Section 3.5.10). Looking at the failure types, they all have an element of substrate failure and this might suggest that the adhesion test conditions are close to the upper limit of substrate strength, in particular the tensile strength of the PMMA substrate. Note however that the earlier adhesion tests from the original compositional range of PE700Ac/MA synthesised demonstrated that adhesion performance fell with higher levels of grafted PE in the copolymers (Table 3.26, Section 3.5.3).

* This refers to the mass ratio of pendant PE chains to poly(acrylate) chains in the final polymer.

† AF = adhesive failure; SF = substrate failure. The percentage areas for each failure type were estimated and averaged over all six replicate adhesion test pieces for each copolymer.

### 3.5.11 **Molecular weight effect on adhesion**

The adhesive performance of an analogous series of DocAc/MA copolymers with decreasing molecular weights was compared (Table 3.47). Since the $M_w$ value is a better indicator than the $M_n$ value of where most mass of a polymer lies the correlation of adhesion performance with this parameter is the more important.

**Table 3.47: Effect of molecular weight on adhesion for the DocAc/MA 1:3.8 copolymers**

| sample | ratio* | ASTM | | | SEC data | | |
|---|---|---|---|---|---|---|---|
| | PE:MA | Shear strength / MPa | Max load at failure / kN | Failure Type | $M_n$ / g mol$^{-1}$ | $M_w$ / g mol$^{-1}$ | PDI |
| **DocAc/MA 1:3.8A** | 1:5.0 | 1.55 | 0.50 | ~100% CF† | 88,000 | 167,100 | 1.9 |
| **DocAc/MA 1:3.8B** | 1:5.0 | 1.27 | 0.41 | ~100% CF† | 12,300 | 58,600 | 4.8 |
| **DocAc/MA 1:3.8C** | 1:5.0 | 0.31 | 0.10 | ~100% CF† | 21,200 | 28,400 | 1.3 |
| **DocAc/MA 1:3.8D** | 1:5.0 | 0.17 | 0.06 | ~100% CF† | 13,700 | 17,300 | 1.3 |

The data in Table 3.47 shows clearly that the lower molecular weight **DocAc/MA** copolymers have much lower cohesive strength than the higher molecular weight ones. The cohesive strength is likely to be a function of the mechanical strength of the copolymer and with all of the observed failures being cohesive, this result was expected. The mechanical strength of a polymer varies with its molecular weight until a threshold is reached when increasing the molecular weight has little or no further effect on the mechanical strength. The $M_w$ at which this threshold occurs

* This refers to the mass ratio of pendant docosyl chains to poly(acrylate) chains in the final polymer.
† 'CF' denotes a cohesive failure

seems to correspond to the critical mass for entanglement. It is worth noting however that it might be expected that the higher molecular weight materials would have higher melt viscosities that could impart better film-forming properties. Increased melt viscosity could also be increasing the thickness of the adhesive layer.

## 3.6 Rationalising the structure-property relationships

### 3.6.1 Background

The experimental data obtained so far have identified those compositions of copolymer adhesives that have given rise to the best adhesion performance, and have also explored some of the molecular structural features that might have contributed this best performance. It is not clear however if our structure/compositional search has arrived at an optimum adhesive, and other structural variants might be synthesised in order to extend this search. However, the experimental data has identified some clear trends in performance versus structure and composition, and instead of continuing a synthesis-based search it was thought to be more valuable to undertake some broad physical-chemical characterisation of a number of existing key materials in order to try and rationalise the structure-performance relationship that has already been established. In attempting to do this three critical regions of a typical adhesive sandwich were identified: i) the PMMA-adhesive copolymer interface; ii) the PP-adhesive copolymer interface and iii) the bulk of the adhesive copolymer. Efforts to shed light on the physical characteristics of all three of these loci were undertaken using particular adhesive copolymers that had proved to give rise to good adhesion and others where the observed adhesion was poor.

### 3.6.2 Characterising the adhesive-substrate interfaces.

#### 3.6.2.1 *Introduction*

In order to characterise the interplay between the adhesive and the two substrates, an ASTM-type adhesion test specimen (**PP-PE700Ac/MA 1:9-PMMA**) was cryo-fractured. Small fragments of the broken specimen which showed the two substrate-adhesive interfaces in cross section were examined by scanning electron microscopy (SEM) and thin sections (78 nm) of the same types of pieces were also examined by transmission electron microscopy (TEM). In addition Energy Dispersive X-ray (EDX) spectroscopy was used to characterise some particle-like features which had been observed by TEM in the copolymer. Although we were also trying to identify any phase-separated domains or other fine structure by TEM in the **PE700Ac/MA**

**1.9** layer**,** specimen staining was not carried out and consequently no features could be observed. A subsequent TEM examination of stained specimens and subsequent morphological elucidation of five copolymers from the **PE700Ac/MA** series is discussed in section 3.6.3.3, these being bulk samples of the copolymers rather than a component in an adhesive sandwich.

### 3.6.2.2 *SEM cross-sections of the adhesive-substrate interfaces*

The small pieces displaying the fracture surface (a cross-section through both substrate-copolymer interfaces) of the adhesive test specimen were embedded on the surface of a SEM specimen stub and coated with a thin film of platinum. The prepared specimens were then examined by SEM.

The scanning electron micrographs of the **PE700Ac/MA 1:9** adhesion test specimen (Figure 3.18) show that the PP substrate surface appears rougher than that of the PMMA, and indeed the adhesive seems to be mechanically interlocked on the PP interface to a greater extent than the PMMA. Since both substrate surfaces were roughened using the same protocols it seems likely that the PMMA surface had been flattened during adhesive test specimen preparation. When the test specimen was prepared it was compressed at 108 °C overnight which, being close to the $T_g$ of the PMMA substrate, may have allowed the PMMA to conform to the smooth surface of the adhesive. The highly crystalline PP substrate would be unaffected at this temperature and seems to have retained its surface roughness. The **PE700Ac/MA** adhesive would have been above its melting point (94 °C) and therefore behaving as a highly viscous liquid film, filling the grooves in the PP surface but smoothing out the similarly soft PMMA surface. There does not appear to be any observable macroscopic mixing of the adhesive between the PP and adhesive, at the other interface the micrographs are inconclusive.

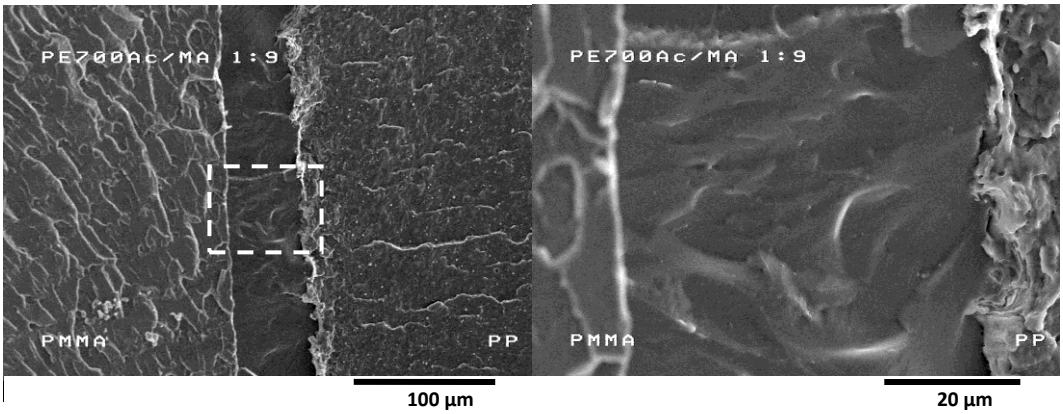


**Figure 3.18: The cross-section of an ASTM test specimen for PP-[PE700Ac/MA 1:9]-PMMA by SEM at two different magnifications. The box in the left image shows the approximate region pictured in the right image.**

The surface of the **PE700Ac/MA 1:9** seems to be homogeneous and at this magnification does not appear to have any features associated with phase separation. In addition there is no apparent difference in the copolymer morphology near to either interface (Figure 3.18).

### 3.6.2.3 *TEM cross-sections of the adhesive-substrate interfaces and subsequent EDX spectroscopy.*

A cross-sectional block face similar to that used for SEM was sectioned using an ultramicrotome (78 nm sections). Although some deformation of the thin sections did occur, they remained sufficiently intact and were subsequently mounted on gold grids and examined by TEM (Figure 3.19).

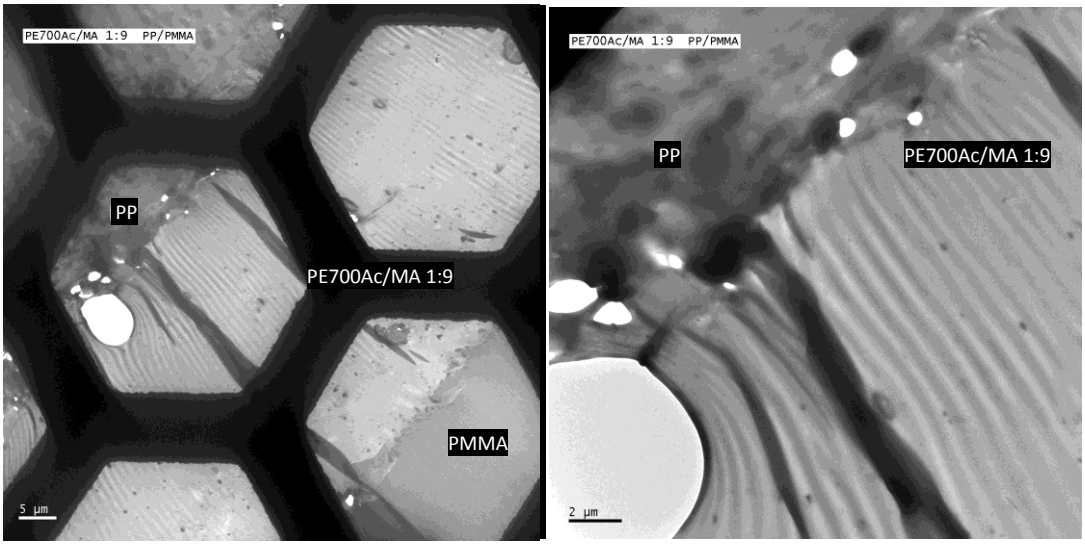


**Figure 3.19: TE micrographs of the PP-PE700Ac/MA 1:9-PMMA test specimen in cross-section. The hexagonal pattern is a gold TEM support grid.**

The transmission electron micrographs of the thin cross sections from the adhesive test specimen highlight the difference in surface roughness already observed by SEM, with voids appearing more numerous around the rougher PP surface (Figure 3.19). The regularly spaced lines apparent in the **PE700Ac/MA 1:9** layer seem likely to be artefacts generated from stresses imparted to the material during sectioning. The lines seem unlikely to be phase separation of the block copolymer since a selective contrast agent (such as the $RuO_4$ employed successfully in section 3.6.3.3) was not used during sample preparation. With no contrast introduced by staining the specimen, if different phases did exist in the copolymer (*i.e.* the PE and PMA) these would appear the same when examined by TEM as neither of them deflect the electron beam strongly as would a heavy metal. However, in the TE

micrographs some small particle-like objects can be seen dispersed throughout the **PE700Ac/MA** layer. These were subsequently examined using TEM at higher magnifications (Figure 3.20).

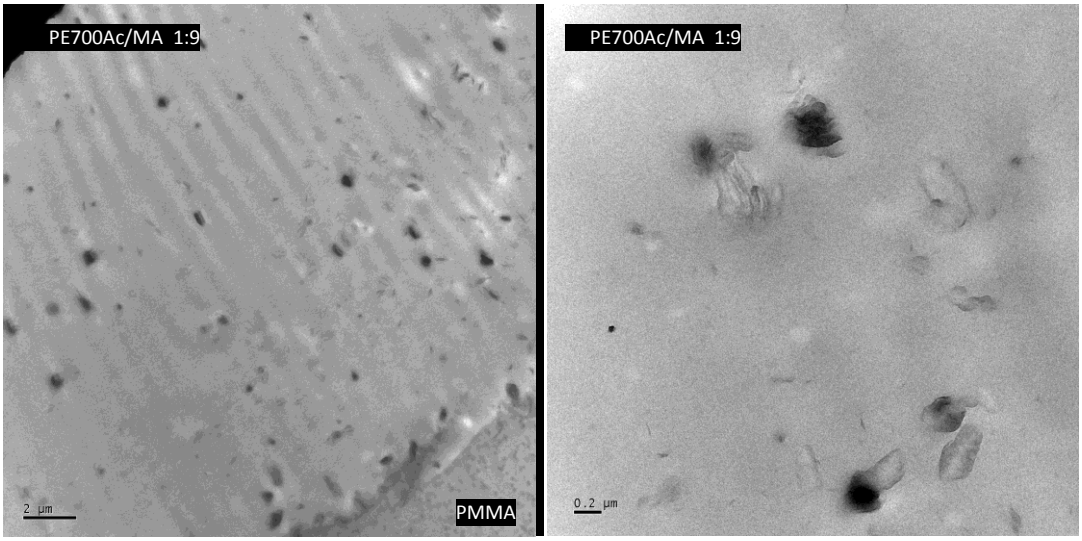


**Figure 3.20: High-magnification TE micrographs of the PE700Ac/MA 1:9 showing detail of the particle-like objects.**

The particle-like objects in the adhesive layer seemed likely to be an impurity introduced at some stage of sample preparation since they were not observed during subsequent additional TEM examination of the same copolymer (see Section 3.6.3.3). Since the objects appear dark in the TE micrographs, this suggests that they contain a heavier element(s) that scatter the electron beam more strongly than the bulk of the copolymer (which contains lighter elements, C, H, O and N and thus appears light coloured). The elemental composition of the objects and the bulk of the copolymer were subsequently characterised in turn by Energy Dispersive X-ray (EDX) spectroscopy, and this provided evidence that particle-like objects were rich in sodium compared to the copolymer. The source of this apparent contamination remains unknown.

### 3.6.2.4 *ULAM/ToF-SIMS of the PMMA-PE700Ac 1:9 interface*

Ultra low angle microtomy (ULAM) across an interface coupled with time-of-flight (ToF) secondary mass spectroscopic (ToF-SIMS) analysis is a powerful methodology for high resolution microscopic imaging of the interface[19]. Bearing in mind the thickness dimensions of our PMMA-adhesive copolymer-PP sandwiches it was not possible to prepare a single sample for microtoming at low angle that would expose both the PMMA-adhesive and PP-adhesive interfaces simultaneously. Accordingly therefore it was necessary to prepare separate PMMA-adhesive and PP-adhesive samples for microtoming and analysis using a preparative procedure as close as possible to that used in preparing the PMMA-adhesive-PP sandwiches for ASTM adhesion testing. The adhesive chosen was **PE700Ac/MA 1:9** and the solvent casting, annealing temperature and applied pressure were kept as similar as possible to try to recreate the adhesion interfaces as accurately as possible. However it was impossible to roughen the substrate surfaces since the ULAM technique requires the adhesive interface to be parallel to the other face of the substrate and in addition the substrate surface had to be as flat as possible so that the interface would be sectioned correctly (Figure 3.21). Unfortunately all attempts to section the PP-adhesive sample failed in that the layers detached too easily. Consequently only the PMMA-adhesive interface could be examined in this way.

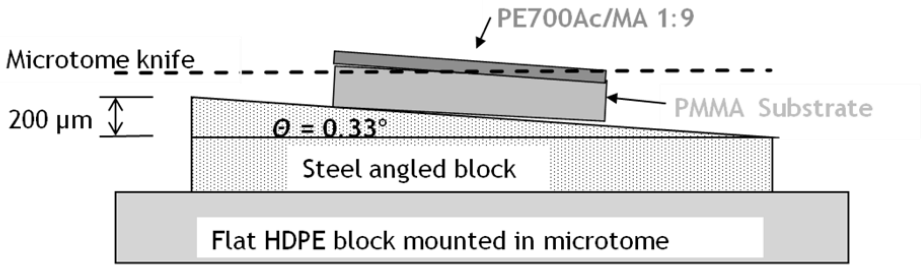


**Figure 3.21: Schematic diagram of the ULAM cross-sectioning methodology used.**

The PMMA-adhesive sandwich was sectioned 1 µm at a time as shown in the cartoon in Figure 3.21 until the previously buried interface became visible. The

specimen was then transferred to a time-of-flight secondary ion mass spectrometer (ToF-SIMS), outgassed and small areas (500 x 500 µm) of the interface were imaged by rastering the ion beam and taking fragmentation mass spectra from each pixel (256 x 256 pixels). Software in the instrument allowed images to be built up which compared the relative intensity of selected diagnostic peaks in the mass spectra of each pixel. The images clearly showed the difference between the fragmentation spectra for the PMMA substrate and the **PE700Ac/MA 1:9** (Figure 3.22).

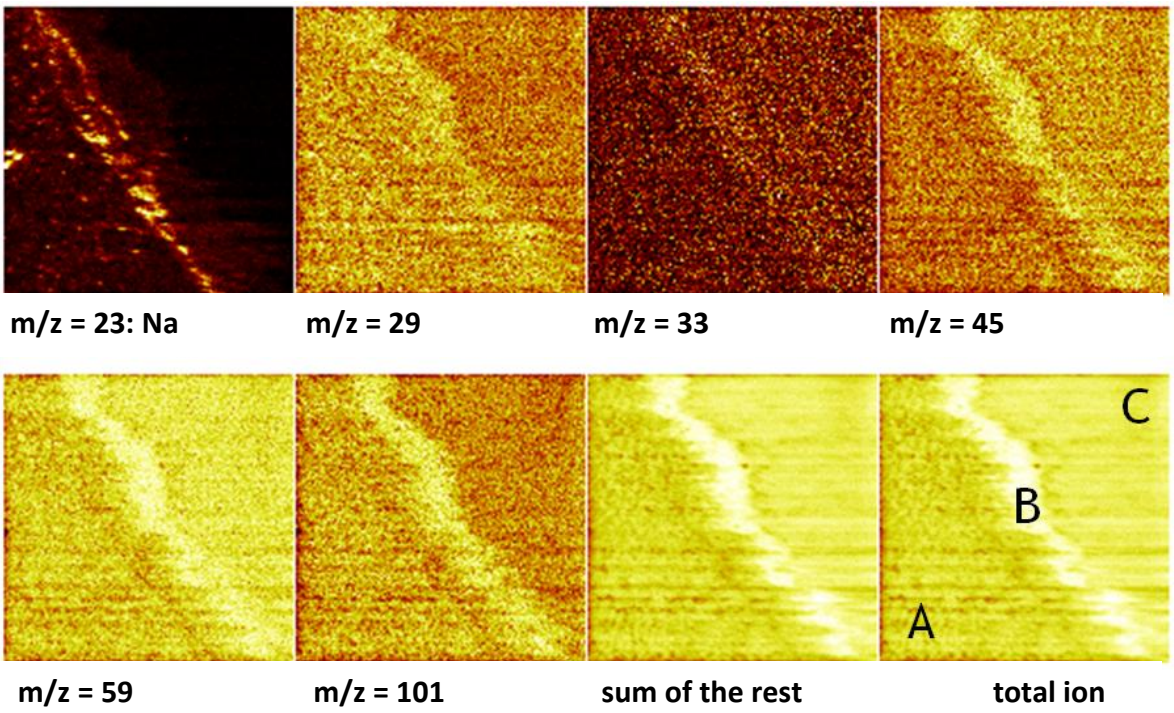


**Figure 3.22: Images derived from ToF-SIMS spectra of a PMMA-PE700Ac/MA 1:9 interface. A = PMMA, B = interface layer, C = PE700Ac/MA 1:9. White = high intensity, Black = low intensity**

The ToF-SIMS derived images (Figure 3.22) show that a distinct layer (B) does exist at the interface between the PMMA and the adhesive and that this is apparent in the relative abundance of more than one ion mass. In terms of mass spectra this interfacial layer certainly has a composition differing from that of both PMMA and the adhesive but it is not possible to deduce a molecular structural difference from these data. Interestingly the PMMA side of the interface seems to be rich in sodium relative certainly to the **PE700Ac/MA 1:9** (C) and to a lesser extent to the PMMA

(A). We believe that this represents the surface segregation of a small molecule mould-release additive present in the PMMA which contains sodium. The presence of such an additive also seems to account for the relatively high intensity of the ToF-SIMS images at the interface (B) since, being of relatively low molar mass (to the two polymers), it would be expected to fragment into ions more completely and therefore be detected at a greater concentration. The images do not however provide conclusive evidence for any mixing of the PMMA and **PE700Ac/MA 1:9** at the interface.

### 3.6.2.5 *Contact angle measurements*

One simple rationalisation about adhesive performance might be that the best adhesives have a surface contact angle that is the best compromise between the surface contact angles of the two substrates. Though this was thought to be a rather naïve theory nevertheless it was thought that it would be valuable to have these data to hand. In order to estimate the energy of a material surface, the angle made between the surface and a droplet of liquid can be measured. The theory of surface wettability has been reviewed in depth by de Gennes[20]. The **PE700Ac/MA** copolymers were investigated along with the commercial polymer substrates which were used for adhesion testing (PMMA, LDPE and PP) and the results are shown in Table 3.48.

**Table 3.48: Contact angle measurement data.**

| Sample | Failure load KN | Contact Angle | | | | Standard |
|---|---|---|---|---|---|---|
| | | 1/° | 2/° | 3/° | Average/° | deviation/° |
| PMMA* | n/a | | | | **68.0** | |
| **PE700Ac/MA 1:9.0** | 0.87 | 58.04 | 62.72 | 49.68 | **56.8** | 6.61 |
| **PE700Ac/MA 1:5.0** | 0.80 | 60.88 | 47.15 | 62.01 | **56.7** | 8.27 |
| **PE700Ac/MA 1:0.99** | 0.47 | 52.38 | 59.38 | 52.08 | **54.6** | 4.13 |
| **PE700Ac/MA 1:0.50** | 0.24 | 59.84 | 64.42 | 66.66 | **63.6** | 3.48 |
| **PE700Ac/MA 1:0.10** | nm† | 89.09 | 82.98 | 62.69 | **78.3** | 13.8 |
| **PE700Ac/MA 1:0.05** | nm† | 81.40 | 92.48 | 93.57 | **89.2** | 6.73 |
| PP* | n/a | | | | **81.0** | |
| LDPE | n/a | 83.49 | 84.24 | 87.61 | **85.1** | 2.19 |

* Raw data and standard deviation values were not provided for these materials.
† nm = not measured

The contact angle is ~68° and the average for PP and LDPE is ~83°. The mid-point between that of PMMA and the polyalkanes is therefore ~76°. Our naïve theory would predict therefore that an adhesive copolymer with a contact angle of ~76° might be optimum for adhesion performance.

Although the results were a little scattered (this was a consequence of the idiosyncrasies of the method) a trend was observed with increasing PE content in the copolymer giving higher contact angles. This trend was expected as the larger the fraction of non-polar PE in the copolymer, the higher the surface energy of that copolymer should be. In fact copolymers **PE700Ac/MA 1:9.0** and **PE700Ac/MA 1:5.0** provide the best apparent shear strength, 0.83 kN, and posses a contact angle of ~57°. This is significantly below that of PMMA and the polyalkanes and is indeed close to the value of 52° for poly(methyl acrylate) homopolymer[21]. Furthermore copolymer **PE700Ac/MA 1:0.99** provides a significantly reduced shear strength, 0.45 kN, and yet possesses a similar contact angle, 55°. These data show clearly that the value of a simple macroscopic surface physical property such as contact angle or surface energy alone does not offer any reliable indication of potential adhesion performance. Indeed with an apparently favourable contact angle for adhesion between PMMA and polyalkanes, the experimentally poor behaviour observed with the PE-rich copolymers suggests that the latter may be a result of their relatively poor bulk mechanical properties rather than a surface or interface effect.

### 3.6.3 **Morphological studies**

#### 3.6.3.1 ***Introduction***

In order to further investigate and rationalise the structure/adhesion property relationships found for these materials, techniques probing their morphology were adopted. Thermal analysis by differential scanning calorimetry (DSC) and transmission electron microscopy (TEM) were available to us.

#### 3.6.3.2 ***Thermal analysis; differential scanning calorimetry***

Some of the key adhesion copolymers were analysed by differential scanning calorimetery (DSC), which gave valuable information on their glass transition temperature ($T_g$) and/or their melting points ($T_m$) in addition to crystallinity data. Initial samples were assessed where the DSC data was taken from the second heating/cooling cycle in each case since this removes the effects of thermal history on the sample. An additional heating/cooling cycle was performed the data from which, in all cases, corresponded to that from the second cycle. This suggests that no decomposition was occurring during the heating (to 140 °C) although thermal gravimetric analysis studies would be of benefit to confirm this, especially as the copolymers have to be heated for extended periods during adhesive testing. In order to measure the degree of crystallinity data from the first heating/cooling cycle was used.

When the **PE700Ac/MA** copolymers were analysed by DSC a clear relationship between the composition and the melting point could be observed. The DSC curves had two distinct melt transitions consistent with the presence of the non-functional PE impurity. The temperature of the melt transition varied with the composition ratio (Figure 3.23). A $T_m$ value 108 °C for the PE700OH starting material was also recorded as a reference. The $T_m$ of linear PE is reported in the *Polymer Handbook*[13] from various references to be in the range of 137-146 °C, but the relatively low molecular weight of the PE700-OH (Mn = 700 g $mol^{-1}$) has a significant effect in reducing this temperature. The presence of the –OH end-group may also influence the $T_m$ but when compared to the molecular weight effect this is likely to be small. In

the **PE700Ac/MA** copolymer series the $T_m$ of the PE phase passed through a minimum with the highest and lowest PE content materials having similar values. These minima seem to reflect the influence of the amorphous PMA phase on the crystalline PE phase with regard to the $T_m$ value, and may reflect solubility effects.

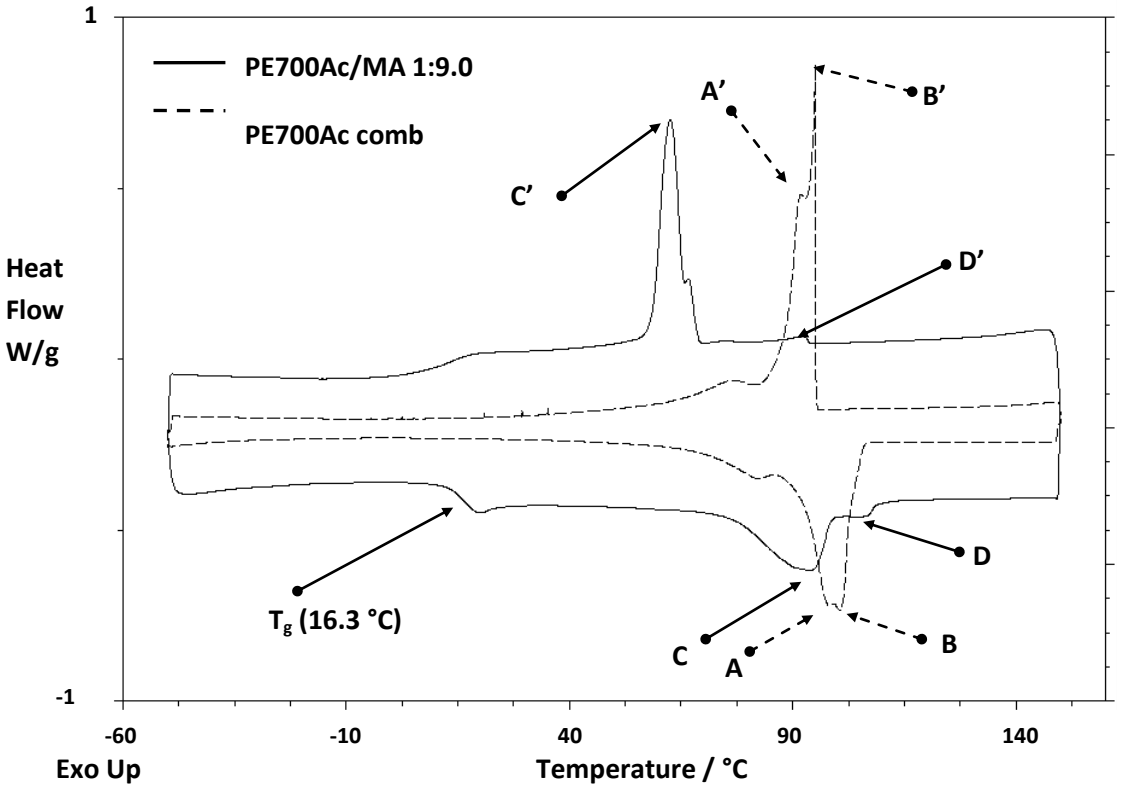


**Figure 3.23: A DSC curve comparison for one PE700Ac/MA copolymer (solid line) and the PE700Ac comb (dashed line). Data was taken from the second heating/cooling cycle.**

**A. Melt transition**
**A'. Crystallisation** } **of the PE segments of the PE700Ac comb copolymer**

**B. Melt transition**
**B'. Crystallisation** } **of the non-functional PE impurity present in the PE700Ac/MA comb copolymer at ~20 wt%.**

**C. Melt transition**
**C'. Crystallisation** } **of the PE segments of the PE700Ac/MA 1:9.0 copolymer**

**D. Melt transition**
**D'. Crystallisation** } **of the non-functional PE impurity present in the PE700Ac/MA 1:9.0 copolymer at ~2 wt%.**

**Table 3.49: Comparison of the $T_m$ and $T_g$ values of the series of PE700Ac/MA copolymers.**

| Sample | Mass ratio* | Thermal transitions / °C | |
|---|---|---|---|
| | PE:MA | $T_g$ | $T_m$ |
| **poly(methyl acrylate)[13]** | 0:1 | 10 | ~ |
| **PE700Ac/MA 1:9.0** | 1:10.0 | 16 | 107 |
| **PE700Ac/MA 1:5.0** | 1:5.5 | 18 | 109 |
| **PE700Ac/MA 1:0.99** | 1:1.1 | 18 | 98 |
| **PE700Ac/MA 1:0.50** | 1:0.6 | * | 99 |
| **PE700Ac/MA 1:0.10** | 1:0.1 | * | 98 |
| **PE700Ac/MA 1:0.05** | 1:0.1 | * | 98 |
| **PE700Ac comb†** | 1:0 | * | 101 |
| **PE700OH** | | | 108 |

For the **PE700Ac/MA** copolymers rich in PMA a $T_g$ can also be clearly seen, as the PE content is increased the polymer has a higher crystalline content compared to PMA homopolymer (see later) and the $T_g$ increases markedly from 10 °C to 16 °C with only 10% PE (Figure 3.24). As the PE content in increased the $T_g$ increases slightly before levelling off and becoming less visible by DSC although it may have been possible to observe it by dynamic mechanical thermal analysis (DMTA).

* Not observed.
† i.e. a homopolymer of PE700Ac

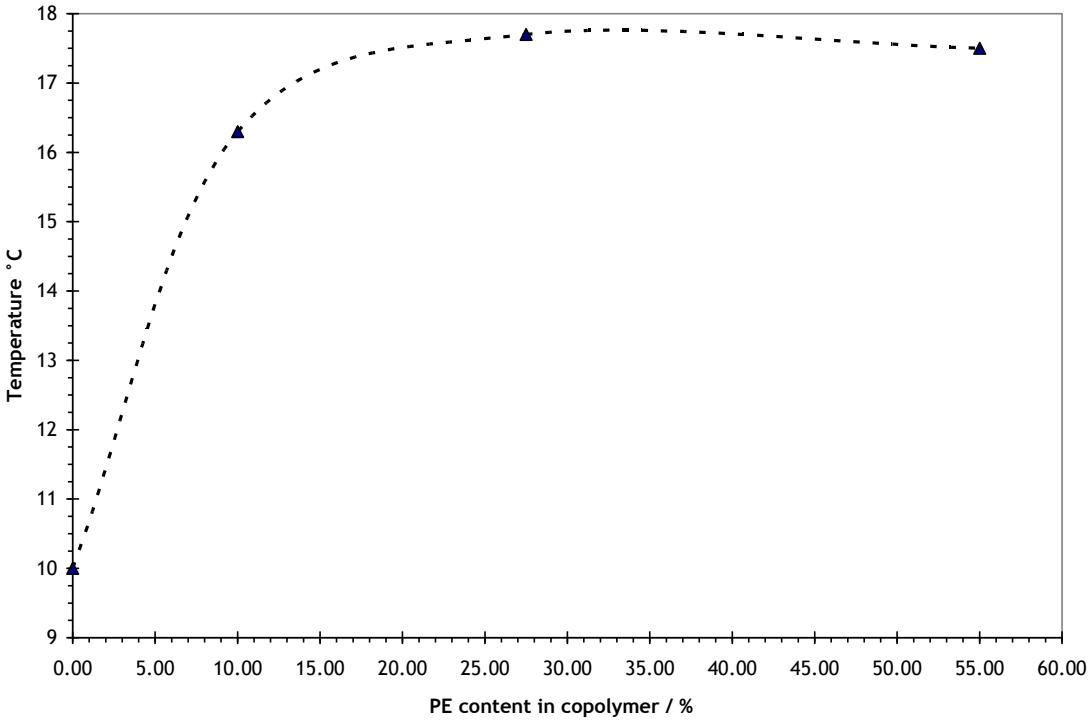


**Figure 3.24: The variation of $T_g$ with PE content for the PE700Ac/MA copolymers.**

The degree of crystallinity of the **PE700Ac/MA** series of copolymers was estimated using a First Law method reported by Kong and Hay[22] (Table 3.50). Essentially the relative size of the melting endotherms measured by DSC (i.e. their $\Delta H_m$) of the copolymers were compared to the measured $\Delta H_m$ (245.3 J $g^{-1}$) of a sample of PE with a crystalline fraction close to 100%[23]. However this assumes that the copolymer behaves in the same way as a PE homopolymer but nonetheless provides a good estimate of the copolymers' relative crystallinity, especially when compared to the transmission electron micrographs which clearly demonstrated the increase in crystalline domains as the PE content was increased (see Section 3.6.3.3). It is worth noting that the measured crystallinity is lower than the theoretical values corresponding nominal PE content (Table 3.50) which is not unexpected as the PE chains are attached to a PMA backbone, which must constrain the PE side chains.

**Table 3.50: Degree of crystallinity for the PE700Ac/MA series of copolymers derived from thermal analysis data from the first heating/cooling cycle.**

| Copolymer | $\Delta H_m$ / J $g^{-1}$ | $T_m$ / °C | Nominal PE content* / % | Degree of crystallinity / % |
|---|---|---|---|---|
| **PE700Ac/MA 1:9.0** | 20.1 | 95 | 10 | 8 |
| **PE700Ac/MA 1:5.0** | 27.1 | 92 | 20 | 11 |
| **PE700Ac/MA 1:0.99** | 98.4 | 98 | 50 | 40 |
| **PE700Ac/MA 1:0.50** | 117.9 | 98 | 80 | 48 |
| **PE700Ac/MA 1:0.10** | 170.8 | 98 | 90 | 70 |

Glass transition temperatures could not be observed by DSC for the **PE700Ac/EHMA** copolymers. The $T_g$ of these copolymers should in theory be lower than that of the **PE700Ac/MA** copolymers as the branched 2-ethylhexyl side packs less efficiently compared with the methyl side chain. Poly(2-ethylhexyl methacrylate) has a $T_g$ of -10 °C, compared to PMA which has a $T_g$ of +10 °C[23]. Observation of the physical properties of the **PE700Ac/EHMA** copolymers reveals that they are in a rubbery state at room temperature, indicating that they are likely to be above their $T_g$.

The melt transition is barely visible in the DSC traces of the **PE700Ac/EHMA** copolymers, especially for those rich in EHMA, becoming more prominent and increasing as the PE content is increased (Table 3.51). The melt transition is likely to arise from the melting of crystalline or semi-crystalline PE microdomains in the PEHMA matrix, with the size and/or number of such domains increasing with increasing PE content giving rise to a larger melt transition at a higher temperature.

* Measured from the feed ratio of PE700Ac monomer fed into the reaction.

Poly(2-ethylhexyl methacrylate) is an amorphous material and as such does not have a clear melt transition. Overall the thermal behaviour of the **PE700Ac/EHMA** series of copolymers does not differ substantially from the behaviour of the **PE700Ac/MA** series and this is consistent with their similar adhesion performance.

**Table 3.51: Thermal analysis data of the PE700Ac/EHMA copolymers.**

| Copolymer | Mass ratio PE:(M)Ac | $T_m$ / °C (DSC) |
|---|---|---|
| **PE700Ac/EHMA 1:24.1** | 1:10 | 102 |
| **PE700Ac/EHMA 1:12.1** | 1:5 | 104 |
| **PE700Ac/EHMA 1:2.4** | 1:1 | 106 |
| **PE700Ac/EHMA 1:1.2** | 1:0.5 | 106 |
| **PE700-OH** | ~ | 108 |

### 3.6.3.3 *Transmission electron microscopy*

Transmission electron microscopy (TEM) can be used to investigate the morphology of a polymer or copolymer if sufficient contrast can be introduced to one of the phases present. Organic polymers typically have low contrast in TEM as light atoms such as carbon or hydrogen do not scatter the electron beam sufficiently. Stains are often used which will covalently introduce heavier elements into the polymer, these scatter the electron beam more effectively and subsequently introduce contrast. In the case of a polymer containing crystalline PE domains, these can be stained selectively over amorphous regions by reacting the sample with aggressive transition metal containing reagents such as $RuO_4$. Sample preparation and staining are essential to provide meaningful TE micrographs and a method was developed to use with the PE700Ac/MA copolymers. A series of five **PE700Ac/MA** copolymers, with a range of compositions from 1:9, 1:5, 1:1, 5:1 and 9:1 (PE:PMA) were solution cast onto PP substrates and annealed in the same way as the adhesion test pieces were prepared in order to achieve as similar a morphology to that found in actual adhesion test-pieces as possible. Small slices of the copolymer film were cut and embedded into a proprietary hydrophobic acrylic resin (Lowicryl HM20) which

effectively supported them as they were cut into thin slices in the ultramicrotome. The thin sections were placed onto Au grids and then stained. Two different methods were used to stain the copolymer slices, one using osmium tetroxide ($OsO_4$)[24] and another using ruthenium tetroxide ($RuO_4$)[25]. When the samples were observed using the TE microscope it was found that the $RuO_4$ had selectively stained some features in the copolymer, while the $OsO_4$ seemed to have had no fixing effect. $RuO_4$ is an aggressive reagent and is known to preferentially stain crystalline over amorphous PE domains[26]. TEM was then used to image the sections at various magnifications.

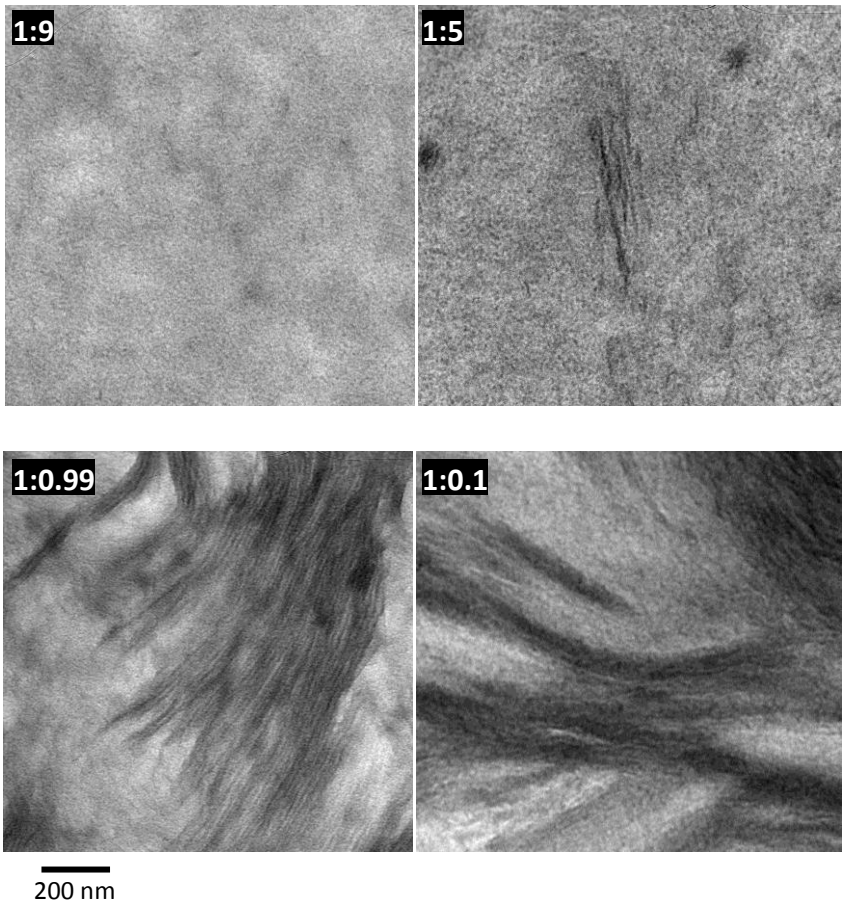


**Figure 3.25: TE micrographs of the $RuO_4$ stained PE700Ac/MA copolymers. The ratios shown in the top right corner of each image represent the PE:PMA ratio in the copolymer under investigation.**

The **PE700Ac/MA 1.9** copolymer (Figure 3.25 top left) seems to show only very small discrete regions of stained PE, which is consistent with the copolymer composition (around 10% 'PE' by mass). The **PE700Ac/MA 1:5** copolymer (Figure 3.25 top right) has more and larger PE rich regions, which is expected as it has a larger PE content than the 1:9 copolymer. The striped, "wheatsheaf" features are consistent with crystalline PE regions[27] and the lamellar thickness was clear enough to measure (d = ~15 Å). The **PE700Ac/MA 1:0.99** copolymer (Figure 3.25 bottom left) had large regions where a semi-crystalline lamellar type morphology was visible. Again these were characteristic wheatsheaf features, and the lamellar

thickness was measured (d = ~15 Å). Small lamellar distances like this are also evidence that the features are indeed crystalline PE and not structures associated with a phase-separated PE-PMA morphology, which would have had lamellar spacings in the order of ~40-50 Å. The size and widespread distribution of these regions is consistent with an increased PE content. The TEM of copolymer **PE700Ac/MA 1:0.1** (Figure 3.25 bottom right) seemed to show a large amount of wheatsheaf-type crystalline PE lamellae in a relatively small proportion of amorphous PMA matrix. Again, this was consistent with an increased PE content compared to the other copolymers.

Comparing all of the micrographs it seems likely that the PE side-chains (and any linear non-functional PE present) prefer to pack together to form crystalline or semi-crystalline lamellar structures within the amorphous PMA matrix. As the PE content is increased the size and amount of these structures increases. This is also consistent with the crystallinity data derived from thermal analysis. In terms of the relative adhesive strength of these copolymers these TEM images would appear to be crucial. Small and highly dispersed PE regions (1:9 and 1:5) seem to be significantly better than either no PE content at all or large and interconnected PE domains (1:0.99 and 1:0.1).

### 3.6.4 **Conclusions from Morphological Studies**

From the morphological studies of the **PE700Ac/MA** copolymers it seems likely that the PE content provides crystallinity. Thus the proportion of crystallinity is determined by the composition of the copolymer. As early as 1969 Bawn proposed that the presence of crystalline domains within an amorphous matrix, such as those observed in the PE700Ac/MA copolymers by TEM, can be thought of as thermally-labile crosslinks[18], and as such these are likely to enhance the toughness of the main copolymer phase. The properties of the **PE700Ac/MA** copolymers are consistent with the presence of such domains, being soft at and above the $T_m$ of the PE phase, much like an amorphous polymer above its $T_g$, and yet hard and strong below the $T_m$ of this phase (although still above the $T_g$ of the main phase). The presence of crystalline domains will alter the mechanical properties of a sample, it follows

therefore that the mass% of the PE phase and the thermal history of a sample of the copolymer will influence its mechanical strength and in this instance the adhesion properties. If a sample is cooled quickly from the melt a large proportion of small crystalline domains will be formed, in contrast slow cooling or annealing will provide a larger proportion of large spherulites. The number and size distribution of PE crystalline domains will of course influence the bulk properties of the copolymers.

## 3.7 Summary and Conclusions

In the present work new graft copolymer materials that could be used as adhesives or compatibilisers for PMMA and PP have been prepared. These materials were targeted as the adhesive to allow laminated structures of PMMA and PP to be constructed, which might then be used as potential replacement materials for PVC which is used currently in the construction industry for window frames, door frames, gutters, drain pipes and cladding. PVC is an excellent material for this purpose especially window and door frames and cladding as a result of its excellent mechanical and weathering properties, however it is difficult to recycle since its decomposition temperature is lower than its melting temperature. In addition to this when PVC burns, the combustion products have been shown to include low levels of highly toxic dioxins[28] as well as stoichiometric amounts of HCl. These combustion products make PVC disposal hazardous and complex, therefore replacements are being sought. PP also possesses suitable mechanical properties for this purpose but does not weather very well. Therefore it has been suggested that a barrier layer of filled PMMA on its surface would greatly enhance the lifetime of PP used in construction. However PP and PMMA are essentially incompatible and a cheap copolymer adhesive is required to create the laminated composite.

PE grafted poly(meth)acrylates were proposed as potentially useful adhesives. The copolymers were made by a grafting 'through' technique using macromonomers and free-radical polymerisation. Acrylate and methacrylate PE macromonomers were prepared in high conversion from commercially sourced polyethylene monoalcohols (PE-OH) by esterification with either acryloyl or methacryloyl chloride. They were isolated by precipitation into an excess non-solvent and characterised by $^{1}$H NMR and FT-IR spectroscopy. These PE macromonomers were then copolymerised, at several different comonomer ratios, using a conventional free-radical solution methodology with a variety of different (meth)acrylate co-monomers (e.g MA, MMA, 2-EHMA) to provide copolymers with a broad range of different properties. The copolymers were isolated by precipitation into an excess of non-solvent, characterised by $^{1}$H NMR spectroscopy and were evaluated in an in-house adhesion test. The best-performing materials were re-tested using an ASTM standard protocol

and were characterised morphologically by DSC and TEM. This allowed us to elucidate several structure/property relationships for the materials studied. In passing a method to free the commercially-available PE-OHs from a non-functional PE impurity (15-20%) was developed using a simple isocratic separation on silica gel. Access to a higher purity PE-OH allowed the influence of the non-functional PE impurity on the structure-property relationships of the adhesives to be established.

The important experimental findings and structure/adhesive property relationships emerging from this study are as follows:

1. Melt formed sandwiches of PMMA and LDPE using poly(methyl acrylate) homopolymer display facile cohesive failure on being stressed although the substrates initially and superficially appear to 'stick together'
2. ~10-20 wt% of PE grafts in various (meth)acrylate ester copolymers provide high adhesive strength in both PMMA-LDPE and PMMA-PP sandwiches. This is the case for the **DocAc/MA, PE460Ac/MA, PE700Ac/MA, PE460Ac/EHMA** and **PE700Ac/EHMA** copolymers.
3. Higher levels of the PE component result in poorer adhesion performance.
4. Simple physical mixtures of PE-OH with *e.g.* PMA in the same mass ratio of the better copolymer adhesives display poor adhesion properties.
5. The presence of a small level of non-functional PE in copolymers already showing good adhesion performance improves the adhesive strength to a small but significant extent.
6. Copolymers that show good adhesive performance for PMMA with LDPE using the 'in-house' test also perform well with PMMA-PP sandwiches in the ASTM adhesion test.
7. Polyacrylate and low $T_g$ polymethacrylate mainchains can each form the basis of effective adhesives whereas high $T_g$ polymethacrylate chains yield brittle ineffective adhesives.
8. **PE460Ac** and **PE700Ac** comb copolymers (*i.e.* homopolymers of each of these macromonomers) are poor adhesives.
9. As measured by contact angle there is no simple correlation between the macroscopic surface nature of the adhesive copolymers and the PMMA and

polyalkane substrates. The best adhesive performance is provided by copolymers with a contact angle (~55°) below that of both PMMA (~68°) and the polyalkane (~85°) substrates.

The mechanism of adhesion was studied first by examination of a PMMA-copolymer-PP 'sandwich' in cross-section by SEM and TEM. For the copolymer-PP interface the microscopy seems to indicate that mechanical interlocking rather than mixing of the adherand and the copolymer is a major component of the adhesive mechanism. The SEM and TEM examination was inconclusive for the mechanism of adhesion at the PMMA-copolymer interface. The PMMA-**PE700Ac/MA 1:9** copolymer interface was additionally investigated using ULAM/ToF-SIMS. The sample preparation suggested that the surface adhesion was good and indeed better than the analogous PP-copolymer sample which delaminated on microtoming. Images generated from the fragmentation spectra of an ultra low angle cross-section of the PMMA-copolymer interface seemed to show that there was layer at the interface which was compositionally different to either the PMMA or the adhesive copolymer. Although complete characterisation of this layer was not possible, it seemed likely to contain a sodium-rich low molecular weight component of the commercial-grade PMMA which had segregated to the surface during manufacture (this was possibly a surfactant type additive known as a mould-release agent which by its nature would segregate to the PMMA surface).

The DSC data for **PE700Ac/MA 1:9** showed unambiguously the presence of a discrete PMA phase and likewise a discrete PE phase. Both the PMA and PE phases show melt/crystallisation transitions and there is a glass transition at ~16°C probably associated with the amorphous region of the PMA phase. At ambient temperature therefore it seems that the major component is a soft PMA matrix in which is located a crystalline PE phase.

The bulk morphology of the **PE700Ac/MA** copolymer series was also characterised by TE microscopy. TE micrographs seem to confirm that the graft copolymers have a bulk morphology comprising crystalline domains of PE within an amorphous PMA matrix. As the PE content of the copolymer is increased the number and size of these domains both increase and once the PE content is greater than 50 wt%, the crystalline

regions dominate and are near continuous through the specimen. Discrete crystalline or semi-crystalline domains such as these within an amorphous polymer matrix are known to behave like thermally labile cross-links, in this case making the copolymer rigid (*i.e.* more tough) at temperatures above its $T_g$ but below its $T_m$. When compared to the main structure/adhesion property relationship already established (*i.e.* ~10-20 wt% PE = good adhesion: 50 wt%+ PE poor adhesion) it can be concluded that the small discrete crystalline PE domains do indeed reinforce the PMA matrix, greatly improving its mechanical strength and thus improving the overall adhesive strength and that a higher proportion of PE grafts weakens the material as the crystalline domains become linked together. The PE domains themselves seem to have low mechanical strength, presumably as a result of the low molecular weight of the PE side-chains (700 g $mol^{-1}$). The degree of crystallinity measured by DSC of the same series of copolymers correlates well with their PE graft content and the size and number of crystalline domains observed by TEM.

Interestingly the use of rather low molecular weight polyethylene monoalcohols was not our choice in that the materials employed (PE460-OH and PE700-OH) were the only ones conveniently commercially available at modest cost. Rather fortunately it seems that such molecular weights are a good choice, allowing the formation of a large proportion of very small crystalline domains of PE at overall low PE content (~10%). Also these components yield PE grafted polyacrylate copolymers that have reasonable solubility and are able to be manipulated fairly easily. Longer PE graft chains might tend to form a small number of larger domains or spherulites, and hence not provide the broad and uniform reinforcement of the PMA phase provided by the large number of smaller domains.

Overall therefore it seems that further optimisation of the graft copolymers identified in this project seems very worthwhile building on the generic structural principals that have been evolved. This would seem to provide a real opportunity to develop a viable PMMA-polyalkane sandwich as a replacement for PVC products.

## 3.8 Future Work

- Fully optimise the synthetic methodology used to prepare the copolymers containing **PE700Ac** and **PE460Ac** with respect to molecular weight, characterising all of the products using high temperature SEC. Subsequently obtain a complete relationship between the polymers' molecular weight and their adhesive performance.

- Prepare and characterise macroinitiators from both the PE700-OH and PE460-OH starting materials used in the present work and subsequently use these to synthesise and characterise a series of polyethylene-*block*-poly(methyl [meth]acrylate) copolymers using the controlled radical polymerisation methodology ATRP, with reference to the work of Matyjaszewski and co-workers[1b]. In particular it is likely that copolymers derived from the purified PE-OH starting materials would be interesting to study in terms of their phase behaviour.

- Fully investigate the adhesive-substrate interfaces to find out the mechanism of adhesion, looking for evidence of interdiffusion using small-angle neutron scattering, although to provide contrast this would require the preparation of deuterated adhesive polymers to study in the PMMA and PP matrices using a synchrotron neutron source.

- Perform a more complete thermal analysis of the copolymers described in the present work involving DMTA to discover all of their $T_g$ values and TGA to ascertain their stability at the elevated temperatures used for heat sealing.

## 3.9 References


(1) (a) Britovsek, G. J. P.; Cohen, S. A.; Gibson, V. C.; Maddox, P. J.; Meurs, M. v. *Angewandte Chemie International Edition* **2002**, *41*, 489(b) Kaneyoshi, H.; Inoue, Y.; Matyjaszewski, K. *Macromolecules* **2005**, *38*, 5425(c) Britovsek, G. J. P.; Cohen, S. A.; Gibson, V. C.; van Meurs, M. *J Am Chem Soc* **2004**, *126*, 10701.

(2) Przybilla, L.; Brand, J. D.; Yoshimura, K.; Rader, H. J.; Mullen, K. *Anal Chem* **2000**, *72*, 4591.

(3) Lin-Gibson, S.; Brunner, L.; Vanderhart, D. L.; Bauer, B. J.; Fanconi, B. M.; Guttman, C. M.; Wallace, W. E. *Macromolecules* **2002**, *35*, 7149.

(4) Pasch, H.; Trathnigg, B. *HPLC of polymers*; Springer: Berlin ; London, 1998.

(5) Chang, T. *J Polym Sci Pol Phys* **2005**, *43*, 1591.

(6) Heinz, L. C.; Pasch, H. *Polymer* **2005**, *46*, 12040.

(7) Muenker, A. H.; Hudson Jr., B. E. *J Macromol Sci -Chem* **1969**, *A3*, 1465

(8) Tsaknis, J.; Lalas, S.; Gergis, V.; Dourtoglou, V.; Spiliotis, V. *Journal of Agricultural and Food Chemistry* **1999**, *47*, 4495.

(9) Burtle, J. G.; Turek, W. N. *J Org Chem* **1954**, *19*.

(10) Stempel, G. H.; Cross, R. P.; Mariella, R. P. *J Am Chem Soc* **1950**, 2299.

(11) Guerbet, M. *Comptes Rendus* **1909**, *149*, 129.

(12) MacDonald, I. I. *Unpublished results* **2006**.

(13) Brandrup, J.; Immergut, E. H.; McDowell, W. *Polymer handbook*; 2d ed.; Wiley: New York,, 1975.

(14) Staudinger, H. *Trans Faraday Soc* **1933**, 18.

(15) Flory, P. J. *Principles of polymer chemistry*; Cornell University Press: Ithaca, N.Y., 1953.

(16) D1005-05; ASTM International: West Conshohocken, PA, 2005.

(17) D3163-1; ASTM International: West Conshohocken, PA, 2001.

(18) Bawn, C. E. H. *Plastics and Polymers* **1969**, *37*, 373.

(19) (a) Hinder, S. J.; Lowe, C.; Maxted, J. T.; Watts, J. F. *Surf Interface Anal* **2004**, *36*, 1575(b) Hinder, S. J.; Watts, J. F.; Simmons, G. C.; Lowe, C. *Surf Interface Anal* **2008**, *40*, 436.

(20) de Gennes, P. G. *Reviews of Modern Physics* **1985**, *57*, 827.

(21) Andrade, J. D.; Ma, S. M.; King, R. N.; Gregonis, D. E. *J Colloid Interf Sci* **1979**, *72*, 488.

(22) Kong, Y.; Hay, J. N. *Polymer* **2002**, *43*, 3873.

(23) Brandrup, J.; Immergut, E. H.; Grulke, E. A. *Polymer handbook*; 4th ed.; Wiley: New York, 1999.

(24) Kato, K. *Journal of Electron Microscopy* **1965**, *14*, 220.

(25) Trent, J. S. *Macromolecules* **1984**, *17*, 2930.

(26) (a) Sano, H.; Usami, T.; Nakagawa, H. *Polymer* **1986**, *27*, 1497(b) Loo, Y. L.; Register, R. A.; Adamson, D. H. *J Polym Sci Pol Phys* **2000**, *38*, 2564.

(27) Woodward, A. E. *Atlas of polymer morphology*; Hanser Publishers: Munich ; New York, 1989.

(28) Katami, T.; Yasuhara, A.; Okuda, T.; Shibamoto, T. *Environmental Science & Technology* **2002**, *36*, 1320.